

A submersible eDNA sampler that enables persistent site assessment of biodiversity

by

Andre D. Hendricks

Submitted in partial fulfilment of the requirements
For the degree of Master of Applied Science

at

Dalhousie University
Halifax, Nova Scotia
April 2022

Dalhousie University is located in Mi'kma'ki, the

Ancestral and unceded territory of the Mi'kmaq.

We are all Treaty people.

© Copyright by Andre D. Hendricks, 2023

Table of Contents

List of Tables.....	vi
List of Figures.....	vii
Abstract	ix
List of Abbreviations and Symbols	x
Acknowledgements.....	xiv
Chapter 1 Introduction.....	1
1.1 Thesis Description and Scope.....	3
1.2 Publications and Conferences	4
1.2.1 Peer-Reviewed Journal Articles.....	5
1.2.2 Conference Proceedings	5
1.2.3 Unrelated to the eDNA Sampler Journal Papers Contributions.....	5
Chapter 2 Literature Review	6
2.1 Smith-Root eDNA sampler.....	6
2.2 Continuous Low-Level Aquatic Monitoring (CLAM)	9
2.3 Subsurface Automated Sampler for eDNA (SASe).....	10
2.4 Phytoplankton Sampler (PPS).....	12
2.5 Modular Autonomous Biosampler (MAB).....	15
2.6 Environmental Sample Processor (ESP) Gen 3	16
2.7 In-Situ Autonomous Biosampler (IS-ABS).....	18
2.8 PolyWAG (Water Acquired Genomics).....	20
2.9 Large Volume eDNA Sampler	20
2.10 Summary Table.....	23
Chapter 3 A Novel eDNA Sampler	26

3.1	Chemicals.....	27
3.2	Fluidic Architecture Configurations.....	28
3.2.1	Push Configuration.....	29
3.2.2	Pull Configuration.....	30
3.3	Fluid Mechanics.....	31
3.4	Electronic Components.....	33
3.4.1	Syringe Pump.....	33
3.4.2	Solenoid Valves.....	34
3.4.3	Pressure Sensor.....	36
Chapter 4 Electrical Design.....		39
4.1	Electronic Architecture.....	39
4.2	Early-Stage Prototyping.....	40
4.3	Circuit Board Designs.....	42
4.3.1	PCB V1 - Adding Power Regulation and Valves.....	43
4.3.2	PCB V2 – Adding Flexibility.....	45
4.3.3	PCB V3 – Adding Pressure Tolerance.....	46
4.4	Final PCB Components.....	47
4.4.1	Voltage Regulators.....	47
4.4.2	Microcontroller Development Board.....	48
4.4.3	Stepper Motor Driver.....	49
4.4.4	Analog to Digital Converter.....	50
4.4.5	RS-232 Line Driver/Receiver.....	51
4.4.6	Octal Low-Side Driver.....	51
4.4.7	Bluetooth Low Energy Module.....	52

4.4.8	SD Card Module.....	52
4.4.9	Backup Battery	53
4.5	Interfacing with Fluidic Architecture	53
4.5.1	Piston Pump	53
4.5.2	Solenoid Valve	56
4.5.3	Pressure Sensor	57
4.6	Power Budget Considerations	58
Chapter 5 Software Design.....		64
5.1	Automation Protocol	64
5.2	Threads	66
5.2.1	Main Thread	67
5.2.2	Backup Communication Thread	67
5.2.3	Pressure Measurement Thread	68
5.3	Interrupts.....	68
5.3.1	Quadrature Encoder Interrupt	69
5.3.2	Home Signal Interrupt.....	70
5.3.3	Scheduler Interrupt.....	71
5.4	Fluid Control	71
5.4.1	Piston Pump Fluid Flow Control	71
5.4.2	Flow Rate Calculation	74
Chapter 6 Unit Testing		77
6.1	Negative Pressure Test	77
6.2	Pump Flow Rate and Volume Test.....	80
6.3	Cross-Contamination Testing	82

Chapter 7 Benchtop System	87
7.1 Benchtop Setup	87
7.1.1 Fluidic Architecture	88
7.1.2 Electronic Section	90
7.2 Food Dye Testing	90
7.3 eDNA Sampling – Actual Biological Sample.....	92
7.3.1 Test 1 (T1) – Pull Configuration.....	96
7.3.2 Test 2 (T2) – Pull Configuration.....	97
7.3.3 Test 3 (T3) – Push Configuration	98
7.3.4 Test 4 (T4) – Push Configuration	98
7.5 Cross-Contamination Test	99
7.6 Conclusion	102
Chapter 8 Submersible eDNA Sampler	103
8.1 System Description	104
8.2 Halifax Harbour Deployment.....	105
8.2.1 Field Sample Collection	105
8.2.2 DNA Extraction and Sequencing	106
8.2.3 Bioinformatics	107
8.2.4 Results	108
8.2.5 Discussion.....	114
Chapter 9 Conclusion and Future Work	117
9.1 Thesis Conclusion	117
9.2 Suggested Future Work	117
References.....	119

List of Tables

Table 2.1 eDNA samplers in the literature and commercially available.	23
Table 2.2: Requirements of a novel eDNA sampler.....	24
Table 6.1: Piston pump flow rate and volume accuracy test with encoder ticks set to 12,500. .	81
Table 6.2: Piston pump flow rate and volume accuracy test with encoder ticks set to 12,000. .	82
Table 7.1: Food dye colouring for each filter membrane and chemicals of the eDNA sampler ..	92
Table 7.2: Mean quantity of BB40 bacteria monoculture captured on filter membranes	101
Table 8.1: Coordinates and time sampled for each of the 6 stations where a successful deployment occurred	110
Table 8.2: DNA metrics of eDNA sampler and Niskin samples at each station (S1-S6) and the pre-filter (PF).....	110

List of Figures

Figure 2.1: Smith Root eDNA sampler	7
Figure 2.2: Subsurface Automated Sampler for eDNA (SASe).....	11
Figure 2.3: Phytoplankton Sampler	13
Figure 2.4: Modular Autonomous Biosampler	15
Figure 2.5: Environmental Sample Processor	17
Figure 2.6: In-situ Autonomous Biosampler (IS-ABS)	19
Figure 2.7: Large Volume eDNA sampler	21
Figure 3.1: eDNA sampler's fluidic architecture	26
Figure 3.2: eDNA sampler's piston pump CAD rendering.....	33
Figure 3.3: eDNA sampler's solenoid valve CAD rendering.....	35
Figure 3.4: eDNA sampler's pressure sensor	36
Figure 4.1: eDNA sampler's electronic architecture diagram	40
Figure 4.2: eDNA sampler's early electronic prototype	41
Figure 4.3: eDNA sampler's PCB v1.....	44
Figure 4.4: eDNA sampler's PCB v2.....	45
Figure 4.5: eDNA sampler's PCB v3.....	46
Figure 4.6: Piston pump's electrical connections	54
Figure 4.7: Piston pump's quadrature encoder signal.....	55
Figure 4.8: Piston pump's home signal	56
Figure 4.9. Power vs Time for spike and hold system	56
Figure 4.10. Wheatstone bridge model of the pressure sensor used in the fluidic circuit.	58
Figure 5.1: eDNA sampler's automation protocol overview	65
Figure 5.2: eDNA sampler's process threads	66

Figure 5.3: System interrupts.....	68
Figure 5.4: eDNA sampler’s pressure data analysis.....	73
Figure 6.1: Negative pressure test setup.....	77
Figure 6.2: Negative pressure test data.....	79
Figure 6.3: Piston pump’s volumetric and flowrate test benchtop setup.....	81
Figure 6.4: Cross-contamination test benchtop setup.....	83
Figure 6.5: Intensity measurements recorded at 520 nm during the cross-contamination tests	86
Figure 7.1: Benchtop setup of the eDNA sampler.....	87
Figure 7.2: Benchtop eDNA sampler manifold.....	89
Figure 7.3: Fluidic implementation of benchtop food dye flow test.....	91
Figure 7.4: Bar plot of top 20 taxon families.....	95
Figure 7.5: Rarefaction curves for observed ASVs and sequence depths.....	96
Figure 7.6: Standard curve of threshold cycle (Ct) vs Log10 quantity of BB40.....	100
Figure 8.1: Submersible eDNA sampler.....	103
Figure 8.2: Rarefaction curves for all samples.....	108
Figure 8.3: Map of Halifax Harbour sampling locations.....	109
Figure 8.4: Stacked bar plot highlighting the top 10 relatively abundant bacterial taxonomic families.....	112
Figure 8.5: Scatterplots showing raw counts of all ASVs.....	113
Figure 8.6: Upset plot of ASVs in each sample as well as the pre-filter (PF).....	114

Abstract

Environmental DNA (eDNA) analysis facilitates the study of biodiversity in aquatic habitats. eDNA samplers automate the sample collection process required for eDNA analysis, reducing the manual labour needed. This thesis describes the development of a novel eDNA sampler capable of self-cleaning and multisample capture and preservation. The submersible eDNA sampler unit was compared to the traditional Niskin Bottle (manual) approach during a transect in Halifax's Bedford Basin. Both approaches yielded comparable results based on the detected bacterial and phytoplankton Amplicon Sequence Variants (ASVs). The presented eDNA sampler will be a valuable tool for biodiversity surveys in Marine Protected Areas (MPA), wind farm installation, site assessments and coral reef restorations. The eDNA sampler will be a timely technology to aid the fulfillment of the objectives described in the recent Kunming-Montreal Global Biodiversity Framework (GBF). Nearly 200 countries agreed to adopt the GBF at the United Nations Biodiversity Conference, COP15, Montreal, Canada.

List of Abbreviations and Symbols

ADC	Analog-to-Digital Converter
ARM	Advanced RISC Machine
ASV	Amplicon Sequencing Variant
AUV	Autonomous Underwater Vehicle
BBMP	Bedford Basin Monitoring Program
BLE	Bluetooth Low Energy
BPC	BioProcess Containers
CAD	Computer-Aided Design
CCD	Charge Coupled Device
CIIMAR	Interdisciplinary Centre of Marine and Environmental Research (Centro Interdisciplinar de Investigação Marinha e Ambiental)
CLAM	Continuous Low-Level Aquatic Monitoring
CPU	Central Processing Unit
DC	Direct Current
DOT	Dartmouth Ocean Technologies Inc.
eDNA	Environmental DNA
ESP	Environmental Sample Processor
FEP	Fluorinated Ethylene Propylene
FKM	Fluro-Elastomer
Gen	Generation

GPS	Global Positioning System
HAB	Harmful Algae Bloom
HCl	Hydrochloric Acid
IEEE	Institute of Electrical and Electronics Engineers
IMR	Integrated Microbiome Resource
IS-ABS	In-situ Autonomous Biosampler
LR-AUV	Long Range Autonomous Underwater Vehicle
LSB	Least Significant Bit
MA	Massachusetts
MAB	Modular Autonomous Biosampler
MBARI	Monterey Bay Aquarium Research Institute
MEMS	Micro-Electro-Mechanical Systems
MOS	Midwater Oil Sampler
MPA	Marine Protected Area
MQ	Milli-Q
NEMA	National Electrical Manufacturers Association
NOAA	National Oceanic and Atmospheric Administration
OLED	Organic Light-Emitting Diode
PC	Polycarbonate
PEEK	Polyetheretherketone
PES	Polyethersulfone
PF	Pre-filter

PGA	Programmable Gain Amplifier
PMMA	Polymethyl methacrylate
PolyWAG	Poly Water Acquired Genomics
PPS	Phytoplankton Sampler
RAM	Random Access Memory
RFD	Red Food Dye
RISC	Reduced Instruction Set Computer
RNA	Ribonucleic acid
RPM	Revolution per minute
RS-232	Recommended Standard 232
RTC	Real-Time Clock
SAS	Subsurface Automated Sampler
SASe	Subsurface Automated Sampler for eDNA
SD	Secure Digital
SDIO	Secure Digital Input Output
SMD	Surface Mount Device
SPE	Solid Phase Extraction
SPI	Serial Peripheral Interface
SRAM	Static RAM
TZP	Tretragonal Zirconia Polycrystal
UART	Universal Asynchronous Receiver / Transmitter
USA	United States of America

USB Universal Serial Bus
USD United States Dollars
WHOI Woods Hole Oceanographic Institution

Acknowledgements

I would like to thank all my family and friends who supported me throughout the two years of my Masters. I would also like to thank the members of the “Sieben Lab”, as we call it, whom I have gotten to know over the years, as they helped motivate me to complete the project.

This thesis has been a large undertaking with an interdisciplinary project combining electrical engineering and biology elements to do an extraordinary task. I want to thank the entire Dartmouth Oceans Technologies Inc. (DOT) team for their help in designing and testing the submersible eDNA sampler. I would like to thank Dr. Julie LaRoche and Dr. Robert Beiko for their support and recommendations throughout the design and testing of the novel eDNA sampler. I would like to thank Connor Mackie for the data collection and analysis for Chapters 7 and 8.

I thank my current supervisory committee members, Dr. Mae Seto and Dr. Craig Brown, and my past committee member Dr. Jacek Ilow for their support and recommendations.

Lastly, I would like to thank my supervisor, Dr. Vincent Sieben, for his support, mentoring and guidance over the years. I fondly remember our first interaction in 2018, when he joined the Engineering faculty at Dalhousie, got his research lab and hired me as his first research assistant for the lab. We started in an empty lab with no equipment and quickly grew. We eventually built a working nitrite sensor within a matter of months.

Chapter 1 Introduction

Increasing human activity in aquatic environments has led to concerns over anthropogenic effects causing issues such as hypoxia, ocean acidification, and eutrophication caused by increased nutrient loading [1]. These impacts can impede growth of certain organisms such as calcifying marine species, whose shells and skeletons can be affected by acidification [2] and promote the growth of other species including those that cause harmful algal blooms (HABs) which harm fish as well as the human economy [3], [4]. The timescale of these changes and their consequent impacts can range from hours to years, and since each ecosystem is unique, changes can be difficult to track, requiring time-resolved *in situ* observations in order to properly assess changes. The recent adoption of the Kunming-Montreal Global Biodiversity Framework (GBF) aims to address biodiversity loss, restore ecosystems and protect indigenous rights [5]. eDNA metabarcoding enables the monitoring of biodiversity in a target location. By tracking the biodiversity of that target location, the effectiveness of mitigation measures to address biodiversity loss and restore ecosystems can be assessed.

Biological monitoring programs have traditionally focused on manual identification of key taxonomic groups of interest; however, these programs can be time consuming and require special training in taxonomic identification. In recent years, with a decrease in the cost of DNA sequencing and the increasing size of nucleic acid databases, environmental DNA (eDNA) is increasingly being used as a proxy for biodiversity in biological monitoring programs [6]. Monitoring eDNA involves studying all DNA present in the environment [7] and is advantageous in multiple ways as it is non-invasive, and widely applicable to microbiota and metazoans alike

using a rapidly evolving suite of analytical methods from sensitive DNA extraction to detection of unique barcode sequences [8]. There are numerous studies that have demonstrated the value of eDNA to study microbial diversity, given the importance of their role in primary production by phytoplankton and biogeochemical cycling of dead organic matter [9]–[11]. For example, biomonitoring of microbiota in aquaculture settings has demonstrated the usefulness of eDNA to detect the rapid microbial response to environmental disturbance and assess management strategies for a sustainable aquaculture industry [9]–[11]. Furthermore, an increasing number of studies have demonstrated the important role that eDNA is destined to play for environmental monitoring of fish biodiversity [12], tracking of marine mammals [13] and other aspects of conservation biology [14].

While disruptive, the current methods for eDNA sampling are often labour intensive, involving the collection of samples using Niskin bottles or similar equipment, followed by separate filtration and preservation steps, often using a peristaltic pump and freezer respectively. The manual components of eDNA sampling and analysis limit its use in remote settings, or in settings where regular around-the-clock samples must be taken, and require a trained individual to perform the process. Extending the applicability of eDNA methods to more-challenging problems requires automation, including the development of automated sampling equipment. Recently samplers have been an active area of research, ranging from single-filter systems to more-complex multi-filter systems. Each unit has varying parameters: such as deployment duration, maximum depth rating, and chemicals/preservatives used. While great progress has been made, we aim to address a current gap between low-cost samplers that are manual and not suitable for extended deployments in harsh conditions, and, large

multi-million dollar and high-performance systems that are too-expensive to deploy at scale. The novel eDNA sampler described in this thesis targets the mid-cost range of systems influenced by the current market.

1.1 Thesis Description and Scope

This thesis project aims to develop a novel eDNA sampler capable of self-cleaning and multisample capture and preservation. The thesis will explore the design stages of development and unit-level testing leading up to deploying a submersible eDNA sampler in the Bedford Basin. The final deployment was a transect of the Bedford Basin, Halifax, in parallel with the traditional Niskin bottle approach. Ultimately, the project was a success as we showed very similar relative abundances in the detection of bacterial and phytoplankton communities.

In Chapter 2 of the thesis, a literature review of eDNA samplers available commercially and in journal articles is presented. This sets the stage for the novel aspects of the eDNA sampler designed in the thesis. In Chapter 3, the fluidic architecture of the novel eDNA sampler is explored, and its operation is discussed. I collaborated with Edward Luy to design the fluidic architecture. In Chapter 4, the electrical architecture and circuit board design of the eDNA sampler is explained along with the early-stage development and its interface to control the fluidic architecture described in Chapter 3. The electrical architecture and PCB version 1 design were my own work. I collaborated with James Smith to design versions 2 and 3 of the PCB. Chapter 5 details the software architecture that controls the eDNA sampler. The software design, firmware implementation, and associated testing was my own work.

In Chapter 6, testing is detailed. The components of the fluidic architecture described in Chapter 3 are unit-tested to determine the pressure sensor's precision, the pump's accuracy and the system's risk of cross-contamination using food dye. The unit testing was my own work. In Chapter 7, a benchtop model of the eDNA sampler is described and evaluated using samples of water from the Bedford Basin, Halifax, to determine the effectiveness of the eDNA sampler and its collection protocol. During this stage, the eDNA sampler also undergoes cross-contamination testing using the bacterial monoculture BB40. The benchtop setup and testing was my own work, with the exception that the fluidic manifold was manufactured by Colin Sonnichsen. Also, the DNA extraction and analysis was performed by Connor Mackie. In Chapter 8, a custom housing created by Dartmouth Ocean Technologies Inc. allowed for the eDNA sampler to be submersible. Chapter 8 explores a comparison test between the eDNA sampler and the traditional approach. The deployment was a collaborative effort between myself and DOT employees. Finally, Chapter 9 considers the future directions and offers suggestions for improvements of the eDNA sampler.

1.2 Publications and Conferences

The following conference proceedings and manuscripts are produced as a result of this thesis work. The material from these peer-reviewed works is used in this thesis and copyright permission has been attained for representing the results.

1.2.1 Peer-Reviewed Journal Articles

- 1 **Andre Hendricks**, Connor Mackie, Edward Luy, Colin Sonnichsen, Lee Miller, Mark Wright, Iain Grundke, James Smith, Joshua Creelman, Mahtab Tavasoli, Arnold Furlong, Robert G. Beiko, Julie LaRoche and Vincent Sieben. “Compact and Automated eDNA Sampler for in situ Monitoring of Marine Environments,” *Sci Rep*, vol. 13, no. 1, Art. no. 1, Mar. 2023, doi: 10.1038/s41598-023-32310-3.

1.2.2 Conference Proceedings

- 1 **Andre Hendricks**, Connor Mackie, Edward Luy, Colin Sonnichsen, Lee Miller, Mark Wright, Iain Grundke, James Smith, Joshua Creelman, Mahtab Tavasoli, Arnold Furlong, Robert G. Beiko, Julie LaRoche and Vincent Sieben, “A Miniaturized and Automated eDNA Sampler: Application to a Marine Environment,” in OCEANS 2022, Hampton Roads, 2022, pp. 1–10. doi: 10.1109/OCEANS47191.2022.9977218.

1.2.3 Unrelated to the eDNA Sampler Journal Papers Contributions

- 1 Colin Sonnichsen, Dariia Atamanchuk, **Andre Hendricks**, Sean Morgan, James Smith, Iain Grundke, Edward Luy, and Vincent Joseph Sieben. 2023, “An Automated Microfluidic Analyzer for In Situ Monitoring of Total Alkalinity,” *ACS Sens.*, vol. 8, no. 1, pp. 344–352, Jan. 2023, doi: 10.1021/acssensors.2c02343.
- 2 Sean C. Morgan, **Andre D. Hendricks**, Mae L. Seto, and Vincent J. Sieben, “A Magnetically Tunable Check Valve Applied to a Lab-on-Chip Nitrite Sensor,” *Sensors*, vol. 19, no. 21, p. 4619, Oct. 2019, doi: 10.3390/s19214619.

Chapter 2 Literature Review

This chapter will focus on the various eDNA samplers developed in the last 20 years. These eDNA samplers range from handheld single-filter systems, capable of a single sample capture per deployment, to multi-filter autonomous systems capable of hundreds of discrete samples captures per deployment.

2.1 Smith-Root eDNA sampler

Figure 2.1 illustrates the Smith-Root eDNA sampler designed by Smith-Root (Washington, USA) and first published in 2018 [15]. As of 2023, Smith-Root sells this sampler at a base price of 7,695 USD [16]. This eDNA sampler is a single-filter handheld sampler containing the electronics in a back-pack-style system, Figure 2.1 - 1. This allows the user to carry the system during deployments easily. The eDNA sampler weighs 10.89 kg without the battery pack installed. The sampler's screen interface, Figure 2.1 – 2, allows the user to program deployment parameters such as target volume and limits for pressure and speed.

The sampler features a simple fluidic system that pulls fluid samples across a 47 mm filter membrane for sample capture using a diaphragm pump. This pulling action, paired with a replaceable inlet tube and filter holder, reduces cross-contamination between sampling events. Figure 2.1 – 4 illustrates the inlet tube and filter holder. However, the single filter means that the user will be required to constantly replace the filter membrane and the sample inlet tube for each deployment location. Additionally, due to the backpack design and 3.6 m pole with a telescoping bipod, the user is limited to sampling close to the surface of the water and in areas

that the user can easily access, Figure 2.1 - 6. Additionally, the user is required to set up a tripod to position the sampler for sample capture.



Figure 2.1: Smith Root eDNA sampler performing sample capture and filter storage immediately after capture. Reprint from [15].

During deployments, the sampler is capable of logging volume sampled data and data from its pressure and GPS sensor. This use of the GPS sensors is advantageous to determine the location of sample capture. The sampler uses 11.1Ah 12.8V power supply is attached to the backpack to power the system that is capable of lasting 6 to 8 hours [15]. With the pump having

a minimum and maximum flowrate of 0.1 L/min and 1.4 L/min respectively with an error of ± 10 % [15].

There have been two recent studies using the Smith-Root eDNA sampler by Pope et al. (2020) and Nolan et al. (2023). In a published study by Pope et al. (2020) [17], the Smith-Root eDNA sampler was used to detect two native amphibians (*Rana sierrae* and *R. cascadae*). These amphibian species are at risk due to population decline caused by disease, habitat alteration and invasive species. The sample collection was performed at 15 meadows in the Sierra Nevada and southern Cascade ranges in California, USA for 65 sample locations. The eDNA analysis was performed alongside visual identification, in which eDNA analysis could match visual results at all sampling locations except for one where the amphibian was seen outside of the sampling area [17].

The eDNA sampler could collect 0.2 to 2.2 L per filter with less than 10 minutes of sampling time. The team found that combining the eDNA analysis with visual methods was ideal for better sample capture. The sample used two filters at the end of the pole to create a duplicate sample collection 25 cm apart. The test also used ethanol preservatives and self-desiccating filters for sample preservation. Multiple samples were collected at each location to increase the chance of detecting DNA related to the frogs. The sampling depth of the sampler was measured at 5 - 10 cm per location [17].

In a separate published study by Nolan et al. (2023) [18], the Smith-Root eDNA sampler was used to detect the brook trout fish species in a conservation effort due to its low population. Samples were collected in southwestern Ontario, Canada. Samples were collected

in Hanlon Creek and Twelve Mile Creek, Ontario. Data was collected and compared during the study between the eDNA analysis and electrofishing techniques. The data from the study showed that the Smith-Root eDNA sampler was collecting Brook trout eDNA throughout Halon Creek and the two main branches of Twelve Mile Creek. Additionally, the Smith-Root could detect eDNA data in locations that had not been detected before using previous methods. The study used 5 µm mixed cellulose ester (MCE) filters [18].

The study highlighted an issue with the Smith-Root eDNA sampler pulling sediment onto the filter membrane due to its lack of a prefilter. The sediment collection onto the filter membrane caused the eDNA sampler to clog quickly. However, it was also assumed that the sediment contained a high concentration of brook trout eDNA [18].

2.2 Continuous Low-Level Aquatic Monitoring (CLAM)

Aqualytical designed the Continuous Low-Level Aquatic Monitoring (CLAM) system in 2014. The CLAM weighs less than one pound and has a spherical shape with a 5 inch diameter [19]. It features a single 47 mm SPE Disk filter and is deployable to 6.1 m [20]. The CLAM has a low flow rate of 5 to 60 mL/min [19], allowing it to utilize the single filter over several hours to capture eDNA. The CLAM can last 36 hours on a single charge, thus allowing it to filter up to 100 L of water during a single deployment [21]. The CLAM has a volume accuracy of $\pm 1\%$ with a rechargeable lithium battery [19]. The user interfaces with it using buttons to stop and start the sampling process, and a screen on the CLAM displays volumes captured when sampling stops.

The CLAM's small design and easy user interface give it an advantage over more advanced eDNA samplers. The user only needs to load the CLAM with the filter for eDNA

collection, press the start button and deploy it into a body of water. Unfortunately, the downside of this design is that only a single sample capture is available during deployments, meaning that the user needs several CLAM devices for multisample deployments. Additionally, preservatives could prevent sample material from being lost during long-term deployments. However, the CLAM does not utilize it. Although the button creates a simple interface, it limits the user from performing advanced actions such as programming a sampling schedule.

As of 2023, the CLAM advertises eDNA functionality on its website, however, there has yet to be a publication that was found to demonstrate the effectiveness of using the CLAM for eDNA sample capture. All currently available publications of the CLAM demonstrate its effectiveness as a tool in contamination studies in aquatic environments.

2.3 Subsurface Automated Sampler for eDNA (SASe)

Figure 2.2 illustrates the Subsurface Automated Sampler for eDNA (SASe) developed by the National Oceanic and Atmospheric Administration (NOAA) in 2021 as an open-source eDNA sampler [22]. This sampler is a single-filter system capable of sample preservation and is submersible up to 55 m [22]. The SASe is small, 11 cm wide x 15 cm long and costs approximately 280 USD to build [22]. The small size and low cost allow for the deployment of numerous samplers simultaneously to improve the spatial resolution of the eDNA collected.

The SASe was first introduced and tested in a 2021 publication by Formel et al. (2021) [22]. Within the journal paper, the SASe underwent two tests using biological samples. The objective of the test was to compare the DNA yield between the manual sampling method and SASe in a lab environment. Both trials involved filtering seawater samples, in which the first test

had the sample spiked with an *Enterococcus faecalis* positive control, while in the second test, the sample remained unaltered. The spiking ensures a higher concentration of DNA in the sample. Three SASe units were used to take nine samples of 1 L of fluid per filter during sampling. The SASe added the preservatives immediately after sample capture. The manual method used a peristaltic pump to individually filter 1 L of samples through five sterivex filter cartridges. After which, the preservative was manually applied to each immediately. The sterivex filter was opened using a PVC pipe cutter to extract the filter membrane. The results of both tests demonstrated a similar relative DNA yield between the manual peristaltic pump method and the SASe.

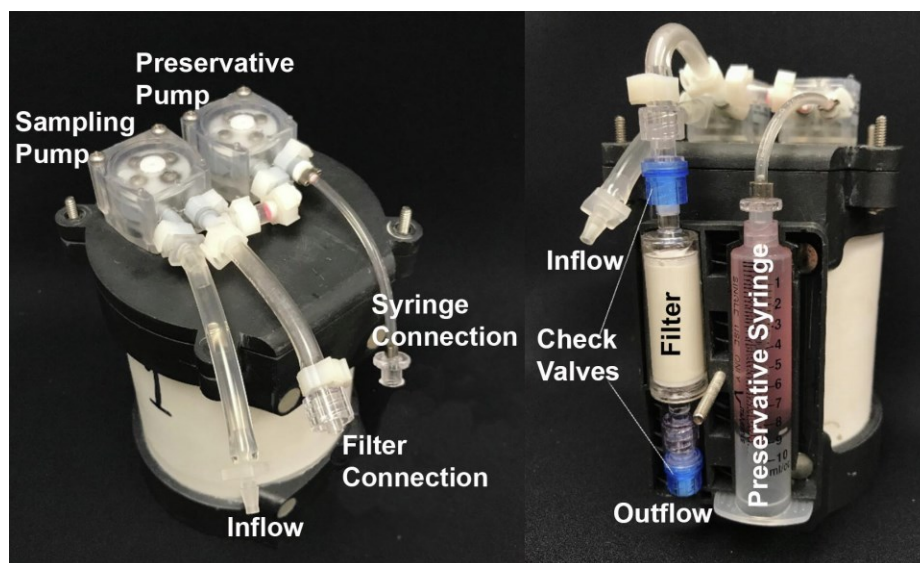


Figure 2.2: Subsurface Automated Sampler for eDNA (SASe) photographs. Reprinted from [22].

The paper also explored the hardware design of the SASe. The system features two peristaltic pumps for sample capture and preservation, respectively, to avoid cross-contamination. Each pump has a volume and flow rate error of $\pm 3\%$ [22]. However, no flow meter is included in the system to verify volumes collected based on membrane loading during

the deployment. The sterivex filter is bordered by check valves on either end to prevent cross-contamination from fluid backflow [22].

A luer lock connects the stervix filter and preservative to the system fluidically, thus allowing for quick swapping after deployments. The luer lock offers a great solution to swap the used components with new ones quickly. A remote control can control the sampler to set the target sample volume and a sampling schedule (date and time) through an OLED screen [22]. The remote control offers an excellent user interface for the user to sync multiple samplers in various locations to perform sampling simultaneously.

The advantage of the SASe is its low cost, allowing multiple systems to be deployed simultaneously for a large spatial resolution. The sample schedule feature allows the samplers to be synced to collect simultaneously. This sample schedule also allows samples to be programmed for any time of the day, which would typically be difficult for a researcher to sample manually. The disadvantage to using multiple SASe units is that each will need to be tracked for retrieval and separately prepped for sampling because each unit can perform a single capture event.

2.4 Phytoplankton Sampler (PPS)

Figure 2.3 illustrates the Phytoplankton sampler (PPS) sold by McLane Labs. The sampler has 24 filters (47 mm), allowing longer deployment periods. The system weighs 60.5 kg and 43 cm x 43 cm x 165 cm (H x W x L) [23]. It is deployable to 5,500 m with a deployment period of 14 months. The system features a gear pump with a 5% flowrate error and a flowrate of 50 – 125 ml/min [23].

However, the downside of the PPS is its size, weight and non-compact design. These factors limit the PPS to be a standalone system that can not easily be attached to an underwater vehicle or deployed by a single person. Further, kinked tubing is a frequently reported experience from our collaborator's (Dr. Julie LaRoche) laboratory in the Department of Biology. Priming of this instrument is also challenging.

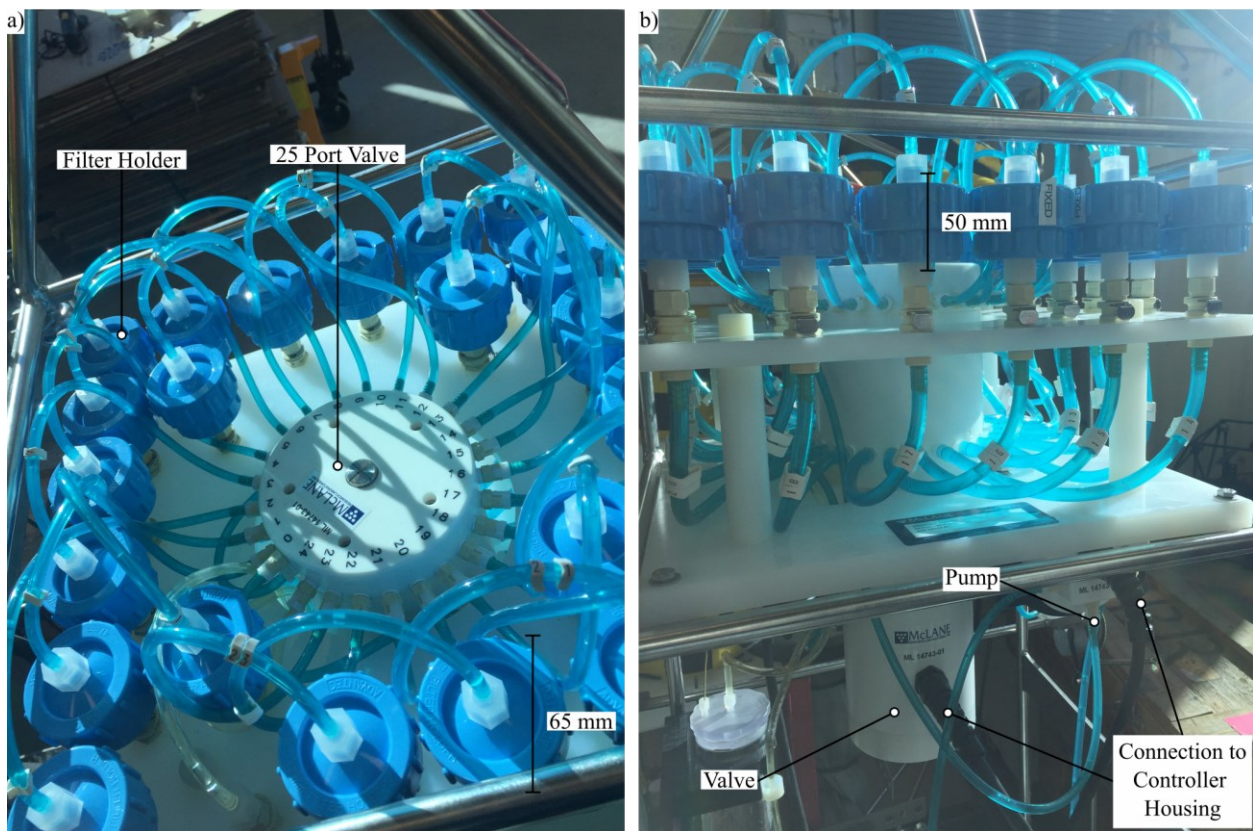


Figure 2.3: Phytoplankton Sampler a) Top view showing fluidic valve, ports, and filter holders b) Side view showing valve, pump, filter holders, fluidic ports and connection to controller housing.

The PPS system has been used in several studies; two are described below. In a published study by McGillicuddy et al. (2014) [24], the PPS was used to monitor a Harmful Algae Bloom (HAB) of *Alexandrium fundyense*. During deployment, the sampler was left in the water

at a depth of 5 m for a sampling frequency of 2-3 days, with the system programmed to capture 2 L of fluid onto a 15 µm Nitex screen. Through the regular sampling event of the PPS, the bloom could be recorded as the cells/L varied throughout the sampling period. However, it was also reported that due to the depth of the PPS, its cell counts reported by the PPS were much lower than samples that were taken closer to the water surface during the spike of the cells/L [24]. The study demonstrated vital features of an eDNA sampler, including long-term deployments, and that power management and preservatives are key considerations.

In another study published by Winslow et al. (2014) [25], the PPS was deployed with several other sensors in the Dry Valley Lakes of Antarctica. The paper's objective was to outline how the sensors were deployed. During the year-long deployment, the PPS was scheduled to sample every 18 days except for three overlapping sample events for replicate sample verification. For the preservation of samples, the system used custom filter housing pre-filled with a DNA preservative solution. After sample capture, the fluid would fill the filter cartridge and preserve the sample. One downside of this was that during long-term deployment, there is a risk of the DNA preservative seeping out of the filter cartridge. Thus, the authors explored the use of an environmentally safe sucrose lysis buffer (SLB) preservative. However, the filter housing was designed to use a preservative less dense than water. The SLB preservative used was denser than water so to accommodate the change, the PPS was deployed upside down.

These studies demonstrate the impressive effectiveness of the PPS in performing long-term deployments due to its ability to collect multiple fluid samples and preserve them over a long period.

2.5 Modular Autonomous Biosampler (MAB)

Figure 2.4 illustrates the Modular Autonomous Biosampler, MAB, developed by Cellula Robotics Ltd. and first published in 2012 [26]. In the publication, the technical specification of the MAB is described; however, no testing was performed. The MAB is a multifilter sampler with sample preservation and self-cleaning features. The sampler weighs 35 kg, is 229 x 1615 mm, and holds up to 200 filters per deployment [26].

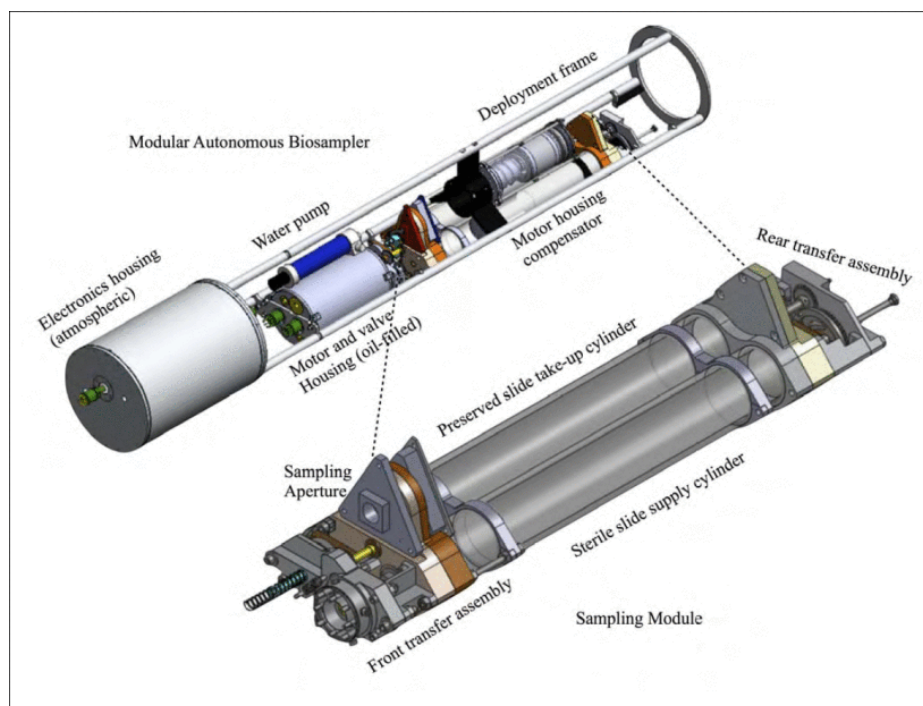


Figure 2.4: Modular Autonomous Biosampler CAD rendering showing exposed internals of the MAB. Copyright © 2012, IEEE. Reprint from [26].

The MAB allows triggering using an RS232 communication channel or 5 V rising edge trigger. The filters used in the sample are the standard 47 mm filter membranes housed in a custom filter slide assembly sandwiched between polycarbonate slide covers to avoid cross-contamination during sample storage. During sampling, filter slides are transferred to the

sampling position from the sterile slide supply cylinder and then to the preserved slide take-up cylinder after sample capture and preservation.

The advantages of the MAB include its large filter capacity and multisample capture and preservation with self-cleaning between sampling events. However, the complex front transfer assembly will likely make the sampler susceptible to mechanical failure. Additionally, its large filter capacity stacked means the sampler must be retrieved by carefully retrieving samples and refilling after deployment. The length of the sampler also makes it difficult to handle by a single individual and requires a team to set up and deploy. Finally, a published paper has yet to demonstrate the system's performance for sample capture with appropriate biological assay comparisons.

2.6 Environmental Sample Processor (ESP) Gen 3

The Environmental Sample Processor (ESP) Gen 3 was developed by the Monterey Bay Aquarium Research Institute (MBARI, California, USA) team in 2015. The sampler is a multifilter sampler capable of multisample capture and preservation with self-cleaning between sample capture events. The ESP Gen 3 was built as an attachment to MBARI's Long Range Autonomous Underwater Vehicle (LR-AUV). The system holds 60 sample collection and processing cartridges [27].

Each sample cartridge is isolated and handles the chemicals required for sample preservation and storage, and waste capture. The compartmentalized packages, allow for fluid isolation between samples and a reduced risk of cross-contamination. However, the downsides of the ESP Gen 3 is the reliance on the AUV shown in Figure 2.5-E, as the sampler is design to be

attached to that specific UAV. Additionally, reliance on separate filter cartridges each holding their own chemicals makes deployment preparation time consuming as chemicals are added to each of the 60 filter cartridges. The cartridges are also custom design therefore creating a dependence on the available cartridges since they are not an off-the-shelf component. Each membrane filter change requires a face plate to be removed with 4 screws (240 for all 60 filters), and therefore, constrains loading/reloading activities to a sterile laboratory/container environment.

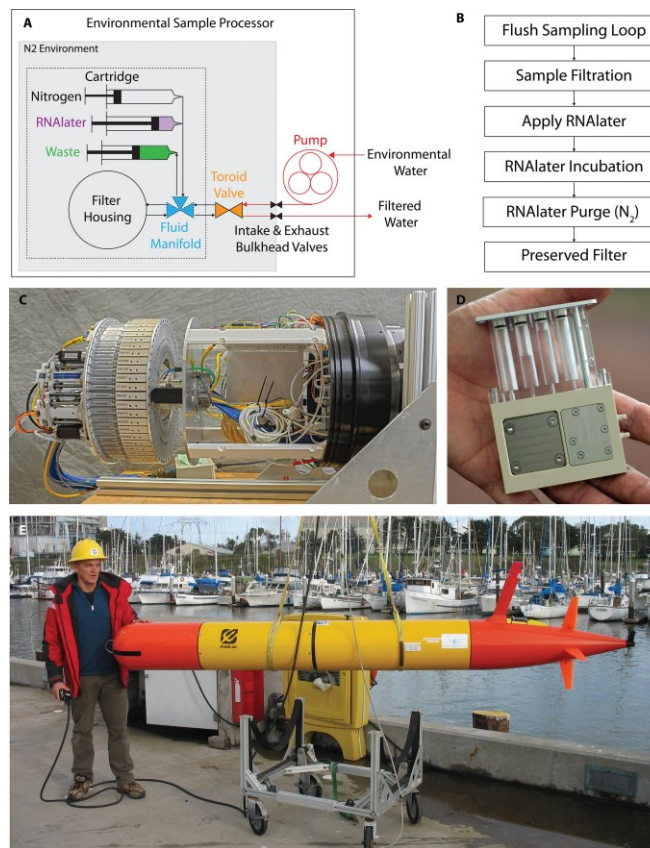


Figure 2.5: Environmental Sample Processor a) Fluidic schematic showing capture on a single filter cartridge b) Sampling protocol c) Exposed internals of the sampler d) Filter cartridge e) Sampler internally attached to a Long Range Autonomous Underwater Vehicle (LR-AUV). Reprint from [27].

In a published study by Yamahara et al. (2019) [27], the ESP Gen 3 was mounted on a LR-AUV to detect several organisms which ranged from microbes, phytoplankton and

invertebrates to vertebrates in the Monterey Bay. The study involved a direct and indirect comparison between the ESP and manual sampling. The direct comparison utilized the benchtop ESP unit while the indirect utilized a peristaltic pump, benchtop ESP and ESP LR-AUV. The study allowed for the eDNA data from the ESP Gen 3 to be logged alongside chlorophyll, temperature, salinity and depth data from the LR-AUV unit. The ESP was capable of filtering 639 to 954 mL within a 58 minute period. The results of the ESP sampling in both direct and indirect cases showed comparable results to the manual approach. The negative controls of the study provided no amplification during the qPCR process, however, SAR11 was amplified.

This study demonstrated the advantage of the ESP being paired with a LR-AUV to get additional sensor data alongside eDNA findings. This could allow for correlations to be made about the eDNA samples and the conditions where the samples were collected. The ESP is one of the most advanced eDNA sampling instruments in the world and is broadly considered to be the pioneering efforts exploring underwater genomic instrumentation.

2.7 In-Situ Autonomous Biosampler (IS-ABS)

The IS-ABS is a 16-filter eDNA sampler capable of multi-sample capture, preservation, and self-clean. The eDNA sampler was developed by the CIIMAR team in Portugal and first published in 2019 [28]. The system is compact and small in size with a diameter of 150 mm and length of 500 mm with a depth rating of 150 m [28].

In the initial published study by Ribeiro et al. (2016) [28], the sampler was compared to the Ocean Sampling Day (OSD) filtration standard procedure using water samples collected 25 km off-shore NW Portuguese coast. The samples were collected in two 20 L carboys and

returned to the lab for the study. The study results showed a similar biodiversity reading in the plankton microbiome diversity at the prokaryotic and eukaryotic levels in the sample fluid for both methods.

The study demonstrated the ease of use for the eDNA sampler in which the system was fully packed and ready to be used with Sterivex-GP filters. The system was sterilized before use and did not require sterilization between samples in addition to automatically applying preservatives to the capture samples. However, the OSD filtration approach required manual cleaning between samples and for the preservative to be manually applied.

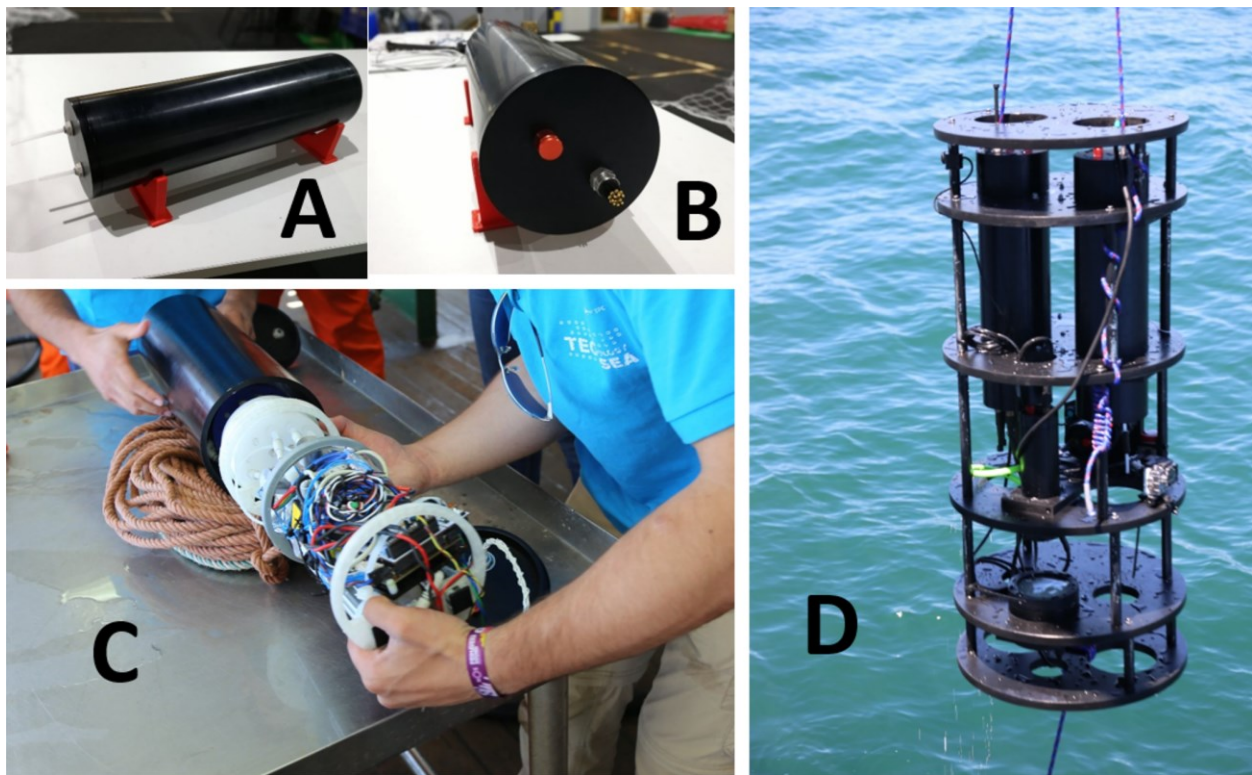


Figure 2.6: In-situ Autonomous Biosampler (IS-ABS) a) Side view showing fluid inlet and outlet ports b) Front view showing external connector interface c) Internal electronics and fluidic system d) Field deployment on a sensor platform. Reprint from [28].

The advantage of the IS-ABS system is its small size, allowing it to be used in areas other than research vessels, such as coastal lakes and riverine. The disadvantage of the IS-ABS design

is that the filter cartridge is not easily accessible. To swap the filter cartridges, the IS-ABS is required to be opened, which is tedious and can damage the instrumentation innards (tubing, wiring, electronics) as shown in Figure 2.6 – C.

2.8 PolyWAG (Water Acquired Genomics)

The polyWAG is a 24-filter sampler developed by a research team at Oregon State University, USA, in 2019 [29]. The polyWAG is openly published on GitHub and costs approximately 6,000 USD to build [30]. The sampler provides a web application user interface to allow the user to schedule deployments, get real-time updates from the sampler and retrieve logs deployment data such as time, pressure and filtered volume. In 2022, the sampler was stated to have used a 47 mm filter holder and could sample 100 – 150 mL of water with an accuracy of $\pm 10\%$ [30].

As of 2023, there have yet to be any papers published on polyWAG demonstrating its sampling performance. However, abstracts and a poster track technical and cost developments of the system [29]–[31].

2.9 Large Volume eDNA Sampler

Figure 2.7 illustrates the large volume sampler designed by Woods Hole Oceanographic Institution (WHOI). The Large Volume eDNA sampler was first published in a journal paper in 2022 [32]. This multifilter sampler can collect up to 12 samples per deployment. The eDNA sampler is deployable to 6000 m and features RS-232 communication for collecting data logs and determining the status of the pumps. The system used a flowmeter on a shared outlet channel to determine the fluid flow volume. Figure 2.7 B. illustrates 2 MOS arrays combined. The Large Volume eDNA sampler is designed to be attached to the Mesobot AUV.

In the initial published study of the Large Volume eDNA sampler by Govindarajan et al. (2022) [32], the system was used to detect the biodiversity of invertebrate taxa in depth ranging from 20 to 400 m in the Flower Garden Banks National Marine Sanctuary. The Sanctuary is a Marine Protected Area (MPA) located in the northwestern Gulf of Mexico. The study compared the Niskin bottle approach to the Large Volume eDNA sampler for sample capture. The study found that samples from the Large Volume eDNA sampler detected approximately 66% more taxa than the Niskin bottle approach. Additionally, the study found that the metazoans eDNA signal decreased with sampling depth compared to the rest of the eDNA signal. During deployment the Large Volume eDNA sampler filtered ~40 – 60 L per filter while the Niskin captured ~2 L of volume. Both capture methods were equipped onto a Mesobot AUV that allowed for sample capture at a set depth. The filter capture process took less than 30 minutes per filter and each deployment lasted less than 4 hours.

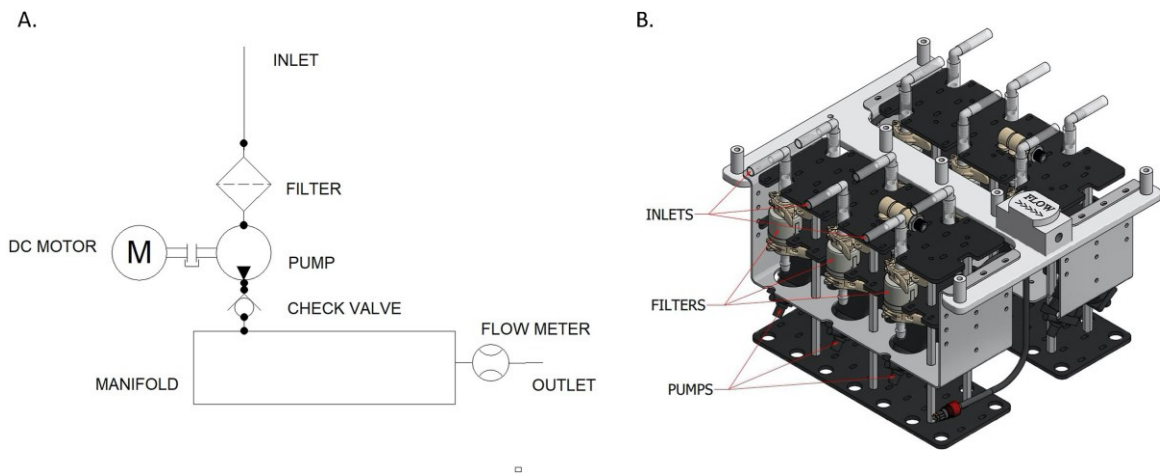


Figure 2.7: Large Volume eDNA sampler a) Fluidic schematic of a single channel of the large volume eDNA sampler b) Rendering of the Large Volume eDNA sampler with 2 MOS arrays of 6 filters each. Reprint from [32].

The Large Volume eDNA sampler was thoroughly cleaned before deployment [32]. Post-deployment, the system was collected, and the samples were immediately preserved due to

the lack of onboard preservatives on the sampler. This lack of preservatives limits the total deployment time capable of the sampler due to filter captured material degrading over time. The eDNA sampler uses a check valve between the filter membrane and sample outlet to minimize cross-contamination and have a separate pump on each inlet channel. However, there is a possible cross-contamination issue between the sampling location due to the lack of isolation between the filter membrane and sample inlet, as shown in Figure 2.7 – A.

The multiple pump design of the Large Volume eDNA sampler offers several advantages, such as ensuring that other channels can still operate if the inlet is blocked. Additionally, the pump array allows for samples to be collected in parallel. As demonstrated in the study by Govindarajan et al. (2022), the fluidic design of the system allows for a large volume to be quickly filtered, thus allowing for a larger biodiversity capture compared of the ambient environment [32].

The disadvantages of this eDNA sampler include its open design, which may lead to snagged cables and algae growth on parts of it. Additionally, the numerous pumps on the system, each with its inlet valves, means that cleaning the fluidic channels can be time-consuming as each channel must be individually connected to the cleaning solution. This time-consuming sampler cleaning can take 1.5 hours for a single person including cleaning the sampler and priming fluidic lines [32].

The study by Govindarajan et al. (2022) demonstrated the need for a depth-rated eDNA sampler to collect eDNA from a range of depths to measure the vertical profile of the aquatic environment concerning the change in biodiversity. The AUV capability allows for the user to

control the sampling locations. In addition to being able to sample large volumes of fluid due to the reduced eDNA concentration with depth. Filtering large volumes increases the chance of detecting the target species.

2.10 Summary Table

The numerous samplers surveyed above have been summarized in Table 2.1 to allow for comparing the various features, advantages, and limitations of each system.

Table 2.1 eDNA samplers in the literature and commercially available.

Year	Instrument	Organisation	Depth	Number of Filters	Filter	Preservation	Self Cleaning	Flow rate (mL/min)
Handheld Sampler (not submersible)								
2018	eDNA Sampler [15]	Smith-Root	Surface	1	47 mm Filter	Y ¹	N ²	100 – 1400
Single Filter Sampler								
2014	Continuous Low-Level Aquatic Monitoring (C.L.A.M) [20]	Aqualytical	6.1 m	1	47 mm SPE Disk	N	N	5 – 60
2021	Subsurface Automated Sampler for eDNA (SASe) [22]	National Oceanic and Atmospheric Administration (NOAA)	55 m	1	Sterivex Filter 0.22 µm	Y	N	
Multi-Filter Sampler								
2008	Phytoplankton Sampler (PPS) [33]	McLane Research Laboratories	5500 m	24	47 mm Filter	Y	Y	50 – 125
2012	Modular Autonomous Biosampler (MAB) [26]	Cellula Robotics Ltd.	200 m	200	47 mm Filter	Y	Y	
2015	Environmental Sample Processor (ESP) Gen 3 [27], [34]	Monterey Bay Aquarium Research Institute (MBARI)	300 m	60	25 mm Durapore Filter 0.22µm	Y	Y	*16
2019	<i>in situ</i> Autonomous Biosampler (IS-ABS) [28]	CIIMAR	150 m	16	Sterivex Filter 0.2 µm	Y	Y ³	54
2019	PolyWAG (Water Acquired Genomics) [35]	Oregon State University	-	24	47 mm Filter Disc	Y	Y	80
2022	Large Volume eDNA Sampler [32]	Woods Hole Oceanographic Institution (WHOI)	6000 m	12	Kleenpak capsule filters	N	N	2000
2022	eDNA Sampler	Dartmouth Ocean Technologies Inc. (DOT)	20 m 3000 m ⁴	9	25 mm Filter	Y	Y	4-30

¹ Requires self-preserving filter.

² Sterilized Filter is provided but lacks acid cleaning protocol.

³ Cleaning is performed with in situ water.

⁴ Deep-rated unit is pressure compensated, filled with mineral oil.

*Calculated value from data.

Currently available eDNA samplers and the literature review have allowed us to elucidate desirable features of an eDNA sampler and to find gaps. This led to the development of the novel eDNA sampler described in the following chapters. These include aspects of self-preservation, multi-sample capture, and methods of cross-contamination reduction such as self-cleaning. There remains a need for an eDNA sampler capable of the following:

Table 2.2: Requirements of a novel eDNA sampler.

Requirement	Feature	Description
1	Single Person Carriable	Weighs less than 30 lbs
2	Power Efficient	Less than 10 W peak
3	Multi-Filter Support	Deployments can perform more than 1 sampling event before swapping filter cartridge
4	Submersible	Submersible to 3000 m
5	Preservatives	Capable of preserving filters after capture for more than 3 months
6	Chemical Cleaning	Capable of cleaning channels with chemicals eg. Acid or bleach
7	Sample Scheduling	Capable of scheduling a Date/Time for sample capture
8	Triggering Capability	Can be triggered by external sensor or computer to start sample capture event eg. UAV triggered
9	Easy access to Filters	Filter cartridge can be replaced in under 5 minutes
10	Optimal Flow rate	Capable of collecting 1 L of fluid within 2 hours. 17 - 30 mL/min

Here we introduce a sampler that addresses the shortcomings of previous samplers and will be described in the following Chapters 3, 4, and 5. This sampler will then be characterised in the Chapters 6, 7 and 8 and shown to be an effective contribution to the requirements list in Table 2.1. While the thesis shows early-stage validation of the eDNA sampler, we expect 10's to

100's of these units will be deployed in numerous studies in the coming years that will further solidify necessity for the eDNA sampler designed in this thesis.

Chapter 3 A Novel eDNA Sampler

This chapter focuses on the fluidic architecture of the novel eDNA sampler. The fluidic architecture is a critical component of the eDNA sampler as it enables the capture and preservation of eDNA samples. The fluid routing design determines fluidic connections and pathways. It was designed to provide routing flexibility using a single pump. Figure 3.1 illustrates two modes of fluidic operation of the eDNA sampler: push mode configuration (Figure 3.1 a)) and pull mode configuration (Figure 3.1 b)). Each mode refers to the eDNA sampler's method of collecting eDNA biomass on the filter membranes (M1 to M9). This design allows the eDNA sampler to accomplish requirements 3, 5, 6, 9 and 10 of the novel eDNA sampler in Table 2.2.

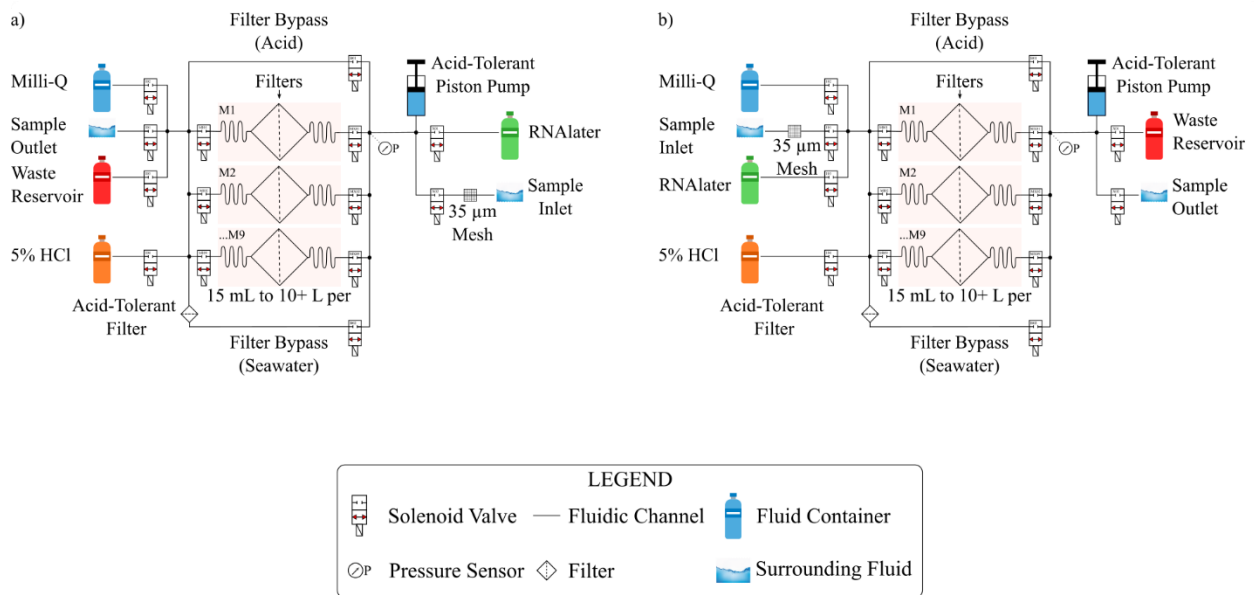


Figure 3.1: eDNA sampler's fluidic architecture. (a) Push configuration (b) Pull configuration.

3.1 Chemicals

The chemicals used by the eDNA sampler illustrated in Figure 3.1 includes 5% Hydrochloric Acid (HCl), RNAlater and purified Milli-Q water. These chemicals are required for each sample capture event to perform self-cleaning on the fluidic channels and to perform sample preservation. HCl is a common disinfectant used in past eDNA work [27], [36]–[38]. Thus, a low concentration of HCl (5%) is used to clean the fluidic channels after sample capture to reduce cross-contamination among distinct sample events.

Purified Milli-Q water is a trademark by Millipore Sigma for a purification system that produces Type 1 water. Type 1 water describes ultrapure water intended for use in highly sensitive procedures. The properties of Type 1 water include a resistivity of 18.2 MΩ·cm at 25 °C and particles less than 0.22 μm. Due to the minimal impurities of Milli-Q water, it is used immediately after HCl cleaning to ensure that HCl does not contaminate the subsequent sample capture and that the fluidic channels remain clean. HCl contamination could destroy DNA that is being captured onto the filter membrane. Milli-Q can also be used as a blank, or negative control if sufficient volumes were loaded.

RNAlater is a commercially sold non-toxic tissue storage reagent comprising high concentrations of quaternary ammonium sulfates and cesium sulfates [39]. It preserves RNA and DNA collected on the filter membranes for several months during long-term deployments by permeating the collected eDNA samples to denature proteases and RNases [39]. Otherwise, the genomic content could degrade rapidly on the filter membranes. RNAlater that passes through the membrane during preservation is collected in the waste reserve due to

environmental concerns regarding its disposal into the ambient environment. The Environmental Sample Processor (ESP) has used RNAlater to preserve samples for up to 21 days [27]. Furthermore, other studies have used RNAlater to preserve DNA for up to 7 years [39].

3.2 Fluidic Architecture Configurations

The eDNA sampler features two modes of fluid operation: pull configuration and push configuration. Each determines the location of the pump in relation to the filter membranes when collecting DNA samples. In the push configuration, during the DNA collection phase, the sample fluid is initially pulled into the piston pump, which then pushes the fluid across the membrane for sample collection. In the pull configuration, during the DNA collection phase, the sample fluid is pulled into the piston pump through the filter membrane channel (M1 to M9) to collect the sample immediately. The fluidic architecture has nine filter membrane channels.

Both configurations of the eDNA sampler utilize a 35 μm inlet filter to prevent large particles from entering the system. The 35 μm inlet filter prevents clogging and ensures that the sampler continues to operate as expected. The particle size limits of the piston pump and solenoid valves determined the size of the inlet filter. Both configurations use the same fluid routing architecture. However, the RNAlater port and waste reservoir port are swapped. The filter bypass (seawater) channel and filter bypass (acid) channel are both used to allow the routing of fluid while bypassing the filter membranes (M1 to M9). The filter bypass (seawater) channel consists of a disposable filter to allow for the filtering of fluid if required, while the filter bypass (acid) channel does not include an inline filter. All the filter membrane channels have comparable fluidic paths.

3.2.1 Push Configuration

Figure 3.1 a) illustrates the push configuration of the eDNA sampler. In this configuration, the piston pump directly connects to the sample inlet and RNAlater. This direct connection allows the piston pump to aspirate either fluid with minimum dead volume before dispensing the fluid through the required filter membrane for either sample capture or preservation. The eDNA sampler generates positive fluidic pressure while dispensing fluid across the filter membrane. This pressure is due to the filter membrane mesh size and the gradual biomass stacking on the filter membrane, which increases the fluidic impedance of the system. The eDNA sampler has a pressure limit of 40 psig; as such, it is crucial to monitor the pressure so as not to exceed the pressure limit. The pressure limit is determined by the fluidic components of the eDNA sampler. The limiting component was the 25 mm filter holder (Advantec 43303010, Polypropylene), that has a maximum pressure threshold of 42 psig. Exceeding the pressure limit risks leaking. Most membrane filters also coincide with this pressure limit and commonly state a maximum transmembrane pressure of 90 psi (~6 bar) to avoid rupturing the thin membranes.

Unfortunately, the push configuration approach introduces the risk of cross-contamination between sample captures. This cross-contamination risk is because fluid samples enter the piston pump before being pushed across the filter membranes for sample capture. The volume chamber of the piston pump thus could see biofouling via microbial growth (and eDNA) from a previous sample capture. Therefore, a vigorous cleaning procedure is crucial to reduce this increased cross-contamination risk.

3.2.2 Pull Configuration

Figure 3.1 b) illustrates the pull configuration of the eDNA sampler. The piston pump directly connects to the sample outlet port and waste reservoir port in this configuration. In contrast to the push configuration, the sample inlet and RNAlater connect to the piston pump through a filter membrane or filter bypass channel in the pull configuration. This minor modification in positioning changes the flow paths and dramatically reduces the risk of cross-contamination since the pump chamber is not shared pre-filter. The reduced cross-contamination risk is due to the fluids being able to pass directly through the filter membranes rather than using the piston pump as a proxy.

The disadvantage of the pull configuration is the negative pressure required to collect DNA samples on the filter membrane. The most significant negative pressure the system can achieve is a vacuum. Therefore, a pressure of approximately -15 psig is achievable for a system relative to atmospheric pressure, or at the surface. This pressure range from 0 to -15 psig is far less than the range of 0 to 40 psig, which is possible in the push configuration. This difference in pressure ranges means that for a similar amount of biomass accumulation, and fluidic impedance, the pressure limit of the pull configuration will be achieved first, leading to less DNA collected for the pull configured compared to the push configuration. Also degassing and bubble nucleation is a substantial problem when pulling vacuum on the surface or shallow waters. However, when the eDNA sampler is deployed in deeper waters this problem goes away due to the hydrostatic pressure applied by the water column. The starting pressure will increase proportional to the depth at a rate of approximately 15 psig per 10 meters, thus increasing the pressure range for the pull configuration. For example, at 20 meters, the pull

configuration should not suffer from bubble nucleation and will have a pressure difference of 45 psig to work with.

3.3 Fluid Mechanics

The Reynolds number is a dimensionless number that correlates the inertial forces of a fluid to its viscous forces. The Reynolds number determines whether a fluid will have a laminar or turbulent flow based on the ratio between these forces. A Reynolds number of less than 2000 indicates that a fluid will have a laminar flow, while a Reynolds number greater than 2000 indicates that the fluid will have a turbulent flow. Laminar flow means fluid flows smoothly with particles travelling in parallel layers. Turbulent flow has eddies that cause the mixing of particles throughout the flow path creating a more chaotic flow. The Reynold's number for this fluidic system can be calculated using the following equation.

$$R_e = \frac{u * d_h}{\nu} \quad (3.1)$$

Where, R_e is the Reynolds number, u is the velocity (m/s), d_h is the hydraulic diameter (m) and ν is the kinematic viscosity (m^2/s). The fluid flow velocity can be calculated using the fluidic flow rate, and the cross-sectional area of the fluidic channels as shown in equation 3.2.

$$\nu = \frac{Q}{A} \quad (3.2)$$

$$A = \pi \times \left(\frac{d_h}{2}\right)^2 \quad (3.3)$$

Using these equations, Reynold's number for the fluidic system of the eDNA sampler can be calculated, assuming that the entire fluidic system of the eDNA sampler can be modelled as a pipe. The minimum diameter in the submersible eDNA sampler's fluidic system is 0.06" (1.52

$\times 10^{-3}$ m), the maximum flow rate during the pump cycle is 60 mL/min (10^{-6} m³/s) and the kinematic viscosity of water at 20 °C is 10^{-6} m²/s.

Using equations 3.2 and 3.3, the fluid velocity can be calculated to be 5.51×10^{-1} m/s. Therefore, Reynold's number can be calculated using equation 3.1 as 837.52, corresponding to a laminar flow within the fluidic system. This analysis can be improved by performing computational fluid dynamics to account for the complex geometry of the fluidic architecture.

Due to the system being in laminar flow, the system can be modelled as an electrical circuit since the relationship between flow rate and pressure drop is linear. This relationship means that the fluidic resistance can be modelled as electrical resistance, fluidic pressure can be modelled as voltage, the flow rate can be modelled as electric currents and compliances within the system can be modelled as capacitance.

The fluidic resistance is caused by the cross-sectional area of the fluidic paths (fluid tubing, solenoid valve, filter membrane and piston pump). As the filter membrane capture particulates, the cross-sectional area available for fluid flow decreases, thus causing an increase in fluidic resistance. This increase can be observed in the pressure measured in the fluidic channel. As the flow rate remains constant with an increasing fluidic resistance, the pressure is expected to increase. Due to the compliance of the fluidic system, which is influenced by the material and components found in the fluidic system, the pressure is expected to slowly dissipate once the flow has stopped to a baseline value.

3.4 Electronic Components

The fluidic architecture features three core electro-fluidic components. This includes a syringe pump, pressure sensor, and several solenoid valves. The eDNA sampler uses these electronic components to select a fluid and control its flow path while ensuring pressure stays in a tolerable region. Chapter 4 covers a detailed analysis of the electrical properties of these components, whereas the following sections detail the mechanical and fluidic properties.

3.4.1 Syringe Pump

Figure 3.2 illustrates the piston pump (LPDA1750330H, Lee Company Ltd.) used within the fluidic architecture of the eDNA sampler. The pump transports the fluid at various speeds throughout the fluidic channels of the eDNA sampler. The pump is a variable volume dispensing pump with a maximum volume of 3000 μL and a precise volume control of 0.1 $\mu\text{L}/\text{step}$ [40]. The pump also has a maximum discharge pressure of 95 psig [40].

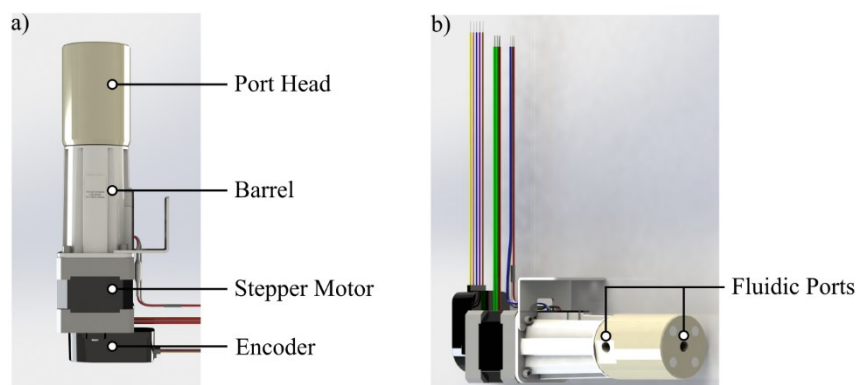


Figure 3.2: eDNA sampler's piston pump CAD rendering (a) Side view of piston pump showing the main sections that make up the unit (b) Isometric view of piston pump showing the fluid ports.

The syringe pump is comprised of several components: the encoder, stepper motor, barrel and port head. The piston pump's encoder and home switch are feedback mechanisms to

determine the position of the piston. The stepper motor is used to move the piston, allowing the system to aspirate or dispense fluid at a controlled speed; the barrel houses the piston. The port head is the wetted section of the syringe pump, thus interacting with the fluid being pumped.

The wetted section of the pump includes the piston, port head and seal. The seal maintains fluidic separation between the port head and barrel. Since the fluids expected to interact with the pump include HCl, a custom pump variant was required. This custom variant used a nickel-based material for the seal's spring that was acid tolerant. The port head and piston are made from polyetheretherketone (PEEK) and tetragonal zirconia polycrystal (TZP), respectively, making them acid tolerant [40]. Although a low acid concentration is used, it is crucial to ensure pump longevity.

The piston pump is connected to the fluidic system of the eDNA sampler by the fluidic ports shown in Figure 3.2 b). The two ports use a ¼ -28 connection. The two ports are internally connected, so external valves are required to control fluid during the aspirate and dispense phase of the piston pump operation.

3.4.2 Solenoid Valves

Figure 3.3 illustrates the solenoid valve (LFNA1250125H, Lee Company Ltd.) used with the fluidic architecture of the eDNA sampler. The solenoid valve directs fluid flow by closing and opening fluidic channels. The solenoid valve is mechanically attached to a manifold using the mounting ports shown in Figure 3.3 b). The solenoid valve is normally closed and is activated to open,

allowing fluid flow. The solenoid valve uses a diaphragm design, thus allowing it near-zero dead volume when closed. However, when open, the dead volume size is 9 μL [41].

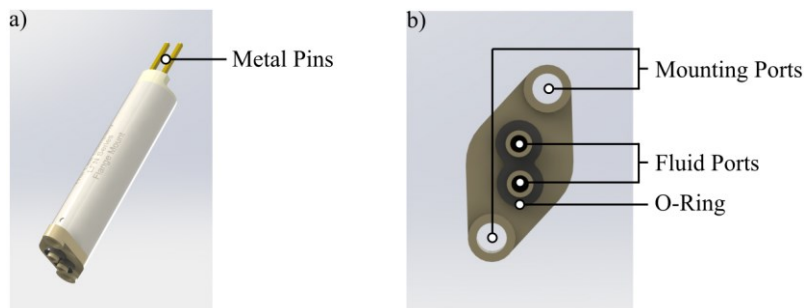


Figure 3.3: eDNA sampler's solenoid valve CAD rendering (a) Side view of the solenoid valves showing the metal pins used to power the solenoid valves, thus opening it (b) Bottom view of the solenoid valves showing the mounting port and O-ring used to create a tight seal with the manifold, in addition to the fluid ports that once opened allows for fluid flow.

The solenoid valves allow for a strong sealing force when the valve is closed. The solenoid valve has an operating pressure of 30 psig, valve proof pressure of 60 psig and a valve burst pressure of 90 psig [40]. The valve-proof pressure is the maximum pressure the system can withstand and still operate within specification. The burst pressure is the maximum pressure the system can withstand before the valves are forced open and are no longer guaranteed to work within specification. The solenoid valves also feature an Fluro-Elastomer (FKM) gasket to provide a seal around the fluidic port to avoid any possible leaks. The pressure ratings of this valve align well with the limits on filter membranes and holders (~40 psig).

The wetted parts of the solenoid valves include the fluidic channel, Figure 3.3 b), and the fluidic seal used to close the channel. The fluidic port and seal are made of PEEK and FKM, respectively. Both materials are resistant to the chemicals used in the eDNA sampler's fluidic architecture. These valves have also been demonstrated in pressure-compensated systems to

operate from 2,100 m to 6,000 m depth [42], and thus are ideal for modifications to realize a deep eDNA sampler at a later date.

Combining the piston pump with the solenoid valves allows for flexibility in sample routing throughout the fluid architecture. Thus, the piston pump can aspirate and dispense from a specified port by opening and closing the relevant solenoid valves and, subsequently, the fluidic channels.

3.4.3 Pressure Sensor

Figure 3.4 illustrates the pressure sensor (26PCFFM6G, Honeywell) used in the fluidic architecture. The pressure sensor is a feedback mechanism to detect changes in the fluidic resistance of the eDNA sampler's fluidic system. This pressure data allows for informed decisions to be made based on the state of the system. These decisions include: switching valves to open/close paths, varying pump speed to have dynamic flowrates, and for safety features to determine when the pump should perform an emergency stop so not to damage internal fluidic components.

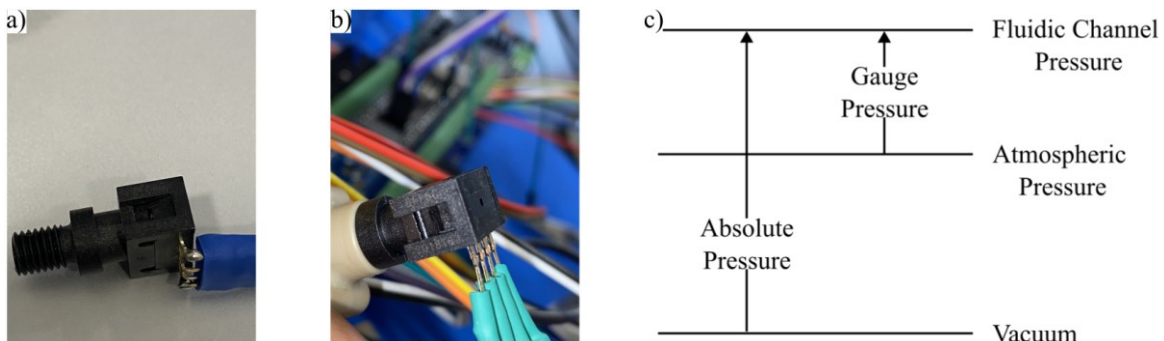


Figure 3.4: eDNA sampler's pressure sensor a) Side view of the pressure sensor showing exposed threading b) Side view of pressure sensor attached to the fluidic circuit by way of the $\frac{1}{4}$ -28 port c) Graph illustrating the difference between gauge pressure and absolute pressure readings.

Figure 3.4 a) is a photograph of the pressure sensor that features a ¼-28 threaded input port that allows for a robust mechanical connection to the fluidic channel and seal. Figure 3.4 b) illustrates the pressure sensor connected to the fluidic channel by threading. This pressure sensor is a 100 psi gauge-style pressure sensor that provides readings relative to the atmospheric pressure that the body of the pressure sensor is exposed to. The backside of the deflecting pressure diaphragm is exposed to ambient through a weeping port, thus making this a relative pressure sensor. This is important for pressure-compensated designs that will see the eDNA sampler filled with mineral oil, in that pressure communication to the external hydrostatic pressure is facilitated.

Figure 3.4 c) illustrates the difference in readings between an absolute pressure sensor and a gauge pressure sensor. The absolute pressure sensor produces a pressure reading relative to a vacuum, while the gauge pressure sensors are relative to the atmospheric pressure the sensor is located. As such, the gauge pressure sensor can produce both positive and negative readings. In Figure 3.4 c), a positive pressure would be measured by the gauge pressure since the fluidic channel pressure is greater than the atmospheric pressure; the inverse would produce a negative pressure reading.

The gauge-style pressure sensor was chosen due to the importance of pressure relative to atmospheric pressure. The fluidic components' max pressure tolerance is based on the atmospheric and internal pressure differential. As such, by using a gauge pressure sensor, thresholds can be established that will be carried throughout the system. The pressure increases as the submersion depth in the ocean increases. Approximately, every 10.1 m down

results in a 14.7 psi pressure increase. Therefore, without pressure compensation, the pressure sensor can detect up to 68.5 m in depth.

With all the core components introduced, the next chapter will detail the electronics used to drive the automation of the novel eDNA sampler.

Chapter 4 Electrical Design

This chapter focuses on the electrical design of the eDNA sampler. The electrical design comprises a printed circuit board (PCB) and the fluidic architecture's electronic components. The PCB includes several components to communicate with the user, store deployment information and interface with the fluidic architecture's electronic components. The fluidic architecture's electronic components comprise a piston pump, pressure sensor and several solenoid valves, which control the eDNA sampler's fluidic system. This design permits the eDNA sampler to accomplish requirements 2, 7 and 8 of the novel eDNA sampler in Table 2.2. The electrical architecture and PCB version 1 design were my own work. I collaborated with James Smith to design versions 2 and 3 of the PCB.

4.1 Electronic Architecture

Figure 4.1 illustrates the finalized electronic architecture of the eDNA sampler. The following sections detail the development of the electronic architecture. The electronic architecture uses off-the-shelf components to control the eDNA sampler. The microcontroller is the central component in the design of the electronic architecture. The microcontroller was selected based on its numerous general-purpose input/output ports, fast 100 MHz core, built-in RTC and connectivity features that included encoder inputs, I2C, SPI, and SDIO. These microcontroller features allowed the electronic architecture to be designed on a single compact PCB with custom firmware without the need for an Operating System (OS). The single PCB design reduces

the failure points of having multiple control modules communicating and the need for communication protocols between these modules.

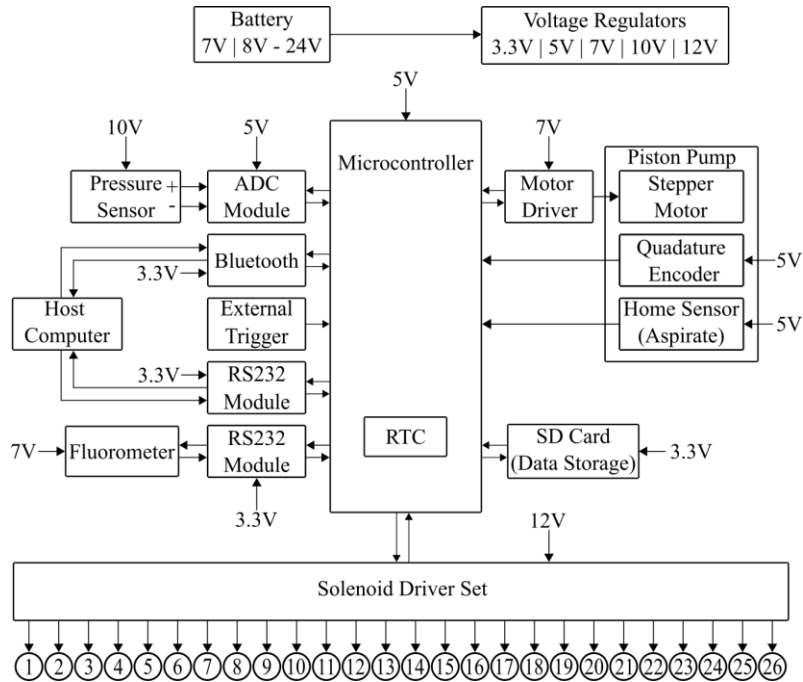


Figure 4.1: eDNA sampler's electronic architecture diagram showing internal electrical connections and components along with interfaces to several peripherals. Modified and reprint from [43].

4.2 Early-Stage Prototyping

Figure 4.2 illustrates the breadboard phase of the eDNA sampler's electronic design and testing. This phase was crucial in determining several viable electronic components required to design the eDNA sampler's final PCB. The breadboard featured several components, including a breadboard power supply module, control buttons, stepper motor driver, Analog-to-Digital Converter (ADC) Module, Advanced RISC Machine (ARM) microcontroller and microSecure Digital (microSD card) module. These components were used to interface with the user, store pressure data and control fluid flow. Thus, allowing for testing several core functionalities required of the eDNA sampler's PCB.

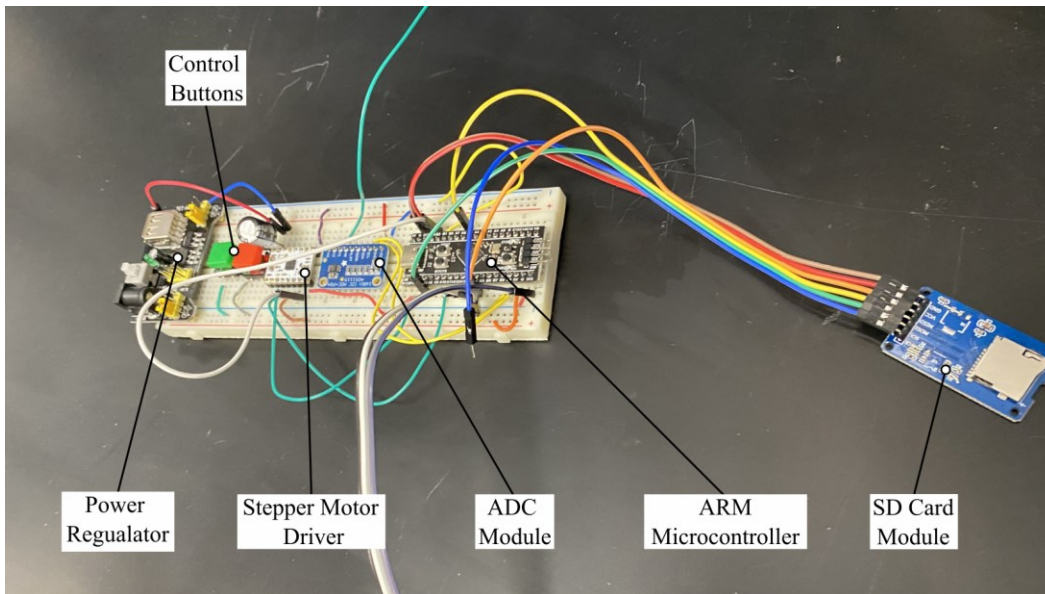


Figure 4.2: eDNA sampler's early electronic prototype used to guide the design of the eDNA sampler's PCB. The breadboard comprises of several components that would later be part of the eDNA sampler's PCB. Additionally, several of the core functionalities of the eDNA PCB was tested on this breadboard.

The fluid flow control was performed using a piston pump controlled using the stepper motor driver and several pins on the microcontroller. The pressure sensor was interfaced with the ADC module, making it possible for the microcontroller to read pressure measurements. Thus, the breadboard system could interface the piston pump and pressure sensor from the fluidic architecture. The microSD card was used to store pressure data during testing while data was transferred to the user.

The communication with the user was accomplished using an external Universal Asynchronous Receiver/Transmitter (UART) to Universal Serial Bus (USB) device. The UART to USB device interfaces the microcontroller directly to the host computer, allowing communication between devices. In early development, the control buttons were used to start (green button) and stop (red button) the piston pump at a pre-programmed speed. However, the firmware was improved to allow these commands to be transmitted over the UART

communication channel. Additionally, a Bluetooth Low Energy (BLE) module was tested for transferring data, thus, allowing the system also to have a wireless means of communication.

The flash memory size requirement increased as the eDNA sampler's firmware became more complex. To meet this requirement, the microcontroller development board used in the breadboard system was changed from the STM32F103 (bluepill) to the STM32F411 (blackpill). This change was decided based on the STM32F411 having a more significant flash memory (512 kB) and a faster CPU core, 100 MHz maximum clock speed. Both microcontrollers are 32-bit ARM devices with the same physical size development board. This allowed for a quick swap during development.

A limitation of the breadboard system was that an external benchtop power supply was required for the piston pump and pressure sensor. This dependence on a benchtop power supply was because the breadboard power supply could only produce 5 V and 3.3 V. However, the pressure sensor and piston pump required 10 V. The PCB design later resolved this issue using several voltage regulators that allowed for several voltages. At this stage, the solenoid valves were not used or tested.

4.3 Circuit Board Designs

A more complete design was required to add valves and integrate more functionality. Using a PCB provides robust electrical connections and mechanical support to its components. Three PCB versions have been designed as more requirements were added throughout the development cycles. The development cycles range from the benchtop eDNA sampler to a fully

submersible 3000 m eDNA sampler. Each version improves upon the previous version's design while keeping the core functionality of the eDNA sampler's PCB.

4.3.1 PCB V1 - Adding Power Regulation and Valves

Figure 4.3 illustrates the eDNA PCB version 1, PCB v1, designed based on the components tested during the breadboard development phase. This PCB design aimed to create a PCB for the benchtop eDNA sampler capable of communicating with the user, storing deployment information and controlling the fluidic system. The PCB v1 used the following components from the breadboard phase: stepper motor driver, ADC Module and ARM microcontroller. The power supply module from the breadboard phase was updated to several DC-to-DC converters to allow a single 7 V input voltage to be converted to meet the voltage requirements of all PCB components and peripherals. The control buttons were completely removed since the firmware was improved to receive commands from the host computer, and the microSD card module was replaced with a microSD card slot on the PCB v1.

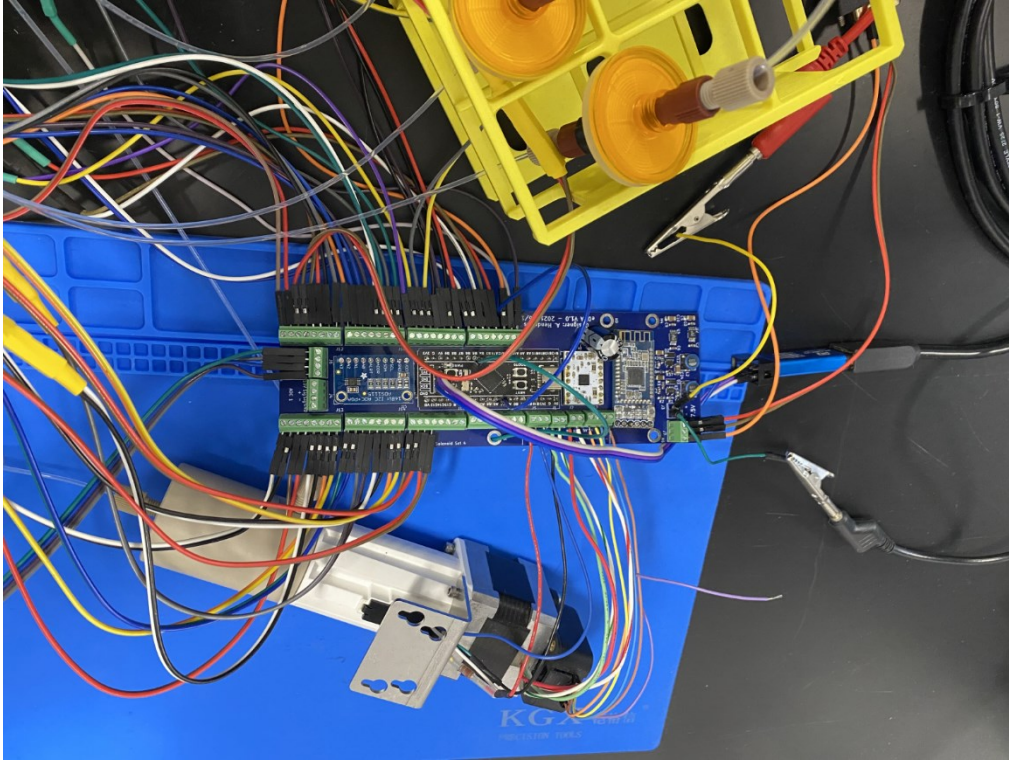


Figure 4.3: eDNA sampler's PCB v1 designed as the first eDNA PCB to be used for benchtop testing of the eDNA sampler.

The following components were added to the eDNA PCBv1: Recommended Standard 232 (RS232) Line Driver/Receiver module, Octal Low side driver and a backup battery slot. The RS232 line driver/receiver module allowed communication over RS232 rather than UART. The octal low-side drivers allowed for interfacing with the fluidic architecture's solenoid valves. The backup battery enabled the microcontroller to keep track of date/time even if the main power had been disrupted. Overall, these components enabled the PCB v1 to interface with all components of the fluidic architecture, communicate with the user and store deployment data.

The PCB v1 also featured several terminal blocks around its perimeter to allow for the connection of peripherals and power. The peripherals include a piston pump, pressure sensor, several solenoid valves and an RS232 communication cable. The power connection provided the main power to the system using a single 7 V input cable.

4.3.2 PCB V2 – Adding Flexibility

Figure 4.4 illustrates PCB version 2, PCB v2, which improved upon PCB v1 in several ways. The same functionality as PCB v1 was maintained with improvements to the mechanical design of the PCB and additional connectors so that a sensor such as a fluorometer could be attached. This PCB version aimed to build a PCB designed for the 20 m submersible eDNA sampler. The improvements include using polyamide to create a flexible section of the PCB to wrap around the solenoid valves in the valve tree on the submersible eDNA sampler. This created a cleaner connection to the solenoid valves compared to the alternative of running 52 lines of electrical wire to the valves. The terminal block connectors were replaced with Molex connectors to ensure more sturdy connections were made with the peripherals. PCB v2 also improved the power input to allow for either a 7 V or an 8 V to 24 V input. Dartmouth Ocean Technologies Electrical Engineers, Merle Pittman and James Smith, designed the improved input voltage circuit used in the eDNA sampler PCB v2 and v3.

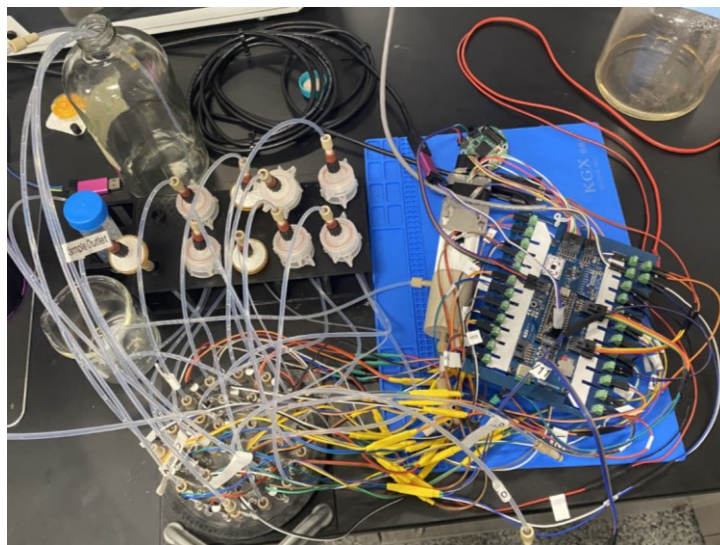


Figure 4.4: eDNA sampler's PCB v2 being testing on the benchtop eDNA sampler. PCB v2 improved on the previous by using a polyamide design to connect to the solenoid valves on the submersible eDNA sampler. Additionally, functionality to attach a fluorometer was added.

4.3.3 PCB V3 – Adding Pressure Tolerance

Figure 4.5 b) illustrates PCB version 3, PCB v3. This version aimed to make a pressure-tolerant PCB capable of being submerged to a depth of 3000 m and improving the positioning of the Molex connectors. This was achieved by making several changes to the design of the PCB. These changes include removing the daughter boards and making the Bluetooth module optional on the PCB. The removed daughter boards were replaced with their Surface Mounted Device (SMD) components and associated support circuitry. The Bluetooth module was made optional due to the module not being pressure tested for the 3000 m depth. The crystal oscillators were replaced with Micro-Electro-Mechanical Systems (MEMS) oscillator (SiT1533, SiTime) and silicon oscillator (LTC6930-5.0, Linear Technologies) for timing, as the original crystals would implode in a pressure compensated system due to cavities in the components.

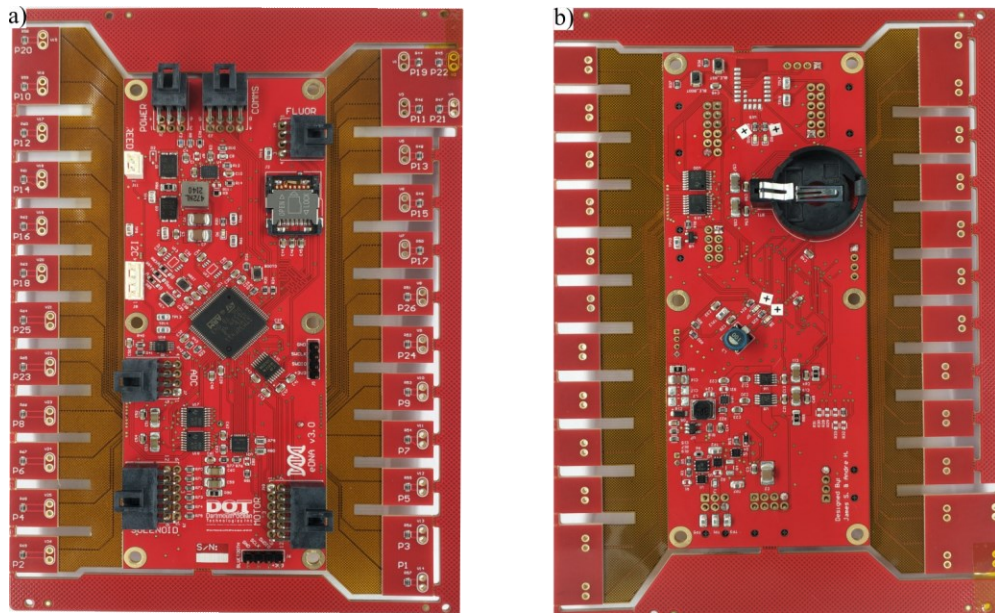


Figure 4.5: eDNA sampler's PCB v3 designed with surface mount components (a) Front View (b) Rear View. Modified and reprint from [43].

4.4 Final PCB Components

This section will explore the components used on the eDNA sampler's PCB and their purpose.

The components used on the PCB are listed below:

- Microcontroller: STM32F411
- Analog to Digital Converter (ADC): ADS1115
- RS-232 Line Driver/ Receiver: MAX3232
- Bluetooth Module: HM-10 (PCB v1), DA1256 (PCB v2), Setebos-I radio module (PCB v3)
- Stepper Motor Driver: DRV8834
- SD card slot
- Octal Low Side Driver: DRV8860
- Battery Holder
- Voltage Regulators:
 - 3.3 V
 - 5 V
 - 7 V: PCB v2 and v3 only
 - 10 V
 - 12 V

4.4.1 Voltage Regulators

The voltage regulators allow a single input voltage to generate multiple voltages ranging from 3.3 to 12 VDC. PCB v1 used an input voltage of 7 VDC. However, PCB v2 and v3 had variable voltage inputs of 7 VDC or 8 VDC to 24 VDC. This improved in PCB v2 and v3 allowed the

submersible eDNA sampler the flexibility to work with multiple different platforms, such as solar-powered buoys and autonomous underwater vehicles (AUV). The voltage requirements for components are as follows:

- 12 V: Solenoid Driver
- 10 V: Pressure Sensor, Stepper Motor Driver (PCB v1)
- 7 V: Stepper Motor Driver (PCB v2 and PCB v3)
- 5 V: ADC module, Bluetooth Module (PCB v1)
- 3.3 V: Bluetooth Module (PCB v2 and PCB v3), RS232 Module, Microcontroller, SD Card Module

4.4.2 Microcontroller Development Board

The microcontroller is the brain of the eDNA sampler. It controls communication with the user, data storage and the fluidic system. This is accomplished using the other PCB components and peripherals that connect to the fluid system. PCB v1 and v2 utilized the development board variant of the microcontroller called the Black Pill (STM32F411CEU6). PCB v3 used the SMD variant of the microcontroller (STM32F411VET6) for required pressure tolerance.

The microcontroller is a 32-bit ARM microcontroller with a maximum clock speed of 100 MHz [44]. The microcontroller variant used has flash storage of 512 kB and 128 KB of SRAM [44], thus allowing for continued firmware improvement. The microcontroller also features several key features [44] used to create additional features on the microcontroller and better interface with the peripherals.

- Real-Time Clock (RTC)

- Backup battery Support
- Hardware Encoder Inputs
- External Interrupts
- SD Card Support

The RTC feature of the microcontroller enabled the creation of a scheduler for the eDNA sampler. The scheduler allows for the sampler to perform its sample capture protocol at a preprogrammed date/time that is set by the user. The external interrupt and hardware encoder inputs allowed for the interfacing of the piston pump's encoder and home signal trigger. The backup battery support allows the RTC to retain the programmed date/time when the power to the eDNA sampler has been disrupted. This achieves requirement 7 of the novel eDNA sampler in Table 2.2. The SD card support allows for the microcontroller to be able to access an SD card for data storage.

4.4.3 Stepper Motor Driver

The stepper motor driver (DRV8834, Texas Instrument) allows the microcontroller to interface with the piston pump. The stepper motor driver controls the piston pump's speed, direction and step size. This translates to the control of fluid flow direction and speed in the eDNA sampler's fluidic system. PCB v1 and v2 used the DRV8834 development board from polulu. PCB v3 used the SMD variant of the stepper motor driver.

The stepper motor driver provided a wide range of input voltages to power the stepper motor. On PCB v1, the stepper motor driver was powered using 10 V from the voltage

regulator. However, due to concerns with power draw requirements, the stepper motor driver was powered with 7 V from the PCB input voltage supply on PCB v2 and v3.

Additionally, the driver provided a max current delivery of 2 A, micro-stepping up to 32 levels [45], sleep mode, directional control and operating temperatures between -40 to 85 °C. The sleep state, direction, step size and steps were controlled by internal logic based on its pin states. The sleep state reduces power consumption when the piston pump is not required to move. A reference voltage value controlled the maximum current. This maximum current on the stepper motor driver was set to 1 A, so as not to damage the piston pump. This current limit helps to achieve requirement 2 of the novel eDNA sampler in Table 2.2.

The step sizes allowed by the stepper motor driver are full-step, 1/2-step, 1/4-step, 1/8-step, 1/16-step and 1/32-step. By reducing the piston pump's step size, the fluid flow becomes smoother. However, there is more power consumed when using microstepping. As such, the eDNA sampler implemented a compromise with a default step size of 1/4-step.

4.4.4 Analog to Digital Converter

The analog-to-digital converter, ADC, interfaces with the pressure sensor in the fluidic system. The ADC allows for an accurate reading and values to be passed to the microcontroller for appropriate measurements. The PCB V1 and V2 utilized a development board. However, PCB V3 featured a surface-mounted device version of the module.

The ADS1115 development module was used as the 16-bit ADC of choice. This module featured an onboard Programmable Gain Amplifier, PGA, required to amplify measured voltage signals. The analog-to-digital converter reads the differential pressure reading from the

pressure sensor. This differential voltage, paired with signal amplification, allows for monitoring precise pressure measures and slight variations in pressure.

This ADS1115's signal amplification and 16-bit resolution were essential due to the microcontroller's built-in 12-bit ADC not having a high enough resolution. The microcontroller's built-in ADC was 12 bits, with a reference voltage of 3.3 V. Thus, the microcontroller's ADC would only produce a step resolution of 0.8 mV, compared to a 15.625 μ V step resolution of the ADS1115 when the PGA is 8x. Section 4.5.3 details the ADS1115 step resolution calculation.

$$R = \frac{V_T}{S_T} = \frac{3.3 V}{2^{12}} = 0.8 mV$$

4.4.5 RS-232 Line Driver/Receiver

The MAX3232 from Texas Instruments was chosen for the RS-232 module. This is an SMD component that was soldered directly to the PCB. This driver chip has two input/output channels and allows for the conversion of UART to RS232.

4.4.6 Octal Low-Side Driver

The Octal Low Side Driver is used to control the solenoid valves required to direct the flow of fluid. Each module of the octal low-side drivers can control eight solenoid valves. Four octal low-side drivers were used to control 26 solenoid valves, allowing for an additional six solenoid valves if required. The DRV8860 38 V 8-Channel Serial Interface Low-Side Driver was the chosen module. It is an SMD component that was directly soldered to the PCB. The driver provides protection and diagnostic features such as Overcurrent Protection, Open Load Detection, Overtemperature Shutdown, Undervoltage Lockout, Individual Channel Status Report and Fault Condition Alarm.

The configurability of the Octal Low-Side drivers included a built-in spike and hold mechanism to be used for opening solenoid valves. This mechanism reduced the power consumption of each solenoid valve from ~900 mW to ~230 mW. Section 4.5.2 further describes the spike and hold mechanism used by the eDNA sampler.

4.4.7 Bluetooth Low Energy Module

The Bluetooth Low Energy Module allows for wireless communication with the eDNA sampler. This wireless means of communication allows for a smartphone or computer to establish a connection. Similar to the RS232 channel, this allows for data transfer and control.

Each iteration of the PCB used a different module to achieve Bluetooth communication. The PCB V1 used the HM-10 module, a popular module in the Arduino community. However, it would be unsuitable when pressure-compensating the unit. The PCB V2 featured the DA1256 Bluetooth module from Dialog; this version is surface mounted. The PCB V3 featured the Setebos-I radio module comprising a Nordic Bluetooth module. This module features an SMD chip shipped with communication firmware and a Bluetooth app to reduce development time.

4.4.8 SD Card Module

The SD Card was attached to the PCB using a microSD card slot. The microcontroller features the built-in protocol, SDIO, required to communicate with the SD card. The SD card allowed substantial amounts of data to be stored long-term between deployments. Data such as pressure measurements, filters used, fluid counts, user configurations, and time-logged filter captures could all be stored on the SD card. So far, a maximum of 32 GB has been tested. Using Bluetooth or RS232 communication channels, data can be retrieved or sent to the sampler.

4.4.9 Backup Battery

The backup battery on the PCB is used to keep track of system time between power cycles. This allows the power supply to be temporarily disconnected, and the system maintains and keeps track of the current time. This is beneficial to several use cases of the eDNA sampler. This included programming the sampler with sample directives and times at a base location.

Afterward, the system can be relocated to the target location for sampling. The system must be powered up at the sample location to perform sampling at the preprogrammed timeslots.

4.5 Interfacing with Fluidic Architecture

One of the primary features of the PCB is to interface with the fluidic architecture's electronic components. This section describes how the PCB was interfaced with the piston pump, pressure sensor and solenoid valves.

4.5.1 Piston Pump

The electrical components of the piston pump (LPDA1750330H, Lee Company Ltd.) comprise a stepper motor, quadrature encoder and home sensor. The stepper motor controls the direction and speed of fluid flow. The quadrature encoder provides feedback on the number of steps and, thus, fluid volume in the piston pump. The home sensor provides feedback on the piston pump getting to its home position, fully aspirated.

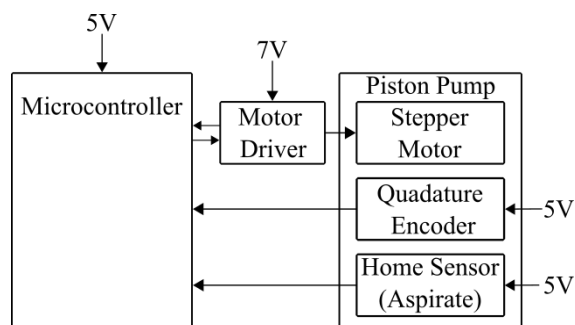


Figure 4.6: Piston pump's electrical connections to the microcontroller on the eDNA PCB. Modified and reprint from [43].

4.5.1.1 Stepper Motor

The piston pump's stepper motor is a NEMA 17 bipolar stepper motor [40]. The stepper motor controls the speed and direction of the piston, which directly correlates to the speed and direction of fluid flow in the eDNA sampler. The microcontroller interfaces with the stepper motor by using a stepper motor driver (DRV8834, Texas Instruments). The driver converts pulses sent by the microcontroller to steps on the pump. Based on the datasheet, the piston pump has a full-step dispense resolution of 1 μL [40]. Therefore, 3000 full steps are required to dispense the piston pump entirely. The NEMA 17 has a full step angle of 1.8° [46]. Therefore, a complete revolution is performed every 200 full steps; 15 revolutions move 3 mL of fluid.

4.5.1.2 Quadrature Encoder

The piston pump's quadrature encoder (E5-200-394-NE-S-D-G-B-S1934, E5 Optical Kit Encoder, US Digital Motion Control Products) directly connects to the microcontroller. This connection is to the encoder timer on the microcontroller. The timer takes the encoder's output signal and uses it to count up or down on the timer count register (encoder register) in the microcontroller's memory address. This counting happens independently of the microcontroller's Central Processing Unit (CPU).

Figure 4.7 illustrates the signals from the encoder. The encoder's output signal consists of channel A and channel B. The channels are out of phase by 90°, and the leading channel can determine the direction the encoder is turning. When channel A is leading channel B, the encoder is moving clockwise. However, when channel B leads channel A, the encoder is moving counterclockwise. The encoder is attached to the piston pump and moves when it does. Therefore, the clockwise motion of the piston pump causes fluid to be dispensed and for the encoder register to count up. In contrast, a counterclockwise motion of the piston pump would cause fluid to be aspirated and the encoder's timer to count down.

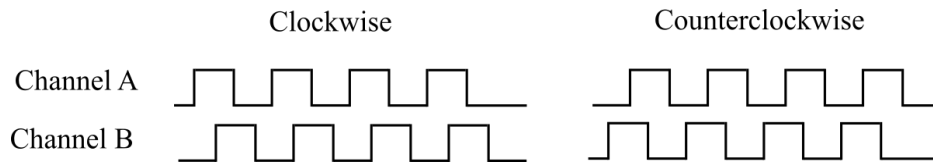


Figure 4.7: Piston pump's quadrature encoder signal for clockwise and counterclockwise directions.

The encoder counts 200 cycles per revolution or 800 pulses per revolution [47], matching the stepper motor's 200 steps per revolution. Therefore, one encoder cycle equals 1 full step by the stepper motor and 1 μL of fluid. The encoder signals are read as pulses, with each encoder cycle containing 4 pulses. Therefore, for each encoder pulse, the microcontroller's encoder timer changes by a magnitude of 1, equivalent to 0.25 μL of fluid. Based on this, the encoder timer must move by a magnitude of 12,000 ticks to move 3000 μL of fluid.

4.5.1.3 Home Sensor

The piston pump's home sensor directly interfaces with the microcontroller. The interface is on an external interrupt pin, which triggers on the rising edge of a pulse such as the one created by the home sensor when the piston entirely dispenses; Figure 4.8.

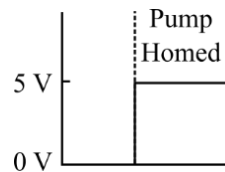


Figure 4.8: Piston pump's home signal showing the voltage transition when the pump is homed.

4.5.2 Solenoid Valve

The solenoid valve used by the fluidic system is in a closed state by default. As such, the solenoid valve must be powered by 12 V to enter an open state. This power delivery is accomplished using the octal low-side driver. However, the issue with the solenoid valves is that it requires 900 mW to open each valve. Depending on the fluidic pathway and period of pumping, the valves might be required to stay open over an extended period. This results in a significant power drain and excess heat each solenoid valve produces. A possible solution to this problem is to implement a spike and hold system using the low-side drivers.

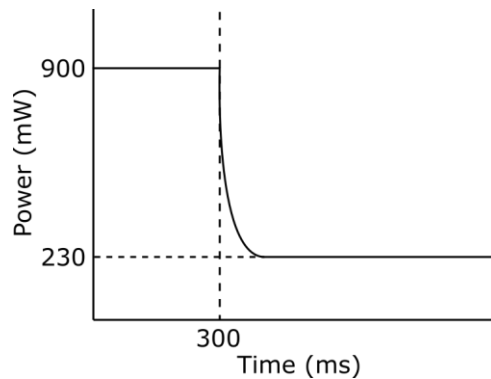


Figure 4.9. Power vs Time for spike and hold system implemented on the solenoid valve.

The solenoid valves are controlled by a spike and hold circuit. This further expands on the usefulness of the solenoid valves. The spike and hold mechanism works by temporarily applying a high voltage across the solenoid valve, after which the current is reduced. This reduction in the current reduces power consumption and heat generation. This is due to the working principle of the solenoid valves; a high current is needed to reduce the maximum air gap. Once the maximum air gap is reduced to the minimum air gap, the current can be reduced, and the valve remains open until power is removed. When there is a maximum air gap, much force is required to move the piston. Thus a more significant amount of current is required. As the air gap decreases and the piston is pulled close to the pole piece, the required force becomes less. Thus the piston can remain in the same position.

The spike and hold system has an energizing time set to 300 ms with a duty cycle of 50 % afterwards. This corresponds to a 300 ms period of the solenoid valves being given full power, after which the voltage applied to the solenoid valve drops to 50 %, which would, in turn, reduce power consumption to approximately 230 mW. When oil-immersed for the pressure-compensated eDNA sampler (deep version), these spike-and-hold parameters will change as oil will be displaced instead of air in the solenoid gaps.

4.5.3 Pressure Sensor

The pressure sensor, 26PCFFM6G, is an analog gauge pressure sensor in the fluidic architecture. The pressure sensor can be modelled as a Wheatstone bridge, as shown in Figure 4.10. The differential voltage between pins 2 and 3 of the Wheatstone bridge corresponds to the changes in pressure. The differential voltage is also 0 V when there is no differential pressure.

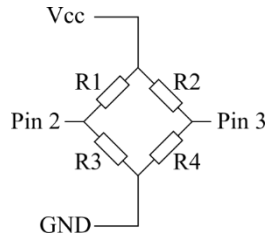


Figure 4.10. Wheatstone bridge model of the pressure sensor used in the fluidic circuit.

The ADC module, ADS 1115, digitalizes the differential voltage so that the microcontroller, STM32F411, can convert the voltage to a pressure reading. The pressure sensor datasheet states a differential voltage span of ± 100 mV that correlates to a gauge pressure span of ± 100 psi, for the nominal voltage of V_{cc} 10 V power. Thus, having a conversion of 1 mV is equal to 1 psi, assuming a linear response.

The differential voltage from the pressure sensor was amplified by 8 to increase its digital resolution. The ADC module's programmable gain amplifier, PGA, accomplished this amplification. This amplification was necessary due to the small voltage range of the pressure sensor's differential voltage. The ADC module's 16-bit resolution corresponded with a Full-Scale Range of ± 512 mV and an LSB resolution of $15.625 \mu\text{V}$ (0.015625 mV). As such, the system could detect changes in pressure up to the resolution of 0.0156 PSI.

4.6 Power Budget Considerations

During deployments with the submersible eDNA sampler, the system will likely be powered using a battery pack. Therefore, it is crucial to know the limitations of the battery pack in terms of the maximum deployment time possible. As such, a series of equations were derived to estimate the maximum deployment time and maximum filterable volume based on the eDNA sampler's electrical characteristics.

To start, equation (4.1) solves for the required battery capacity B_C , based on the eDNA sampler's known idle wattage W_I , peak wattage W_P , hours in idle usage H_I and hours in peak usage H_P . The unit for B_C is Watt-hour (Wh).

$$B_C = (W_I \times H_I) + (W_P \times H_P) \quad (4.1)$$

The total deployment time H_D , is the summation of the hours the system spends idle and at peak, as shown in Equation (4.2). Therefore, idle and peak usage hours are a percentage of the total deployment time, as shown in Equations (4.3) and (4.4). R_I is the percentage of time in idle usage, and R_P is the percentage of time in peak usage. Both R_P and R_I need to summate to 1 (100 %) as shown in equation (4.5).

$$H_D = H_I + H_P \quad (4.2)$$

$$H_I = H_D \times R_I \quad (4.3)$$

$$H_P = H_D \times R_P \quad (4.4)$$

$$R_P + R_I = 1 \quad (4.5)$$

By substituting equations (4.3) and (4.4) into equation (4.1), the dependence of knowing the hours in idle usage and peak usage shift to know the total deployment time and the percentage of time the system will be in idle and peak wattage usage as shown in equation (4.6). From equation (4.6), the total deployment time can be made the subject of the equation, shown in equation (4.7).

$$B_C = H_D((W_I \times R_I) + (W_P \times R_P)) \quad (4.6)$$

$$H_D = \frac{B_C}{(W_I \times R_I) + (W_P \times R_P)} \quad (4.7)$$

Equation (4.8) takes equation (4.4) and makes the percentage of time in peak usage the subject. Equation (4.9) takes equation (4.3) and makes the percentage of time in idle usage the subject in addition to substituting equation (4.2) after making the hours in idle its subject. Thus, the percentage of time spent in either idle or peak are written in terms of the hours spent in peak usage and the total deployment time.

$$R_P = \frac{H_P}{H_D} \quad (4.8)$$

$$R_I = \frac{H_D - H_P}{H_D} \quad (4.9)$$

By substituting equations (4.8) and (4.9) into equation (4.7), the total deployment time can be expressed in terms of the battery capacity, idle wattage, peak wattage and hours in peak usage as shown in equation (4.10). Equation (4.10) can be further simplified, as shown in equation (4.11).

$$H_D = \frac{B_C}{\left(W_I \times \frac{H_D - H_P}{H_D}\right) + \left(W_P \times \frac{H_P}{H_D}\right)} \quad (4.10)$$

$$H_D = H_P - \frac{W_P H_P}{W_I} + \frac{B_C}{W_I} \quad (4.11)$$

When using equation (4.11) to estimate the total deployment time, there is a maximum for hours in peak usage $H_{P,MAX}$, based on the battery capacity and peak wattage, as shown in equation (4.12).

$$H_{P,MAX} = \frac{B_C}{W_P} \quad (4.12)$$

Equation (4.13) solves for the total volume of fluid pumped during a deployment. V_T is the total volume pumped in Litres, and F_A is the average flow rate in ml/min. The 0.06 coefficient is used for unit conversion.

$$V_T = 0.06F_A \times H_P \quad (4.13)$$

Equation (4.14) solves the number of filter captures possible based on the total volume pumped by the eDNA sampler. Where V_C is the average volume captured per filter and V_R is the average volume of reagent/chemicals used per filter capture. All volumes are in terms of Litres.

$$N_F = \frac{V_T}{V_C + V_R} \quad (4.14)$$

The equations derived above can be used to determine the maximum volume and number of filters based solely on the power consumption and battery pack capacity for the eDNA sampler, as described in Chapter 8's eDNA sampler deployment. For the deployment, the battery pack used has a 561.6 Wh capacity, the peak wattage is 10 W, the idle wattage is 1 W. The average flow rate is estimated to be 10 mL/min with an estimated 1 L sample capture per filter and 0.06 L usage of fluid per sample capture. The equations below solve for the maximum number of filter captures possible with the eDNA sampler.

$$H_{P,MAX} = \frac{B_C}{W_P} = \frac{561.6}{10} = 56.1 \text{ hours}$$

$$V_T = 0.06F_A \times H_P = 0.06 \times 10 \times 56.1 = 33.66 \text{ L}$$

$$N_F = \frac{V_T}{V_C + V_R} = \frac{33.66}{1 + 0.06} = 31.8 \approx 32 \text{ Filters}$$

The equations formulated above are useful when planning battery powered deployments of the eDNA sampler. A scenario that can be used to show the effectiveness of

these calculations is as follows. A team of researchers require a study using the eDNA sampler in which the system will be primed and left to operate autonomously until completion with a 561.6 Wh battery. As such, the system is limited to only 9 sample capture event since the filter cartridge holds only 9 filters. For each sample capture event, the sampler filter 1 L of sample fluid and uses 0.06 L of on-board chemicals for cleaning and sample preservation. The average flow rate during the sampling events is estimated to be 10 mL/min. During the sampling event, the sampler uses 10 W, while using 1 W during idle times between sampling events. With these parameters, the equations above can be used to calculate a maximum deployment time of 17.7 days. Thus, allowing the researchers to planning the sampling events according. Unfortunately, the deployment is limited to less than 1 month. The calculation for this deployment is shown below.

$$H_P = \frac{V_T}{0.06F_A} \times N_F = \frac{1.006}{0.06 \times 10} \times 9 = 15.09 \text{ hours}$$

$$H_D = H_P - \frac{W_P H_P}{W_I} + \frac{B_C}{W_I} = 15.09 - \frac{10 \times 15.09}{1} + \frac{561.6}{1} = 425.79 \text{ Hours} = 17.7 \text{ Days}$$

Using the same scenario described above, however with a lower idle wattage of 0.05 W the sampler is capable of being deployed for close to 1 year. This reducing in the idle wattage significantly increases the duration of the studies that can be performed with the eDNA sampler from less than a month ($W_I = 1 \text{ W}$) to approximate 1 year ($W_I = 0.05 \text{ W}$). The calculations for the reduce power system is shown below.

$$H_D = H_P - \frac{W_P H_P}{W_I} + \frac{B_C}{W_I} = 15.09 - \frac{10 \times 15.09}{0.05} + \frac{561.6}{0.05} = 8229.1 \text{ Hours} = 342.9 \text{ Days}$$

With the eDNA sampler's PCB introduced along with its components and peripherals, the next chapter will detail the software used to control the eDNA sampler.

Chapter 5 Software Design

This chapter focuses on the software architecture of the eDNA sampler. The firmware controls the entire eDNA sampler and the system's process to communicate with the user, store deployment information and control the eDNA sampler's fluidic system. This design helps the eDNA sampler to accomplish requirements 7 and 8 of the novel eDNA sampler in Table 2.2. The software design, firmware implementation, and associated testing was my own work.

5.1 Automation Protocol

Figure 5.1 a) illustrates the default sampling protocol of the eDNA sampler along with the estimated completion time for each protocol step. The eDNA sampler performs the sampling protocol whenever triggered by a sample capture event. The sample capture event can be triggered by a scheduled date/time, manually by the user, or triggered by a sensor like a fluorometer attached to the eDNA sampler. Users can also program a custom sampling script into the eDNA sampler's SD card storage or manually over a computer terminal for greater control. The custom script contains the sampling protocol, which sets the number of active valves, collection volume, time limit and minimum flow rate for each step.

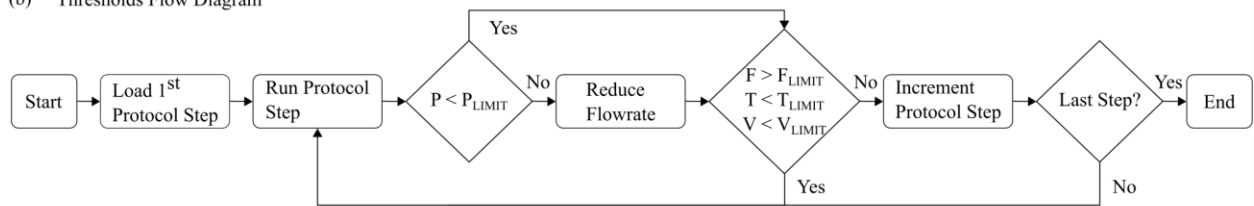
In Figure 5.1 a), the "Sample Prime" step commences the sampling protocol and prepares the sampler by flushing its internal channels with the intended environmental sample fluid. Thereafter, the sampler is now ready to perform the "Sample Capture" step. This step pushes the sample fluid through the selected filter membrane (M1 through M9) for fluid capture. To preserve the material collected on the filter, the "RNAlater Preservation" step pushes the RNAlater through the selected filter membrane. The "MQ Flush" step then uses

Milli-Q to flush RNAlater from the system to avoid it being in contact with 5% HCl that is used in the next step. The “Acid Clean” step cleans the sampler’s internals of contaminants, by using 5% HCl. After that, the “MQ Flush” step flushes the 5% HCl from the channels using Milli-Q. This process cleans the sampler and prepares it for the next sample capture.

(a) Sampling Protocol



(b) Thresholds Flow Diagram



(c) Pressure Profile

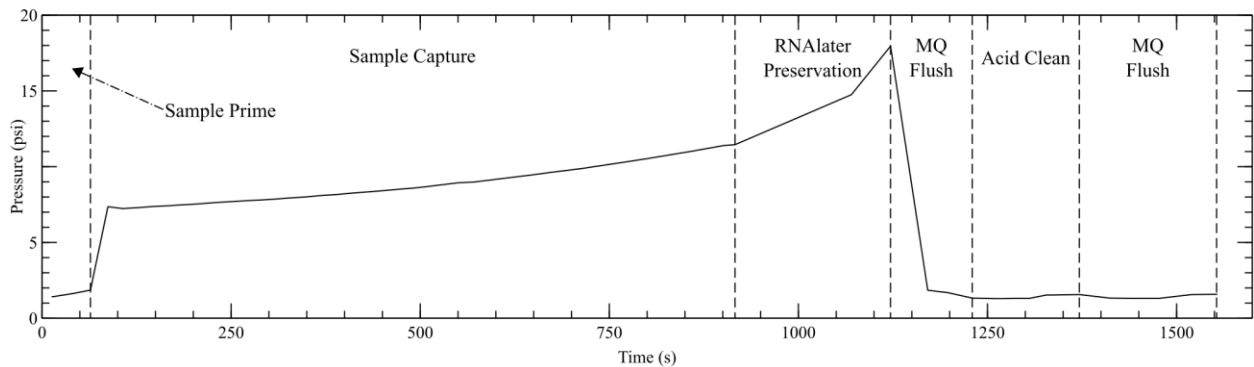


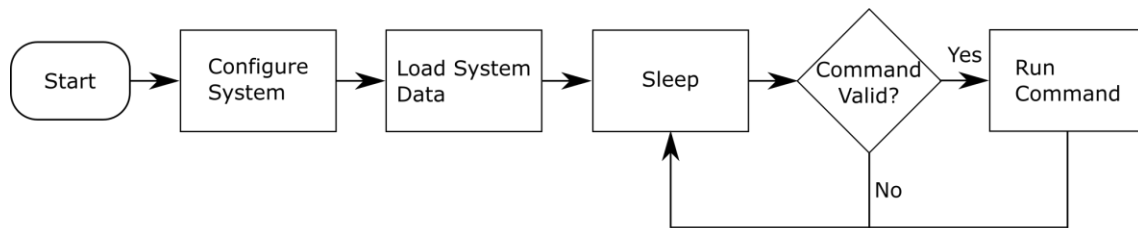
Figure 5.1: eDNA sampler’s automation protocol overview (a) Protocol used to capture and preserve sample then clean fluid channels. (b) Thresholds flow diagram used to load and run protocols within a safe user-specified operating region (F - Flowrate, P - Pressure, T - Time, V - Volume). (c) Pressure data captured during the sampling process on a $0.22\ \mu\text{m}$ polycarbonate filter membrane. *The sampling time is dependent on protocol-specified flowrate and fluid turbidity. The time shown above is for 20 ml/min in ideal conditions. Reprint from [43].

The algorithm shown in Figure 5.1 b) is executed whenever sample capture event is triggered. This algorithm runs the steps shown in the sampling protocol and monitors volume, pressure, and time to ensure that the sampler stays within a tolerable running condition. The algorithm starts by running a series of checks. The first priority is to check the pressure and

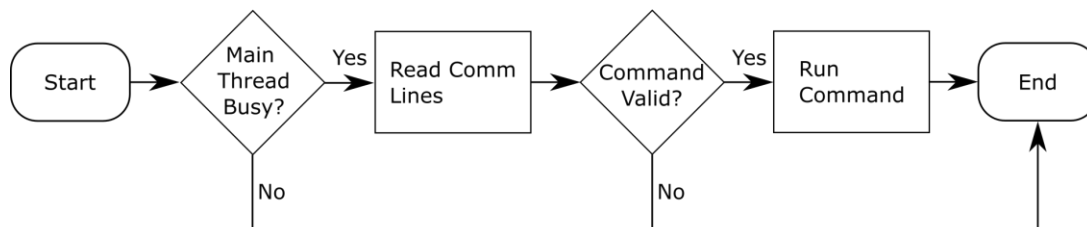
ensure it is within the system safe limit and does not exceed a pre-set pressure limit. If the pressure is greater than that limit, the system reduces the flow rate by a pre-set 40 %. Next, the system checks the flow rate, time-elapsed and volume since the start of the protocol step, in that order. If any of these secondary priorities limits exceeded the sampler moves to the next step in the script. This procedure then repeats until there are no steps left in the sampling protocol. The sampler then enters an idle state (sleep/low power in later versions) and waits for an interrupt to trigger the sampling protocol once more. Figure 5.1 c) illustrates the pressure profile of a recent eDNA sampler deployment in which the sampling protocol shown in Figure 5.1 a) was performed.

5.2 Threads

a) Main Thread



b) Backup Communications Thread (1 Hz)



c) Pressure Measurement Thread (10 Hz)

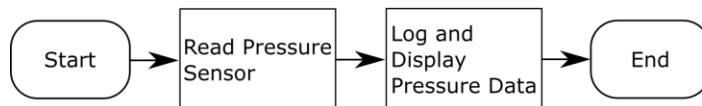


Figure 5.2: eDNA sampler's process threads used to maintain real time system operation on the eDNA sampler a) The main thread that is created during power on and executes all commands. b) Backup communication thread used to execute tasks when the main thread is busy. c) Pressure measurement thread that is used to read pressure data at a constant interval.

Figure 5.2 illustrates several “threads” used in the eDNA samplers’ firmware to allow for real-time operations and control. The “threads” are implemented using timer interrupts and the nested vector interrupt controller (NVIC) to handle pre-emptions. The threads are only active when the eDNA sampler is not in sleep mode.

5.2.1 Main Thread

Figure 5.2 a) illustrates the flow diagram of the main thread in the software architecture. This thread is created when the eDNA sampler is first powered and is used to create all other threads. During bootup, this thread configures the modules and peripherals of the eDNA sampler. The peripheral configuration includes ensuring the pump is in the home position (fully aspirated) and configuring the backup communication thread and pressure measurement thread. Afterward, system configuration data, such as the scheduler information and chemical volume usage status, is loaded from the microSD card.

After that, the main thread puts the eDNA sampler into a sleep state to conserve power. The eDNA sampler exits the sleep state when a scheduled sample capture event is required, or valid command is received on the communication line. After completing the command or sample capture event, the eDNA sampler enters sleep mode.

5.2.2 Backup Communication Thread

Figure 5.2 b) illustrates the flow diagram of the backup communication thread. This thread operates only when the main thread is busy completing a command. The backup thread is intended for quick commands that take less than a second to complete. Commands that take longer to complete risk hindering the command being completed by the main task. The backup

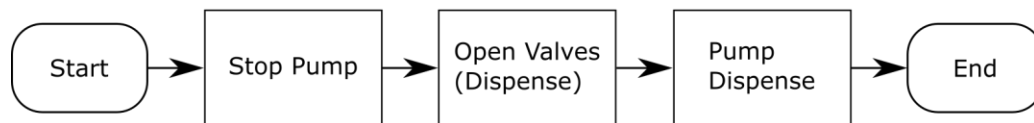
communication thread performs commands such as system status. The default frequency of this thread is 1 Hz.

5.2.3 Pressure Measurement Thread

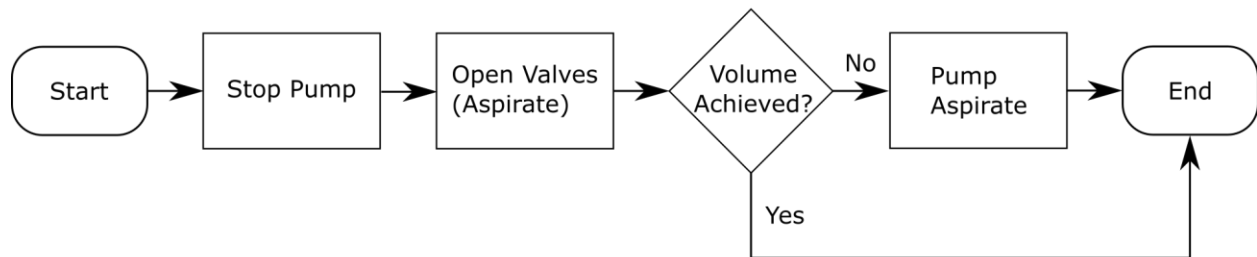
Figure 5.2 c) illustrates the flow diagram of the pressure measurement thread. This thread is activated when the eDNA sampler is executing a sampling protocol. This thread reads pressure measurements from the pressure sensor at regular intervals. The pressure measurements read by this thread are used in calculations related to the piston pump, logged to the microSD card and sent through the communication line to the user for viewing. The user can disable the logging and communication lines features through commands to the eDNA sampler.

5.3 Interrupts

a) Quadrature Encoder Interrupt



b) Home Signal Interrupt



c) Scheduler Interrupt

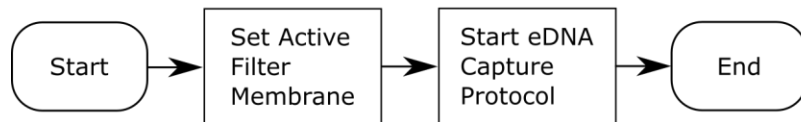


Figure 5.3. System interrupts used in the eDNA sampler.

Figure 5.3 illustrates several interrupts used to interface with the piston pump and to wake the eDNA sampler for sampling events. These interrupts allow the eDNA sampler to maintain real-time execution by keeping the microcontroller's Central Processing unit (CPU) usage low, thus allowing the microcontroller to execute time-critical tasks when required.

5.3.1 Quadrature Encoder Interrupt

Figure 5.3 a) illustrates the Quadrature Encoder Interrupt, triggered when the piston pump's encoder has performed a pre-set number of ticks. Each encoder tick corresponds to a volume of fluid. Therefore, a pre-set number of encoder ticks can be calculated based on the pump cycle's required fluid volume. The maximum fluid volume per pump cycle is 3000 μL based on the size of the piston pump. The Quadrature Encoder Interrupt is triggered when the necessary encoder ticks are achieved.

When the interrupt is triggered, the eDNA sampler stops the piston pump. Next, the eDNA sampler waits until the pressure reading is within one psi of a predetermined baseline pressure. When the fluidic system reaches baseline pressure, the fluid channel for the pump's aspirate phase is closed. Subsequently, the eDNA sampler opens the fluid channel for the pump's dispense phase. The eDNA sampler waits until the pressure reading is within one psi of a predetermined baseline pressure. The eDNA sampler uses solenoid valves to open and close the proper fluidic channels. The sampling protocol specifies the pump speed and proper fluidic channels for the aspirate and dispense phases in the pumping cycle.

Finally, the eDNA sampler changes the direction of the pump to dispense the fluid and sets the pump speed to the value specified in the sampling protocol. The equations below can

be used to translate between an encoder tick reading on the eDNA sampler's PCB and the volume of fluid aspirated by the pump.

$$V = \frac{(E_B - E_C)}{E_T} \times V_T \quad (5.1)$$

$$E_C = E_B - \frac{(V \times E_T)}{V_T} \quad (5.2)$$

Where, E_B is the Base Encoder Count, E_C is the Current Encoder Count, E_T is the Total Encoder Ticks and V_T is the total piston pump volume. With the current configuration of the eDNA sampler the following are constants, $E_B = 30,000$, $E_T = 12,000$ and $V_T = 3,000 \mu L$. E_C varies based on the position of the pump's piston.

5.3.2 Home Signal Interrupt

Figure 5.3 b) illustrates the Home Signal Interrupt, triggered when the pump has entirely dispensed, and the piston is in the home position. When triggered, the eDNA sampler stops the piston pump. Next, the eDNA sampler waits until the pressure reading is within one psi of a predetermined baseline pressure. When the fluidic system reaches baseline pressure, the pump dispense phase's fluid channel is closed. Subsequently, the eDNA sampler opens the fluid channel for the pump's aspirate phase. The eDNA sampler waits until the pressure reading is within one psi of a predetermined baseline pressure.

Finally, the eDNA sampler verified that the total volume required was pumped. If not, another pump cycle is initiated with the encoder interrupt set to aspirate only the remaining fluid volume. If the remaining fluid volume exceeds 3000 μL , the encoder interrupt's tick is set

for 3000 μL . Otherwise, the encoder interrupt's tick is selected based on the remaining fluid volume and equation (5.2).

5.3.3 Scheduler Interrupt

Figure 5.3 c) illustrates the Scheduler Interrupt, triggered when a preset RTC alarm is triggered. When the scheduler interrupt is activated, it sets an active filter membrane (M1 to M9) based on a preprogrammed schedule table. The schedule table includes the date/time and the filter membrane the sampling protocol will use. By default, the scheduler uses the sampling protocol described in Figure 5.1.

5.4 Fluid Control

5.4.1 Piston Pump Fluid Flow Control

Figure 5.4 a) illustrates the pressure build-up in the fluidic system's pressure as biomass accumulates on a filter membrane. This test used seawater collected from Bedford Basin, Halifax. Figure 5.4 c) illustrates the visual changes in the filter membrane as the eDNA sampler collects a large amount of biomass onto a 0.2 μm 25 mm filter.

Figure 5.4 b) illustrates a four-phase cycle required when using a piston pump to move fluid. The four-phase cycle comprises aspirate, wait, dispense and wait. The aspirate phase fills the piston pump with fluid. After that, the waiting phase keeps the aspirate phase's fluidic channel open until pressure stabilizes before switching to the dispense phase's fluidic channel and waiting until pressure stabilizes. Next, the piston pump enters the dispense phase and dispenses fluid into the fluidic system. Finally, the pump enters the waiting stage to switch from

the dispense phase's fluidic channel to the aspirate phase's fluidic channel while ensuring baseline pressure before each switch.

The piston pump's wait phase relies on pressure sensor measurements, a predetermined baseline pressure and a hardcoded timeout value. Using the pressure sensor measurement rather than a fixed waiting time to determine baseline pressure optimizes the system's performance. This performance optimization is because as the eDNA sampler performs the sampling protocol, the channel's fluidic resistance changes, meaning it takes longer for the pressure to stabilize. Having a fixed wait time would mean that system would either be waiting longer than required to collect eDNA samples or switching the channels too quickly, resulting in fluid not being correctly collected. The longer wait times would limit the temporal resolution of the eDNA sampler. At the same time, the premature switching of the valve would result in a significant error in collected fluid volume as the biomass of the filter membrane increases. Therefore, pressure sensor measurements and a predetermined baseline pressure optimize the wait time and volume accuracy.

The user can set the predetermined baseline pressure manually or automatically during the sampling protocol. The automatic approach involves the eDNA sampler opening the appropriate fluidic channels so that the pressure measurements can reflect the baseline pressure for the depth the system resides. The limitation of using a predetermined baseline pressure is that it is assumed that the system will remain at the designated sampling depth until the sampling protocol is completed. A solution to this would be to include a second pressure sensor for measuring ambient pressure to be used as the baseline pressure value.

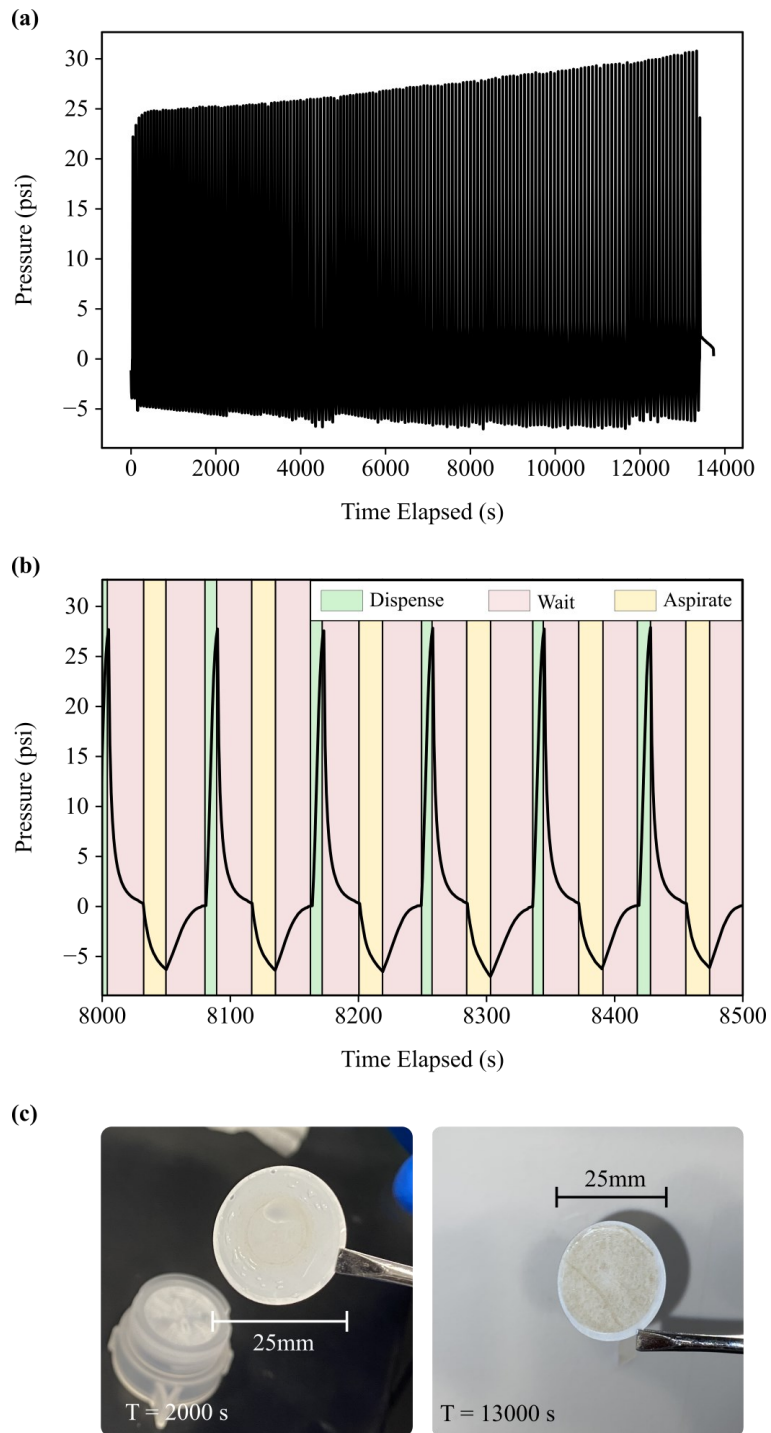


Figure 5.4: eDNA sampler's pressure data analysis (a) Pressure data captured during the sampling process on a $0.22 \mu\text{m}$ polycarbonate filter membrane. (b) Same data as in (a), but zoomed-in pressure cycle to highlight the syringe pump control scheme used. (c) Retentate on the porous membrane, during the early stages of filtration and near the end of filtration. The filter is removed for DNA extraction and downstream processing and analysis. Reprint from [48], © 2022 IEEE.

The piston pump's wait phase uses a hardcoded timeout value for scenarios where organic matter clogs the eDNA sampler fluidic channel. The system's fluidic pressure does not return to the predetermined baseline pressure. The timeout value, 5 minutes, allows a maximum time for the eDNA sampler to wait before resuming the phases of the piston pump cycle. During deployments in the field, the baseline pressure can be collected by opening the eDNA sampler's inlet valve to measure the hydrostatic pressure at the current depth.

5.4.2 Flow Rate Calculation

The microcontroller can control the flow rate of the piston pump using the stepper motor driver. This flow rate control is because of the relationship between the stepper motor steps and the volume of fluid pumped. Equation (5.3) shows this relationship and solves for the step frequency needed to be generated by the microcontroller to achieve a specified flow rate at a specified step angle.

$$F = \frac{R_T}{V_T} \frac{360^\circ}{A} \frac{f}{60} \quad (5.3)$$

Where, F = Step Frequency, R_T = Total Revolutions for full stroke (Constant: 15), V_T = Volume of syringe (ml) (Constant: 3 mL), A = Step angle (based on the step size), f = Flow rate of syringe (ml/min). Based on known step size, the step angle for the pump's piston can be calculated using the following:

$$A = S \times 1.8^\circ \quad (5.4)$$

Where S = Step Size (1, 1/2, 1/4, 1/8, 1/16 and 1/32) and A is the Step Angle. Smaller step sizes allow for a smoother flow with more power (2 coil pairs activated vs 1 coil pair). Larger step sizes allow for a rougher but more rapid flow rate.

The total revolutions for full stroke can be calculated based on the volume per full step for the piston pump, V_s . Based on the piston pump's datasheet the volume per full step is 1 μ L. The total number of revolutions required can be calculated by determining the maximum volume range of the pump and volume per full step for the piston pump. Equation (5.5) produces a total revolution needed to pump fluid that is valid for all step sizes, given that the size of the pump remains at 3 mL. This constant has a value of 15, along with the volume of the syringe pump, which will maintain its constant valve of 3 mL.

$$R_T = \frac{V_T * A}{360^\circ * S * V_s} = \frac{V_T * 1.8^\circ}{360^\circ * V_s} \quad (5.5)$$

$$= \frac{V_T}{200 * V_s}$$

By combining equation (5.3) and (5.5), the equation for calculating the necessary step frequency can be simplified to the following:

$$F = \frac{V_T * A}{360^\circ * S * V_s} \frac{1}{V_T} \frac{360^\circ}{A} \frac{f}{60} = \frac{f}{60 * S * V_s} \quad (5.6)$$

Therefore,

$$F = \frac{f}{60 * S * V_s} \quad (5.7)$$

An example of this calculation would be to run the syringe pump at 20 mL/min with a step size of ¼. The calculation would go as follows:

$$f = 20 \text{ mL/min}$$

$$S = \frac{1}{4}$$

$$F = \frac{f}{60 * S * V_s} = \frac{20}{60 * \frac{1}{4} * 0.001} = 1333.33 \text{ Hz} \quad (5.8)$$

Therefore, as shown in Equation (5.8), for the piston pump to produce a flow rate of 20 mL/min at a step size of ¼, the step frequency needs to be 1333.33 Hz.

With the fluidic, electronic, and software designs rationalized and described, the eDNA sampler was put through the verification processes to evaluate each sub-unit's performance. These details are described in the next Chapter.

Chapter 6 Unit Testing

This chapter focuses on the unit testing performed with the eDNA sampler to verify functionality during its development process. The unit testing was my own work.

6.1 Negative Pressure Test

The negative pressure test was performed using the fluidic system shown in Figure 6.1 b). This test was performed to verify that the eDNA sampler was capable of interfacing with the piston pump and pressure sensor. Additionally, this test was meant to determine the drift in readings from the pressure sensor. In this test, purified Milli-Q water was used so there would be no buildup on the filter membrane, causing a shift in pressure readings over time. During aspirate pump phase fluid was pulled through the filter membrane, however, during the dispense phase fluid was pushed through the fluid channel without the filter membrane as shown in in Figure 6.1 b).

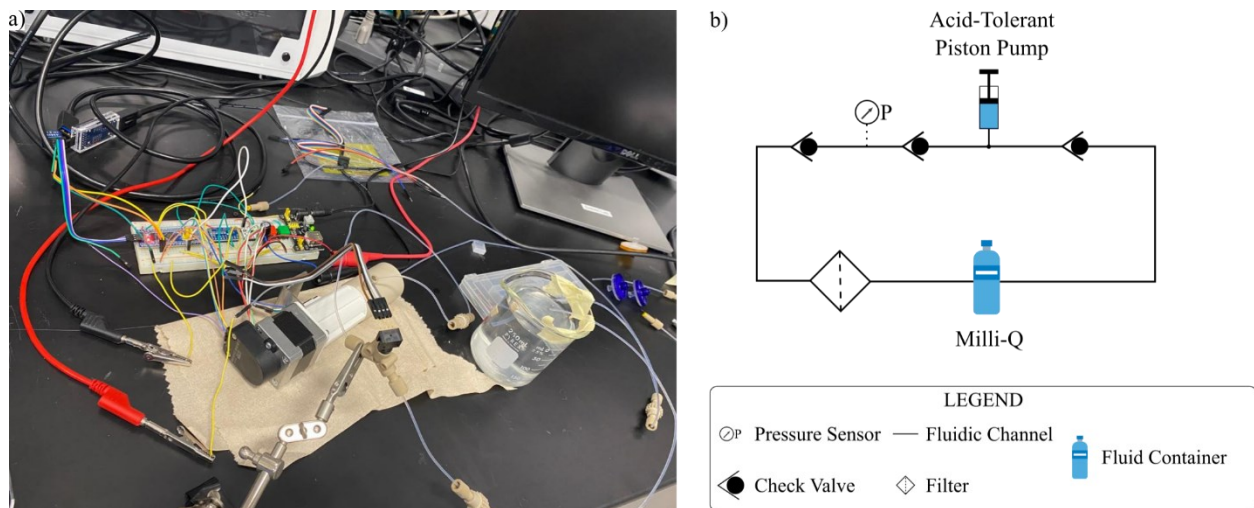


Figure 6.1: Negative pressure test setup (a) Benchtop setup used to test negative pressure (b) Fluidic architecture used to test negative pressure.

The fluidic circuit was built using IDEX 1520XL tubing, check valves (TKLA9502130D, Lee Company Ltd) and the eDNA sampler's pressure sensor and piston pump. The fluidic system was controlled by the breadboard eDNA sampler design shown in Figure 6.1 a). The piston pump was programmed to operate at 5 ml/min per dispense and aspirate phase, thus creating an average effective flowrate of 2.5 ml/min per pump cycle.

Sequentially, the filter holder was changed, going from no filter, to a 0.2 μm PES filter (83-1826-001, Sarstedt), to a 0.45 μm PES filter (83-1826, Sarstedt), and finally back to no filter. The 0.2 μm filters were combined in series for up to 3 filters. The 0.45 μm were combined in series for up to 5 filters. Combining the filter membranes in series is expected to cause a linear change in pressure proportional to the number of filters, akin to voltage increases with added series resistors and constant current (flow rate). During this test, a hardcoded wait phase of 1 second was used rather than the pressure sensor. This was due to the test occurring early in the development phase of the eDNA sampler.

Figure 6.2 a) illustrates the pressure reading measured during the negative pressure testing. A minimum of 6 pump cycles were performed with each combination of filters. A pressure spike is measured between filter combinations due to manually changing out the filter membrane. The combination of the 3 Filters (0.2 μm) in series generated a negative pressure of approximately -8 psi, which did not follow the expected linear pressure growth as the number of filters in series increased. This outlier in the data was likely due to an air bubble getting into the filter.

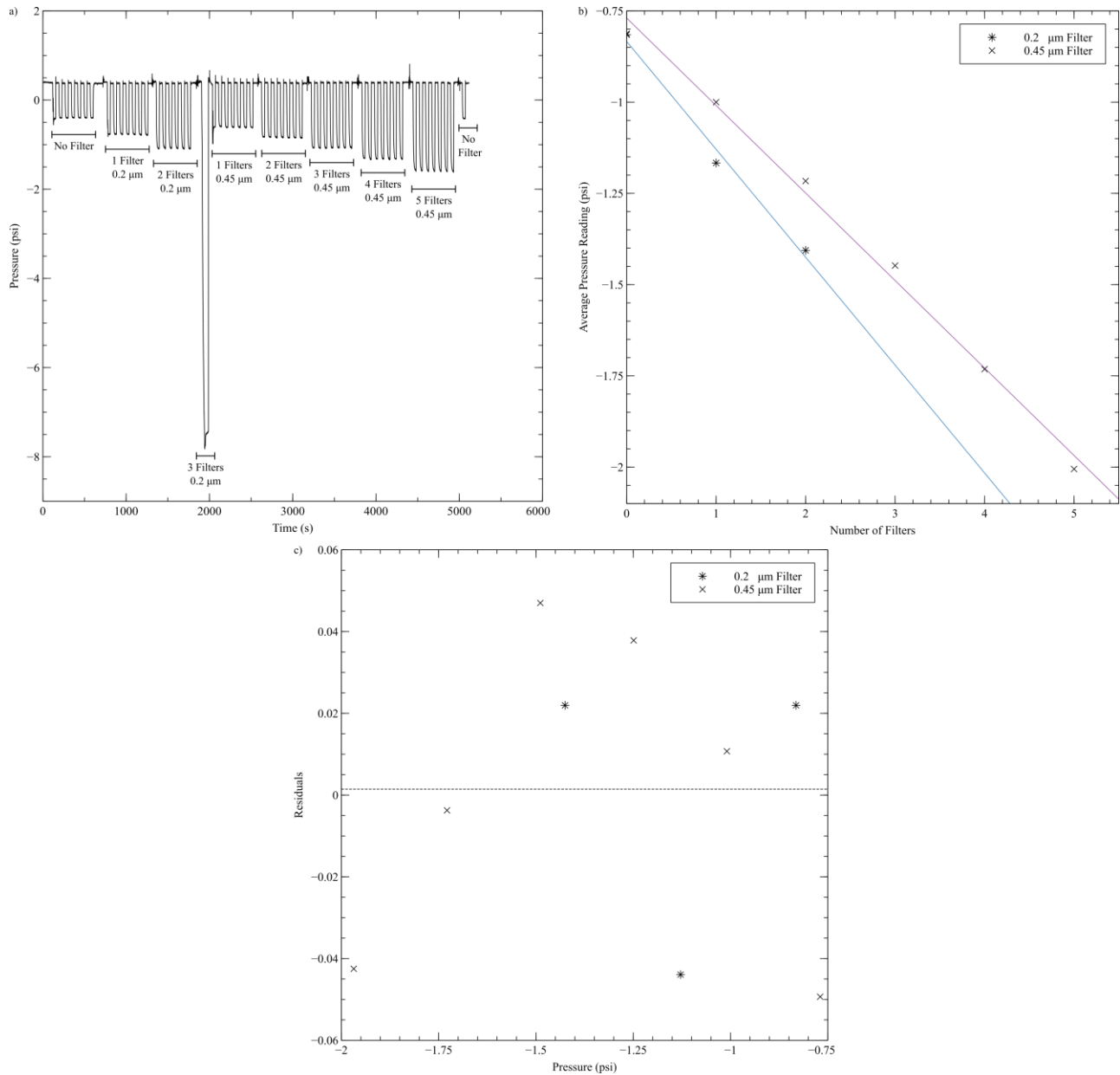


Figure 6.2: Negative pressure test data a) Pressure vs Time measurements for a pull configuration eDNA sampler as various filters are added in series to produce fluidic impedance in the system. b) Average pressure recorded for each size filter vs the number of filter membranes of the specified size that was in series. c) The residual plot of the average pressure reading vs number of filter plot shown in (b).

Figure 6.2 b) illustrates the Average pressure readings vs the number of filters for the 0.2μm and 0.45 μm filters. The outlier filter combination of 3 filters (0.2 μm) was removed not to skew the line of best fit. The lines of best fit for the 0.2 μm and 0.45 μm were linear, as expected. The residual of the plots is illustrated in Figure 6.2 c). Based on the residual, all

pressure readings for the filters were within 0.1 psi of their expected value. This demonstrated the drift of the pressure sensor reading to be within 0.06 psi over the 100 minutes of testing in Figure 6.2 a), making it within a suitable range for the eDNA sampler.

6.2 Pump Flow Rate and Volume Test

The pump flow rate and volume test was performed to determine the error associated with the pump's flow rate and volume accuracy. The microcontroller controls the piston pump, so this test validates the formulas and firmware are implemented correctly. The test setup is shown in Figure 6.3 a), in which the piston pump pulls fluid from a 250 mL breaker and pushes it into a graduated cylinder for measuring.

Before testing, the fluidic system was primed, so air bubbles did not affect the reading. During testing, 3 mL of Milli-Q is collected in the 10 mL graduated cylinder using the following flow rates: 5 mL/min, 10 mL/min, 20 mL/min and 40 mL/min. The fluid volume collected was measured using a laboratory analytical balance, as shown in Figure 6.3 b). The graduated cylinder was dried and tared on the analytical balance (PX84, Ohaus Corporation) before each volume collection. The Milli-Q was measured using the analytical balance under the assumption that the density of water used in the experiment was 1 g/mL.

The pump's flow rate was measured by updating the firmware on the eDNA sampler's PCB to use the microcontroller's systick timer, which has an accuracy of 1 ms to record the time it takes to complete the aspirate and dispense pumping phase distinctly.

The firmware translates the number of encoder ticks to volume based on equation (5.1). As such, the number of ticks representing the pump capacity of 3 mL was hardcoded in the

firmware. Theoretically, this value is 12,000 ticks for 3 mL. However, in the early development of the eDNA sampler, a value of 12,500 ticks was used in error. The value has since been rectified to the correct 12,000 ticks. Therefore, data were collected for 12,000 and 12,500 ticks for this series of tests. Table 6.1 shows data collected using the 12,500 ticks and Table 6.2 shows the data collected using 12,000 ticks.

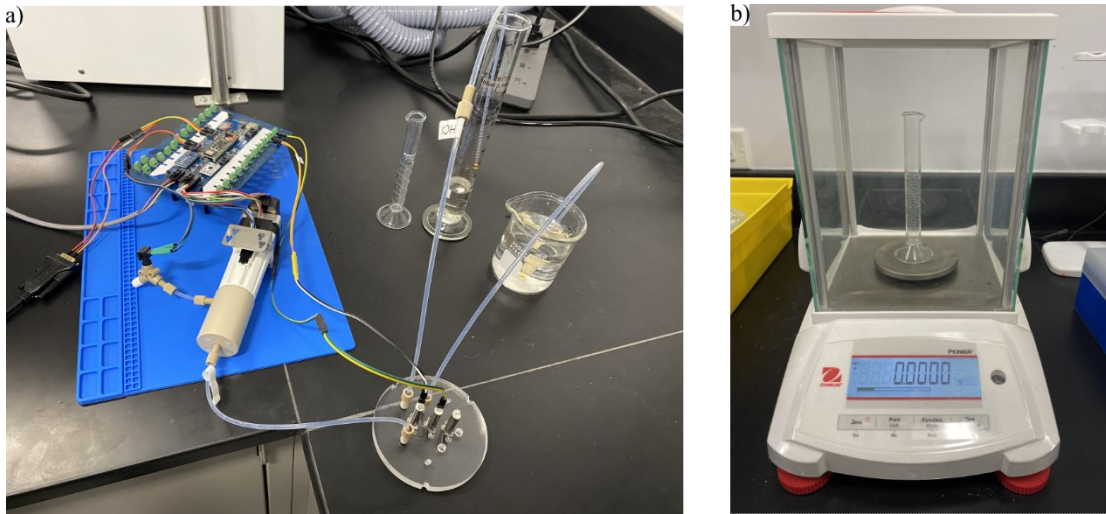


Figure 6.3: Piston pump's volumetric and flowrate test benchtop setup for volumetric and flow rate accuracy of piston pump used in eDNA Sampler (a) Benchtop configuration for volumetric test showing the 10 mL graduated cylinder (b) 10 mL graduated cylinder tared on a laboratory analytical balance to measure fluid volume precisely.

Table 6.1 illustrates the flow rate and volume measurements from the test when using the 12,500 ticks. The results show that the errors for both the pump's flow rate and volume accuracy is within 4.3 % and 4 % respectively.

Table 6.1: Piston pump flow rate and volume accuracy test with encoder ticks set to 12,500.

Flow rate (mL/min)		Volume (mL)		Percentage Error (%)	
Set	Measured	Set	Measured	Speed	Volume
5	4.79	3.0000	3.1028	4.11	3.43
10	9.59	3.0000	3.1008	4.13	3.36
20	19.20	3.0000	3.0980	4.02	3.27
40	38.29	3.0000	3.1186	4.29	3.95

Table 6.2 illustrates the flow rate and volume measurements from the test when the 12,000 ticks. The results of using the correct value improves the flow rate and volume accuracy, with errors less than 0.8 %; a significant improvement over the results shown in Table 6.1. Therefore, this demonstrates the formulas and firmware used to control the piston pump are working within a tolerable degree of error. These figures are comparable with the manufacturers stated error in the datasheet of less than 0.5 % [40].

Table 6.2: Piston pump flow rate and volume accuracy test with encoder ticks set to 12,000.

Flow rate (mL/min)		Volume (mL)		Percentage Error (%)	
Set	Measured	Set	Measured	Flow rate	Volume
5	4.99	3	2.9843	0.11	0.52
10	9.99	3	2.9773	0.13	0.76
20	19.99	3	2.9785	0.07	0.72
40	38.93	3	2.9827	0.18	0.58

6.3 Cross-Contamination Testing

The cross-contamination test uses a dye to quantifiably evaluate the eDNA sampler for the degree of cross-contamination. Using a dye allows for more immediate feedback since a lab is not required to process the samples; eDNA amplification and sequencing takes days to months depending on the backlog and would slow the design iterations. As such, a spectrometer on the eDNA sampler's output port would be able to measure any unexpected changes in light intensity from unwanted dye carry-overs. The cross-contamination test was performed using 0.05% Red Food Dye (RFD) as the sample fluid while the sampling protocol was being performed. The sampling alternated using 0.05% RFD and purified Milli-Q per filter membrane to determine cross-contamination. The 0.05% RFD was chosen based on the dynamic intensity range measured on the spectrometer, other food dye concentrations are viable based on the

same criteria. The main objective of the cross-contamination test is to measure the residuals of the 0.05% RFD based on the fluidic architecture's dead zones and cleaning protocol. Figure 6.4 illustrates the test bench for the food dye cross-contamination test.

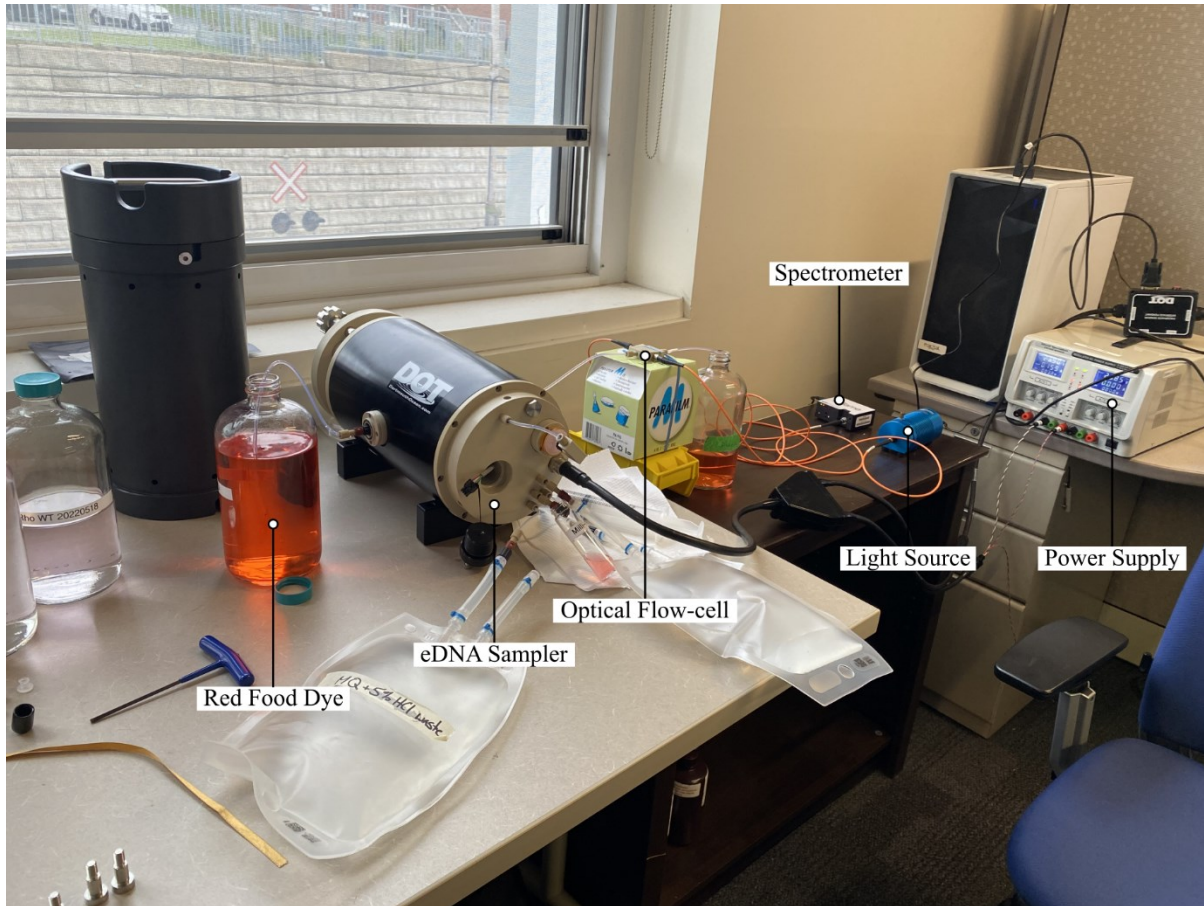


Figure 6.4: Cross-contamination test benchtop setup for eDNA sampler using red food dye and optical measurements.

The use of 0.05 % RFD is the first stage of testing for cross-contamination, which involves the detection of dead zones in the fluidic architecture. This use of RFD is due to it being comparable to biological samples such as micro-organisms suspended in fluid. However, unlike RFD, a biological/particulate sample can attach to the walls of the fluidic channels or get trapped in corners. Further, these microbes can multiply over time, creating a biofilm that would make cleaning more difficult. As such, in the following stages of cross-contamination

testing using biological samples, disinfectants would be required along with testing of parameters such as flow rate, disinfectant concentration and exposure time. Dead zone testing in the fluidic architecture could be improved by performed computational fluid dynamics to isolate the specific areas in the fluidic architecture responsible for the dead zones.

A modified version of the sampling protocol illustrated in Figure 5.1 was performed. The modified sampling protocol included an Acid clean step followed by a Milli-Q Flush before executing the sampling protocol steps shown in Figure 5.1 (a).

For the sampling protocol, 125 mL of sampling fluid was captured using filter membranes M1 to M6. Filter membranes M1, M3 and M5 collected 0.05 % RFD solution. Filter membranes M2, M4 and M6 collected purified Milli-Q. All chemicals in the eDNA sampler were replaced with purified Milli-Q. As the sample fluid leaves the eDNA sampler's output port, it passes through an optical flow cell (79027, FIA Lab, 10 mm optical path) with a light source (HL-2000-FHSA, Ocean Optics) and spectrometer attached. The spectrometer (Flame, Ocean Optics) has a saturation intensity of 65,536 counts based on the Charge Coupled Device (CCD) and 16-bit ADC.

Figure 6.5, shows the intensity measurements recorded by the spectrometer at a wavelength of 520 nm, the center of the dye absorbance peak. The figure illustrates that during sampling of the 0.05 % RFD, the intensity readings plunge and plateau at a minimum of approximately 3000 units. A low light reading signifies that most (approx. 90%) of the light in the 520 nm wavelength has been absorbed by the dye and does not reach the detector as per the Beer-Lambert Law, which states that the light absorbance is directly proportional to the

concentration of solution [49]. Next, the cleaning protocol starts, and the intensity reaches its maximum of approximately 38,000 units, signifying that the RFD has been removed from the system.

More importantly, at the start of the Milli-Q sampling, the intensity suddenly drops at time 3942 s (Intensity Drop 1), 8610 s (Intensity Drop 2), 12793 s (Intensity Drop 3) and 13295 s (Intensity Drop 4) in Figure 6.5. These intensity drops lasted for 15 s, 23 s, 22 s and 1 s for intensity drops 1 to 4, respectively. These intensity decreases indicate that red food dye remained in the system post-cleaning. We quantified this by performing a time-wise integration of the signal intensity. Based on the effective flow rate of 10 mL/min used by the eDNA, the equivalent volume of ~2.5 mL, ~3.8 mL, ~3.6 mL and ~0.2 mL was required to flush the intensity drops 1 to 4, respectively. The RDE carry-over percentage for each intensity drop is 2.0 %, 3.0 %, 2.9 % and 0.2 %, respectively. The RFD carry-over measures the RFD percentage from the prior 125 mL RFD sample capture that remained post-cleaning. The intensity drops indicate that we may have a carry-over volume close to the amount of Milli-Q required to remove the RFD (intensity drops). These are likely to cause cross-contamination during the sampling of biological samples.

Intensity drops 3 and 4 observed during the sample capture of filter membrane M6 is a different behaviour than observed for the sample capture M2 and M4. The sample captures M2 and M4 only contained a single intensity drop at the start of the protocol's cleaning step. The M6 flush showed a second intensity drop (intensity drop 4) and was likely due to the geometry of the valve manifold. This result needs to be repeated and confirmed, and if necessary will need to be investigated more systematically in a future study.

While important to minimize cross-contamination, the system performs multiple flushes between sample captures to minimize carry-over. Further optimization of the system may be required to drive this 2-3% figure lower, after validating the entire eDNA sampler unit with real samples on the bench, which is the topic of the next Chapter.

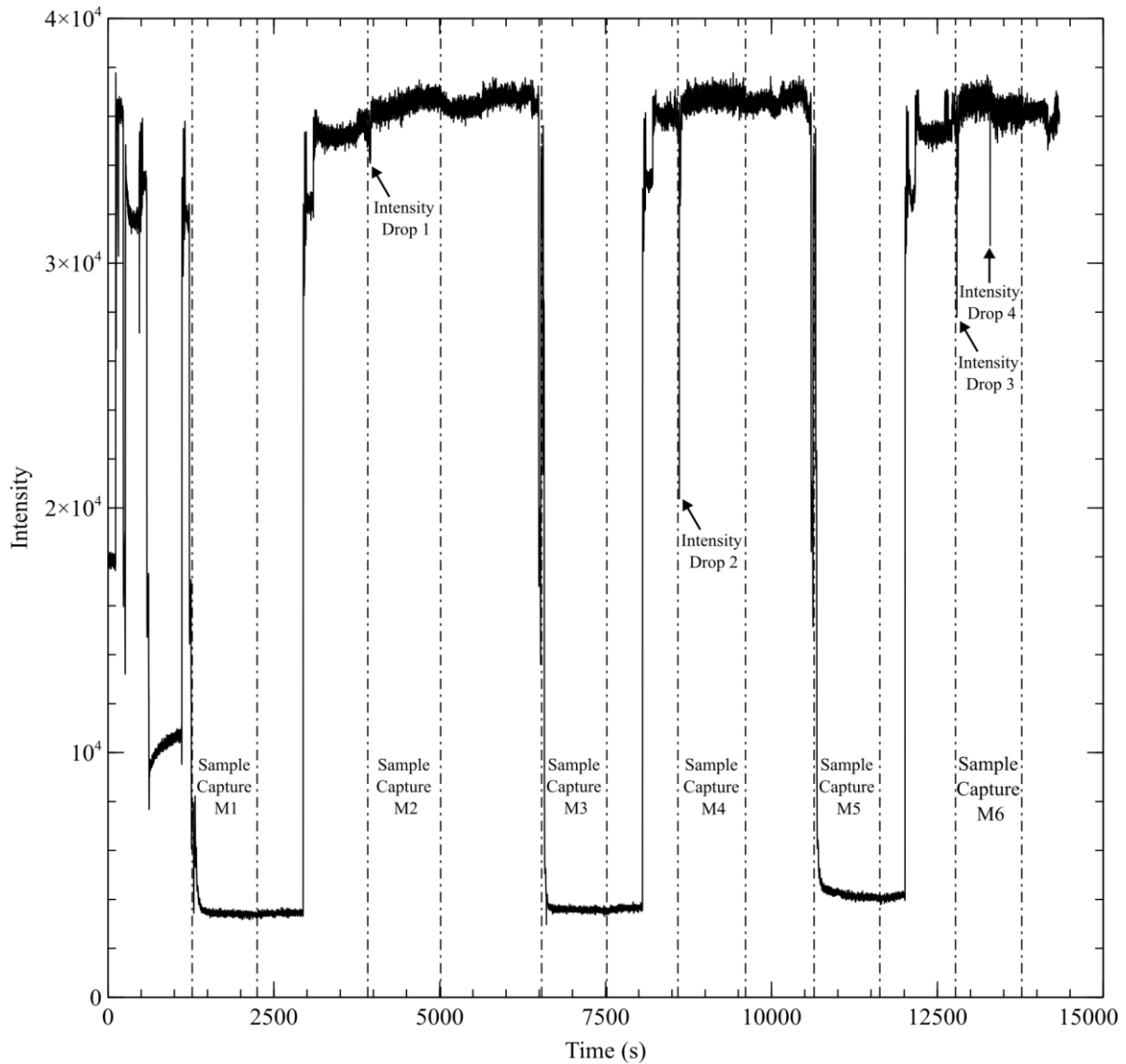


Figure 6.5: Intensity measurements recorded at 520 nm during the cross-contamination tests. Sample Capture M1, M3 and M5 used 0.05 % Red Food Dye (RFD) as the sample fluid. Sample Capture M2, M4 and M5 used purified Milli-Q as the sample fluid. All other steps in the protocol were performed with purified Milli-Q.

Chapter 7 Benchtop System

This chapter focuses on the complete eDNA sampler's benchtop setup and the various tests to verify its functionality. This process served as a crucial step to verify the system design before finalizing the fully assembled and submersible eDNA sampler design. The benchtop setup was used to verify the fluidic architecture design, software control and sampling protocol effectiveness. The benchtop setup and testing was my own work, with the exception that the fluidic manifold was manufactured by Colin Sonnichsen. Also, the DNA extraction and analysis was performed by Connor Mackie.

7.1 Benchtop Setup

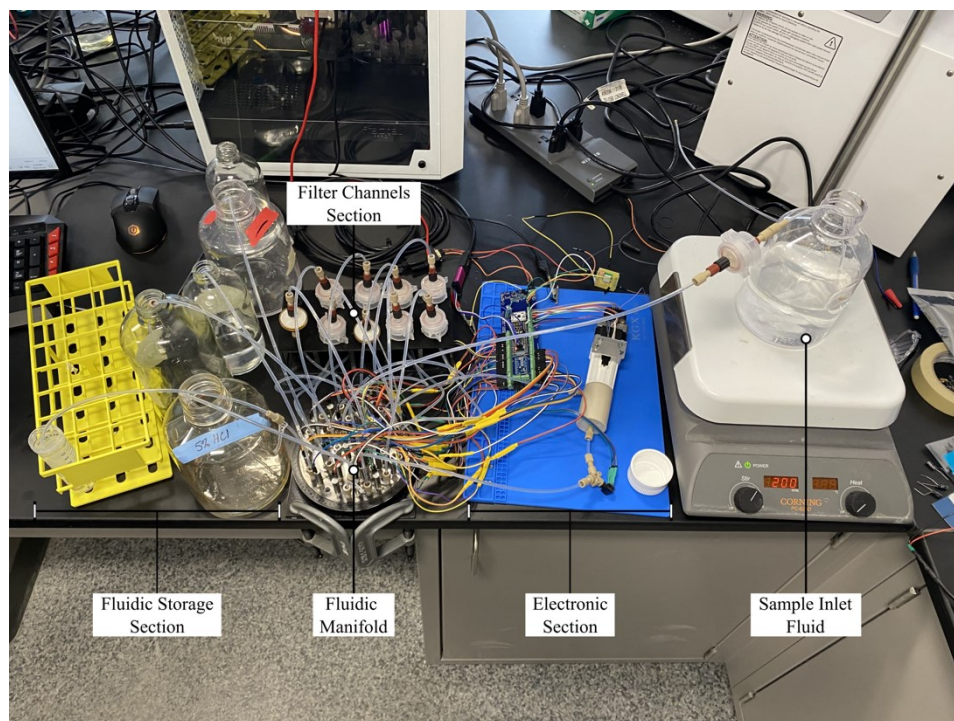


Figure 7.1: Benchtop setup of the eDNA sampler with fully developed fluid architecture for sample capture.

Figure 7.1 illustrates the benchtop setup of the eDNA sampler. This setup consists of several components: Fluidic Storage Section, Fluidic Manifold, Filter Channels Section, Electronic

Section and Sample Inlet Fluid. The Fluidic Storage Section consists of the fluids: RNAlater, 5% HCl and Milli-Q used in the sample capture protocol and two bottles for sample outlet and waste reservoir capture. The Fluidic Manifold comprises the fluid channel routings and solenoid valves to control the states of those channels: opened or closed. The filter channels section consists of fluidic channels with an inline filter; this includes filter membrane channels (M1 to M9) and the filter bypass channel (seawater). The electronic section consists of the eDNA PCB, piston pump and a pressure sensor for communication interface and fluid control. The sample inlet fluid is placed on a stirring plate to constantly stir the sample fluid to ensure that particles are thoroughly mixed and not settling at the bottom of the “sample chamber” before entering the fluidic sample inlet.

7.1.1 Fluidic Architecture

The benchtop implementation of the fluidic architecture is shown in Figure 7.1.

7.1.1.1 Fluidic Manifold

Figure 7.2 illustrates the fluidic manifold used in the eDNA sampler’s benchtop setup. The manifold was designed and produced in collaboration with a postdoctoral fellow, Colin Sonnichsen. The manifold routes all fluids within the eDNA sampler and is made from polymethyl methacrylate (PMMA). This material is chemically inert to all fluids that are intended to be routed through the eDNA sampler. The manifold comprises 1 mm deep and 1 mm wide fluidic channels, ¼-28 ports and fittings for 26 solenoid valves.

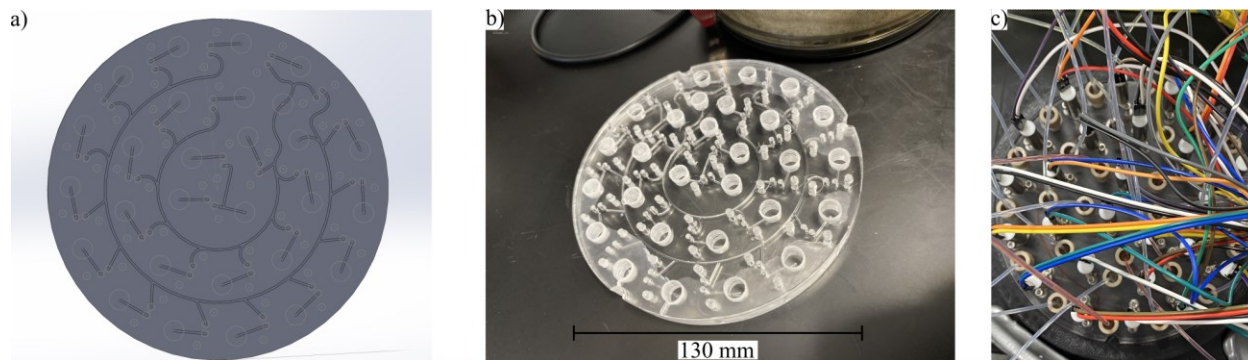


Figure 7.2: Benchtop eDNA sampler manifold (a) SolidWorks model of eDNA sampler's benchtop fluidic manifold (b) Fabricated eDNA sampler's benchtop fluidic manifold using PMMA (c) Fully populated eDNA sampler's fluidic manifold.

Figure 7.2 c) illustrates a fluidic manifold that has been populated with 1-eighth Fluorinated Ethylene Propylene (FEP) fluid tubing using the ¼-28 Polyetheretherketone (PEEK) connectors and solenoid valves. The tubing fluidically links the filter membranes, fluid storage sections, sample inlet and fluidic electronics (Piston Pump and pressure sensor).

7.1.1.2 Fluidic Storage

The fluidic storage section on the eDNA sampler's benchtop setup holds several fluids. The fluids stored in this section are 5% HCl, RNAlater, purified Milli-Q, waste and sample outlet. Each fluid was stored separately in distinct chemically inert containers of assorted sizes.

7.1.1.3 Filter Channels Section

The Filters system features an array of 7 distinct filter holders (Advantec 43303010, Polypropylene), each 25 mm diameter for filter membranes M2 to M6 and M8 to M9. The fluid channels filter membranes M1 and M7 were damaged during the fluidic manifold's fabrication process. A 0.45 µm Sarstedt Polyethersulfone (PES) syringe filter is used for the filter bypass channel (seawater). A custom rack was 3D printed to fit the filter holders and a disposable filter securely.

7.1.1.4 Sample Inlet Fluid

The sample inlet fluid container is placed on a stirring plate with a magnetic stirring bar placed inside the container. The stirring plate is set to 200 RPM to thoroughly mix the sample fluid and ensure particles do not settle at the bottom of the container. The sample inlet fluid is connected to the fluidic manifold using a 1-eighth Fluorinated Ethylene Propylene (FEP) fluid tube. The sample inlet tube has an inline filter holder fitted with a 35 μm filter mesh to prevent large particles from entering the fluidic system.

7.1.2 Electronic Section

The electronic section comprises an eDNA PCB, a syringe pump and a pressure sensor. The piston pump and pressure sensor are fluidically connected to the fluidic manifold through a Y-connector made of PEEK. The eDNA PCB electrically connects to the 26 solenoid valves, piston pump and pressure sensor to control the fluidic operations of the eDNA sampler. The eDNA PCB is powered by a benchtop power supply set to 7 V and connected to a desktop to communicate data.

7.2 Food Dye Testing

The food dye test was performed to verify the fluidic architecture and software control of the eDNA sampler. The benchtop setup for the test is similar to the eDNA sampler benchtop setup described in Chapter 7.1, with modifications to the implementation of the fluidic architecture. Modifying the fluidic architecture includes using a syringe filter for the filter membrane channels and using various food colouring instead of the actual fluids. These modifications

allow a visual examination of the fluid flow paths to verify the correct procedures. Figure 7.3 a) illustrates the setup before starting the filter sample protocol.

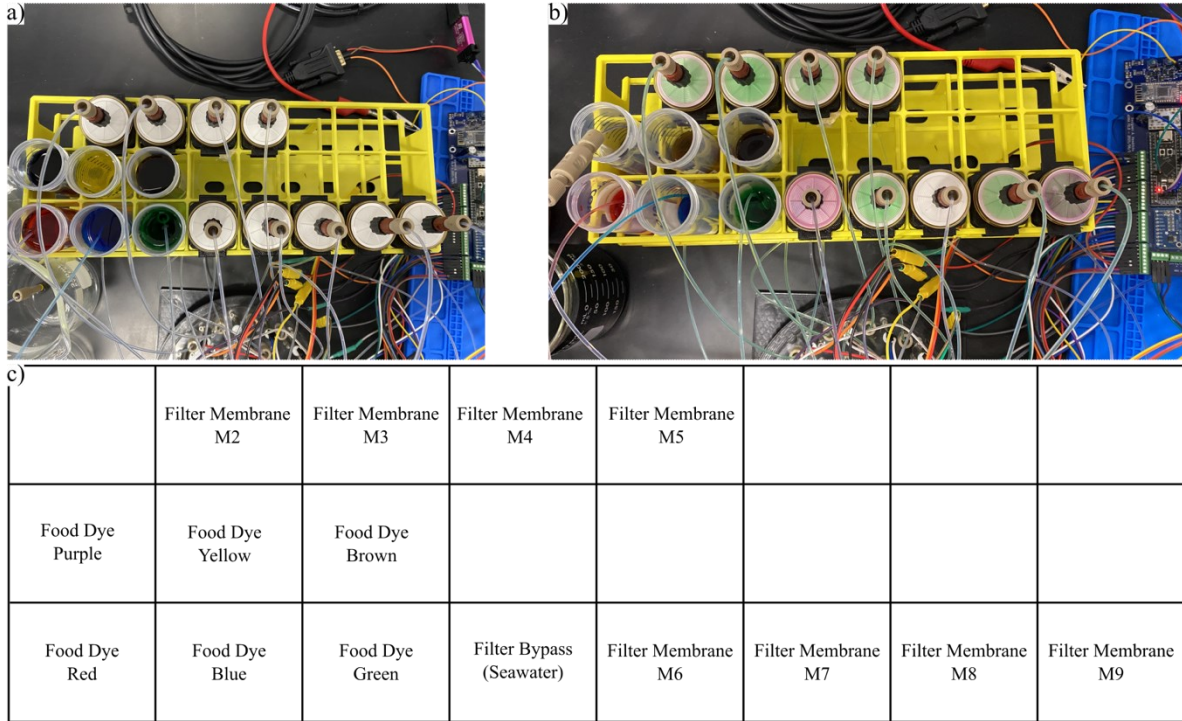


Figure 7.3: Fluidic implementation of benchtop food dye flow test (a) Rack holding rack for food dyes and filters prior to sampling capture running (b) Rack holding rack for food dyes and filters after running sampling capture (c) Food dye and filter membrane positions on the rack.

Table 7.1 summarizes the various food dye colours used for each filter membrane and fluids: RNAlater, Purified Milli-Q and 5% HCl. The sampling protocol was performed for Filter Membranes M2 to M6 and M8 to M9. The positions of the food dyes and filters on the rack are shown in Figure 7.3 c). During the sampling protocol during the sample capture step, the sample inlet tube was moved to the food dye colour representing the filter membrane, as summarized in Table 7.1.

The results of the food dye test were purely visual. Figure 7.3 c), filter membranes M2 to M6 and M8 were coloured green to demonstrate that the filters were preserved after

collection. The image was captured during the start of the RNAlater preservation step. Thus, filter membrane M9 is slightly green as the previous dye is flushed out.

Table 7.1: Food dye colouring for each filter membrane and chemicals of the eDNA sampler. The colours allowed for fluid flow to be tracked throughout the eDNA sampler so to verify fluidic paths and firmware.

Fluidic Channel / Chemical	Food Dye Colour
Filter Membrane 1	-
Filter Membrane 2	Purple
Filter Membrane 3	Yellow
Filter Membrane 4	Brown
Filter Membrane 5	Purple
Filter Membrane 6	Yellow
Filter Membrane 7	-
Filter Membrane 8	Brown
Filter Membrane 9	Purple
RNAlater	Green
5% HCl	Red
Milli-Q	Blue

In conclusion, the food dye test verified the functionality of the fluidic architecture design and software control. The user could trigger the sampling protocol from a desktop terminal to collect sample fluid on a specified filter. Based on the visual analysis during the sampling protocol execution, the software could route fluid into the correct channels.

7.3 eDNA Sampling – Actual Biological Sample

After verifying fluidic architecture design and software control using food dye testing, the next set of tests used seawater as the sample fluid to verify the sampling protocol's effectiveness. This series of tests determined if the eDNA sampler could produce filter membrane samples capable of being sequenced in a genomic facility/lab, specifically, Integrated Microbiome Resource (IMR) at Dalhousie University. The biological samples used during this series were

collected from the Bedford basin at a depth of 1 m through the Bedford Basin Monitoring Program (BBMP).

A modified version of the sampling protocol illustrated in Figure 5.1 was performed. The modified sampling protocol did not perform acid backflow into the sample inlet or perform the sample preservation step with RNAlater. Additionally, the modified sampling protocol included an Acid clean step followed by a Milli-Q Flush before executing the sampling protocol steps shown in Figure 5.1 (a).

During the benchtop testing, 25 mm, 0.2 μm Isopore polycarbonate (PC) membranes (SKU: GTTP02500) were housed in Advantec polypropylene filter housings (Item# RK-06623-32) to perform sample capture. Immediately after the sample capture step of the sampling protocol, the filter membrane was removed using sterile equipment so as not to introduce contaminants. The filter membrane was then placed in a 2 mL screwcap tube and immediately frozen in a CryoShipper for transport back to the LaRoche lab. Once at the LaRoche lab, the samplers were stored at -80°C until they were ready to be extracted and sequenced.

The filter membrane extraction was performed in the LaRoche Lab, while the sequencing was performed in the IMR lab at Dalhousie. The DNA extraction was performed using the DNeasy plant kit from Qiagen with modifications according to the LaRoche lab protocol; details found in the reference [50]. Once extracted, the DNA concentration and purity were measured using a nanodrop spectrometer. From the extracted DNA, 10 μL was sent to the Integrated Microbiome Resource (IMR) Lab at Dalhousie for 16S V4V5 Illumina Sequencing. Figure 7.4 and Figure 7.5 illustrates the results of the sequencing performed for Test 1 (T1) to

Test 4 (T4). The main objective of Test 1 (T1) to Test 4 (T4) was to validate the eDNA sampler's ability to collect biological samples capable of being successfully sequenced. Test 1 and Test 2 were performed using the eDNA sampler's pull configuration. Test 3 and Test 4 were performed using the eDNA sampler's push configuration. Each Test was performed at different points in time, up to several weeks apart. Each Test had sample water collected within the week the testing took place. The precise composition is not of importance for these initial tests, but the fact that the relative abundance resembles the Bedford Basin historical trends is important.

Figure 7.4 illustrates the eDNA sequencing data in a rarefaction curve. The rarefaction curve plots the observed ASVs vs the sequencing depth. ASVs are clusters of highly related DNA sequences that are treated as a single homogeneous unit; each is assigned to a particular taxonomic group such as species, with multiple ASVs potentially mapping to the same group. Sequencing depth is the number of reads based on the alignment of nucleotides. The observed ASVs increases exponentially as the sequencing depth increases until the plot tapers. The taper in the plot signifies that an adequate sequence depth was used to detect majority of the ASVs in the sample being sequenced. Figure 7.4 compares the filter membranes of each test by comparing the number of observed ASVs. The control samples (MilliQ) are expected to have significantly fewer observed ASVs than the biological samples.

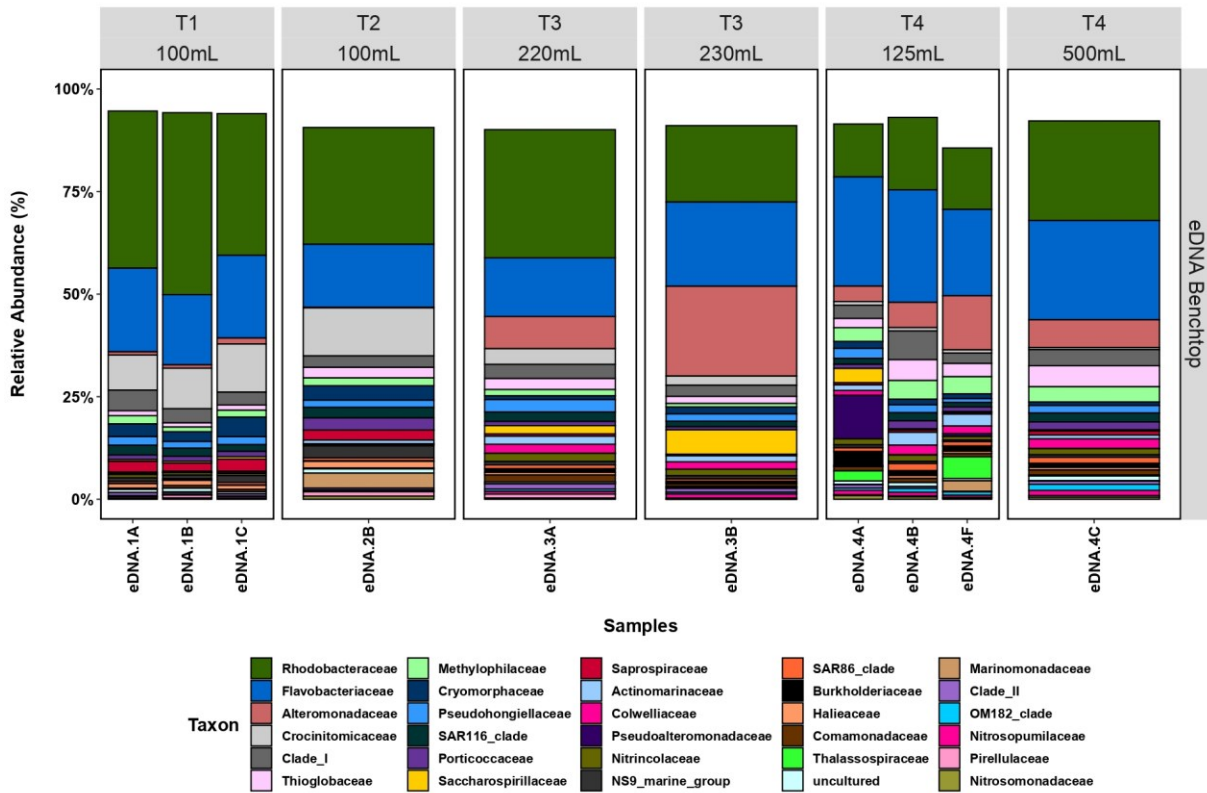


Figure 7.4: Bar plot of top 20 taxon families for T1 to T4 test procedures that were carried out on the eDNA sampler's benchtop unit. T1 and T2 were performed using the pull configuration of the eDNA sampler. T3 and T4 were performed using the push configuration of the eDNA sampler.

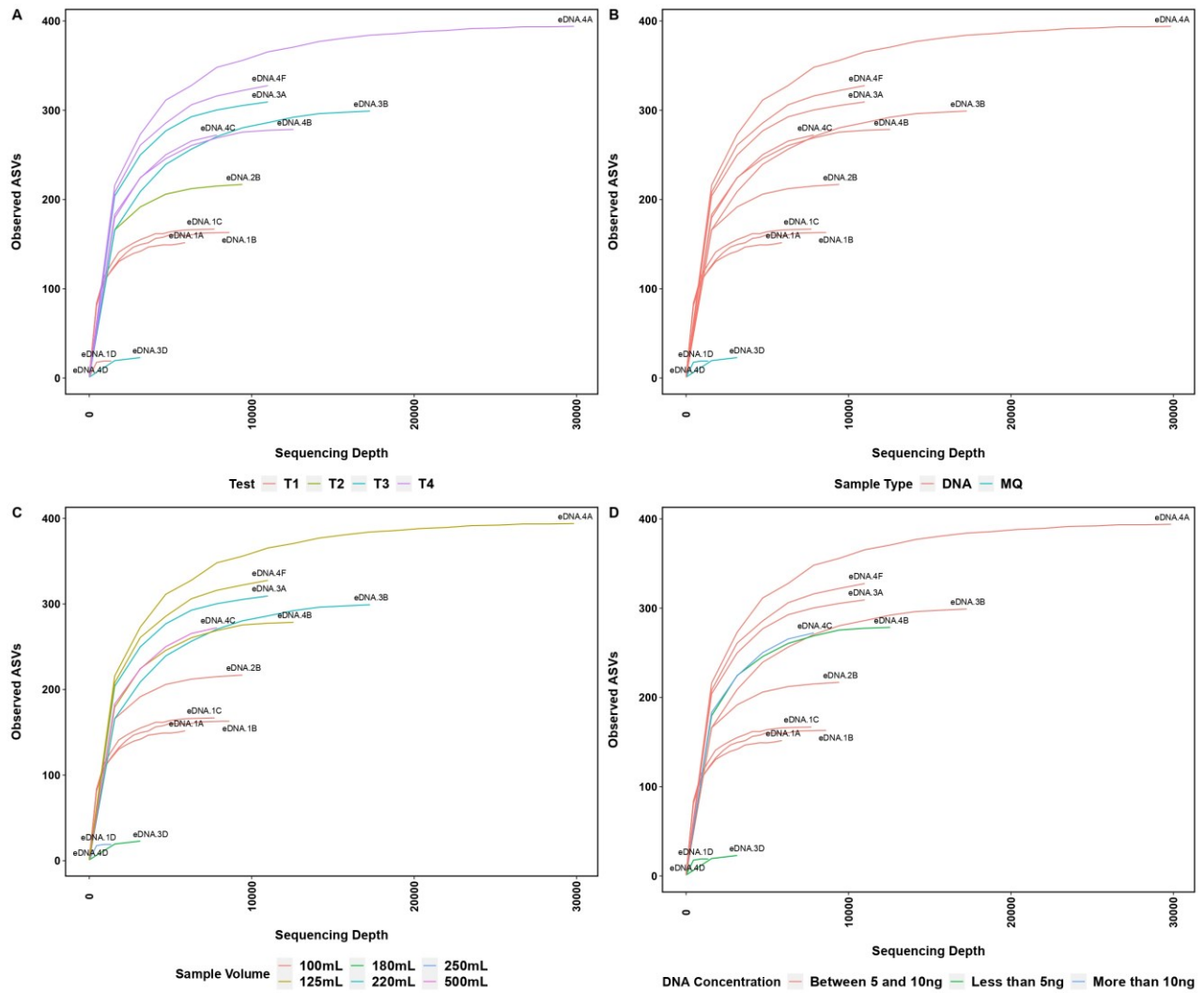


Figure 7.5: Rarefaction curves for observed ASVs and sequence depths. Colour coded based on (a) Test T1 to T4 (b) DNA vs Milli-Q sequences (c) Volume filtered (d) DNA concentration extracted from each sample.

7.3.1 Test 1 (T1) – Pull Configuration

The objective of test T1 was to test the eDNA samplers' effectiveness when using the pull configuration in triplicate. The sample fluid used in this test was collected through BBMP and stored in a refrigerator until it was brought to the Sieben lab for sampling.

Filter membranes, M1 to M4, were used during the sampling protocol for sample capture. However, filter membrane M4 captured purified Milli-Q as a negative control for the test. The filter volume for M1 to M3 was 100 mL, and M4 was 250 mL.

In the results, filter membranes M1 to M4 are referred to as eDNA 1A to eDNA 1D. Figure 7.4 illustrates the top 20 Taxon families found during DNA sequencing. Among the 3 sample captures, a similar relative abundance for the taxon families can be observed. Figure 7.5 illustrates the observed ASVs vs sequencing depth for each sample capture. The observed ASVs for eDNA 1A to eDNA 1C are reasonably similar, while their negative control eDNA 1D showed a small amount of ASVs (~10, compared to ~150 for 1A to 1C) likely due to minor cross-contamination as expected from the dye tests in Chapter 6.

7.3.2 Test 2 (T2) – Pull Configuration

The objective of test T2 was to test the eDNA samplers' effectiveness when using the pull configuration. The sample fluid used in this test was collected through BBMP and stored in a refrigerator until it was brought to the Sieben lab for sampling.

Filter membrane M1 was used during the sampling protocol for sample capture. The filter volume for M1 was 100 mL. In the results, Filter Membranes M1 is referred to as eDNA 2B. Figure 7.4 illustrates the top 20 Taxon families found during DNA sequencing. The filter membrane could be sequenced and showed several taxon families. Figure 7.5 illustrates the observed ASVs vs sequencing depth for each sample capture. The observed ASVs for eDNA 2B (~200) showed a relatively high ASVs count, higher than those collected during Test 1 (~150).

7.3.3 Test 3 (T3) – Push Configuration

The objective of test T3 was to test the eDNA samplers' effectiveness when using the push configuration in duplicate. The sample fluid used in this test was collected through BBMP and stored in a refrigerator until it was brought to the Sieben lab for sampling.

Filter membranes, M1 to M3, were used during the sampling protocol for sample capture. However, filter membrane M3 captured purified Milli-Q as a negative control for the test. The M1, M2 and M3 filter volume was 220 mL, 230 mL, and 180 mL, respectively.

In the results, Filter Membranes M1, M2 and M3 are eDNA 3A, eDNA 3B and eDNA 3D, respectively. Figure 7.4 illustrates a comparable top 20 Taxon families found in eDNA 3A and eDNA 3B. Figure 7.5 illustrates the observed ASVs being similar between eDNA 3A and eDNA 3B. Figure 7.5 also illustrates the negative control eDNA 3D (~10, compared to ~300 for 3A and 3B) as having an insignificant amount of ASVs observed.

7.3.4 Test 4 (T4) – Push Configuration

The objective of test T4 was to test the eDNA samplers' effectiveness when using the push configuration. The test also compares sampling volumes for any noticeable advantages. Additionally, similarities between triplicates were also examined. The sample fluid used in this test was collected through BBMP and stored in a refrigerator until it was brought to the Sieben lab for sampling.

Filter membranes, M1 to M5, were used during the sampling protocol for sample capture. However, filter membrane M5 captured purified Milli-Q as a negative control for the

test. Filter membrane M1 to M3 sampled 125 mL of sample fluid. Filter membranes M4 and M5 sampled 500 mL and 125 mL, respectively.

In the results, Filter Membranes M1, M2 and M3 are eDNA 4A, eDNA 4B and eDNA 4F, respectively. Filter Membranes M4 and M5 are called eDNA 4C and eDNA 4D. Figure 7.4 illustrates a comparable top 20 Taxon families found in which the triplicate eDNA 4A, eDNA 4B, and eDNA 4F. Figure 7.5 illustrates the observed ASVs being similar between samples captured. It can be noted that even though eDNA 4C filtered the largest volume of fluid during this test, its observed ASVs were not larger compared to the other filter membranes (~280, compared to ~400 for 4A, ~310 for 4F and ~280 for 4B). Therefore, filtering 500 mL of sample fluid did not provide different results for detecting the top 20 taxon families compared to filtering 125 mL. However, for rare species, large volumes (litres) may be required [32]. Water turbidity and membrane filter area are the limiting factors for volume of water that can be filtered and are thus not instrument limitations.

7.5 Cross-Contamination Test

Cross-contamination testing was performed on the eDNA sampler to determine the effectiveness of cleaning the benchtop unit before moving the system over to the assembled system. This cross-contamination testing was performed with a bacteria monoculture grown in the LaRoche lab called BB40. The qPCR primer and probe for detecting this bacteria culture are known; thus, no DNA sequencing was needed. Figure 7.6 illustrates the results of the cross-contamination test.

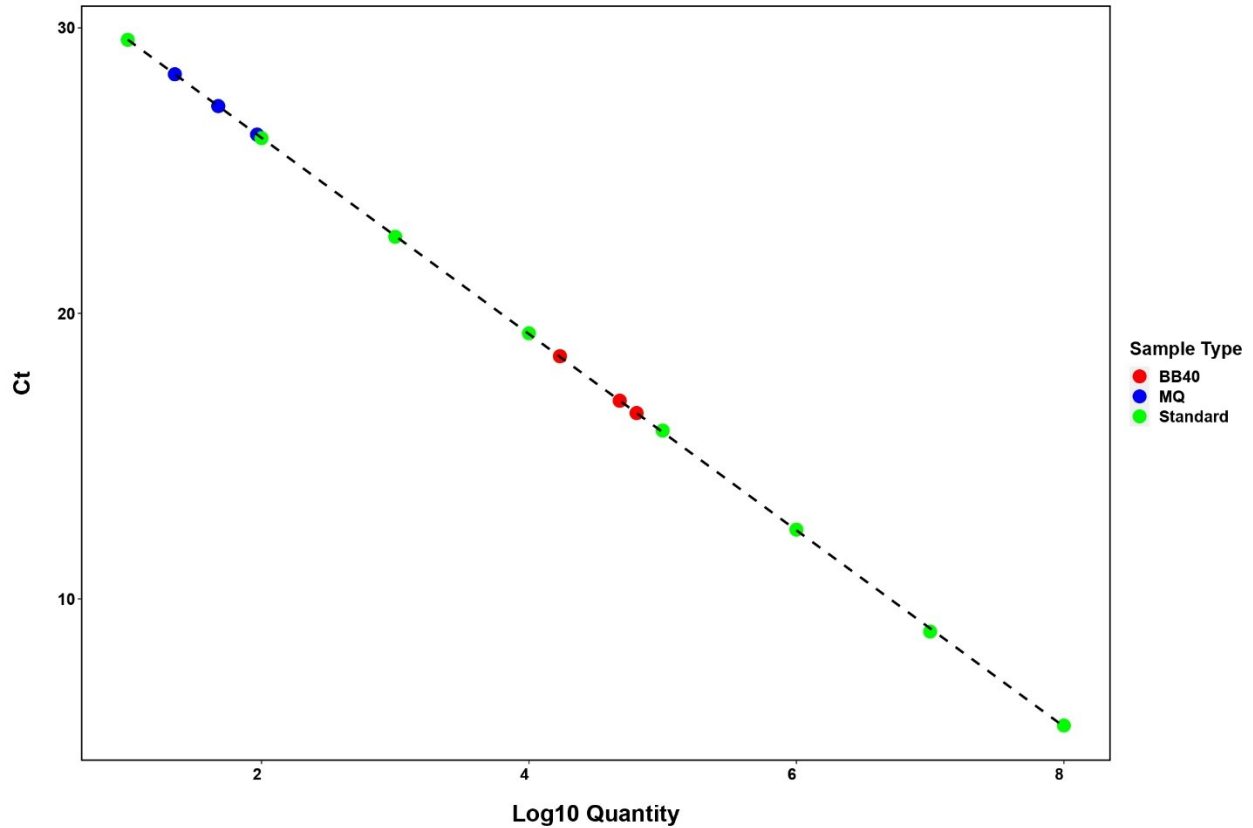


Figure 7.6: Standard curve of threshold cycle (Ct) vs Log10 quantity of BB40 including Ct values from the cross-contamination test performed on the eDNA sampler. Demonstrating less than 0.2% contamination on the eDNA sampler.

A modified version of the sampling protocol illustrated in Figure 5.1 was performed. The modified sampling protocol included an Acid clean step followed by a Milli-Q Flush before executing the sampling protocol steps shown in Figure 5.1 (a).

The cross-contamination test was performed with filter membranes M1 to M6, in which each filter collected 125 mL of sample fluid. The sample fluid used by the eDNA sampler alternated between purified Milli-Q water and the bacteria monoculture BB40. The sampling protocol shown in Figure 5.1 was performed. The filter used during this testing was the 25 mm, 0.2 μm PC membranes housed in Advantec polypropylene filter housings. Immediately after the sample capture step of the sampling protocol, the filter membrane was removed using sterile

equipment so as not to introduce contaminants. The filter membrane was then placed in a 2 mL screwcap tube and immediately frozen in a CryoShipper for transport back to the LaRoche lab. Once at the LaRoche lab, the samplers were stored at -80 °C until they were ready to be extracted and processed.

Figure 7.6 illustrates the results of the cross-contamination test, Table 7.2 shows the mean quantity of BB40 collected on each filter membrane. The results show that the purified Milli-Q filter samples measured a BB40 quantity of less than 0.2%. This reduction in BB40 quantity demonstrates that the cleaning procedure of the eDNA sampler was capable of reducing the cross-contamination between filter membrane capture events, but there is room for further optimization.

Table 7.2: Mean quantity of BB40 bacteria monoculture captured on filter membranes during cross-contamination testing.

Sample Name	Mean Quantity	Remaining percentage
BB40-A	78843	0.118%
MQ-A	93	
BB40-B	49542	0.046%
MQ-B	23	
BB40-C	64620	0.074%
MQ-C	48	

7.6 Conclusion

The tests performed on the eDNA sampler's benchtop setup were capable of verifying the effectiveness of the eDNA sampler's design. The eDNA sampler could perform multiple sample captures, self-clean and preserves samples when required. The samples captured were successfully extracted and sequenced in laboratory. Cross-contamination was minimal, less than 0.2%, indicating that variance in the relative abundance was due to inadequate mixing and subsampling. The novel eDNA sampler design is now ready to be packaged in a submersible enclosure and compared in field to the traditional approach of using Niskin bottles, described in the next Chapter.

Chapter 8 Submersible eDNA Sampler

This chapter is based on the published manuscript “Compact and Automated eDNA Sampler for in situ Monitoring of Marine Environments” by Andre Hendricks et al. [43]. The compact and automated eDNA sampler is the final stage of the eDNA sampler that is submersible and currently commercially available. This submersible housing design helps the eDNA sampler to accomplish requirements 1, 4 and 9 of the novel eDNA sampler in Table 2.2. The entire mechanical design was created by Dartmouth Ocean Technologies Inc., while the entire electrical, fluidic and software design was my thesis work described in the preceding chapters. This is the first field validation of the novel eDNA sampler.

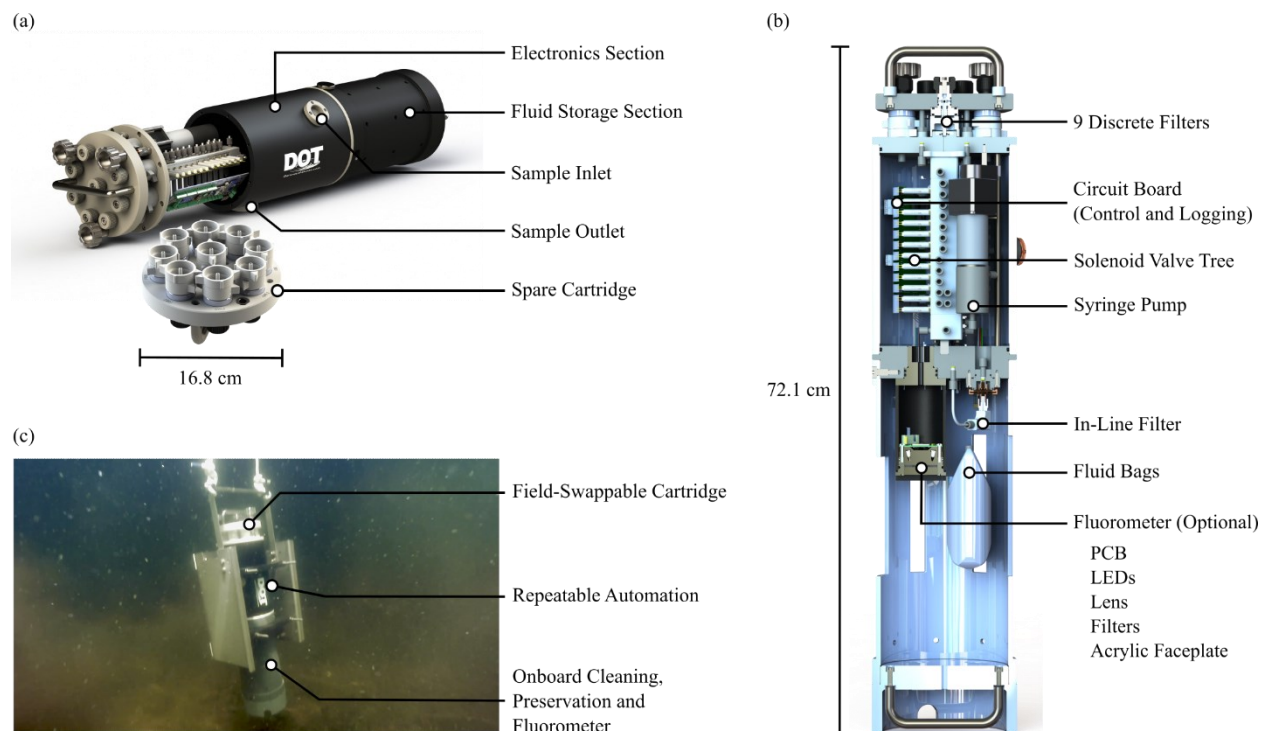


Figure 8.1: Submersible eDNA sampler (a) 3D CAD rendering of the DOT eDNA sampler with partially exposed electronics section. (b) Cross-sectional view of the DOT eDNA sampler, highlighting all compartments, fluid storage bags and attached fluorometer. (c) Fully built DOT eDNA sampler deployed underwater. Reprint from [43].

8.1 System Description

Dalhousie University has collaborated with Dartmouth Ocean Technologies, Inc. (DOT) to create a novel eDNA sampler that features a simple modular approach that has three detachable sections: filter cartridge, electronics section, and fluid storage section, shown in Figure 8.1. The fully assembled unit has a length of 72.1 cm and a width of 16.8 cm, weighing 11.3 kg in air and 3.3 kg in salt water. It is capable of cleaning between sample captures, preservation of captured samples and has 9 discrete filters, each 25 mm in diameter. Different filter membranes can be loaded into the filter holders (Advantec 43303010, Polypropylene), thus allowing for a wide variety of membrane materials and pore sizes to be used based on targeted species. The eDNA sampler's filter cartridge is made from Polyetheretherketone (PEEK) material and holds the 9 filter holders. Once the filter cartridge is loaded with clean filters it can be attached to the electronics section of the eDNA sampler. This fast swap approach allows for multiple filter cartridges to be prepared and then loaded into the sampler as needed. The filter cartridge is secured by 3 knobs that are indexed to the electronic section to avoid assembly error.

The eDNA sampler's electronics section is the core of the instrument. It houses a pump and custom valve tree, along with a custom printed circuit board (PCB) for automation and data logging. The PCB and software are detailed in Chapter 4 and Chapter 5, respectively. The valve tree consists of the fluid routing manifold, a pressure sensor, tubing inter-connections, and solenoid valves for the sampler. The valve tree also has ports that are used to fluidically couple to the filters on the filter cartridge, and to access the fluid bags loaded with reagents and stored in the fluid section of the sampler. The eDNA sampler draws 1 W at idle and 10 W at peak.

The eDNA sampler's fluid storage section houses and protects all the required fluids and an optional fluorometer. The fluids stored in this section are as follows: 5% hydrochloric acid (HCl) (cleaning), RNAlater (preservation), purified Milli-Q water (rinsing) and waste. The fluids are stored in 100 and 500 mL Labtainer™ BioProcess Containers (BPC) and connected to the Electronics section with 1/4 - 28 tapped ports. The waste bag is used to hold chemicals that are deemed not safe to flush into the ocean or surrounding waters. RNAlater is used to preserve the collected samples, 5% HCl is used to clean the system fluid lines and backflow the sample inlet, and Milli-Q is used to flush the system between protocol steps. The 5% HCl and Milli-Q are effective at reducing cross-contamination that might take place in the system tubing and manifolds between sampling events. HCl and RNAlater used in this study were of analytical grade and supplied by Fisher Chemical (Waltham, MA, USA).

8.2 Halifax Harbour Deployment

8.2.1 Field Sample Collection

As a first test of how this eDNA sampler performs *in situ*, the sampler was deployed during a transect of the Halifax Harbour into the Bedford Basin, shown in Figure 8.3. The unit was deployed 5 m deep and the first portion of the sampling protocol was run, where 125 mL of water was filtered through a 25 mm diameter, 0.22 µm polycarbonate (PC) membrane (Millipore). The sampler was deployed for the entire time the boat was on station (15-17 min), ensuring the full 125 mL was captured. After pulling the sampler back on deck, the second portion of the script was run, where 6 mL of RNAlater was pumped across the membrane for preservation and the “Acid Clean” step was performed. Due to the time constraints of maintaining station, this 2-step approach was implemented; however, both steps are trivial to

combine when the sampler is deployed as intended and without human intervention. Samples were stored in RNeasy in the cassette overnight, after which they and the 35 µm pre-filter were removed and stored short-term in a -20 °C freezer, then longer term in a -80 °C freezer prior to extracting the DNA. Though the sampler preserves the samples with RNeasy automatically, filters were frozen as recommended for long term storage due to the unknown timeline between the transect and DNA extraction.

Comparative bottle samples were taken at the same stations directly next to the sampler using a 5 L Niskin bottle attached to a rope. The bottle samples were taken at the same time and depth as the eDNA sampler. These bottle samples were then filtered in duplicate on deck using a peristaltic pump through 47 mm diameter, 0.22 µm PC membranes (Millipore). Between 660-1140 mL of water was filtered for each duplicate, after which membranes were immediately frozen in a cryoshipper primed with liquid nitrogen. Prior to deployment, the Niskin bottle was thoroughly cleaned using 5% HCl. The protocol is to rinse the Niskin bottle immediately after use with tap water to remove the salt. Afterwards, ¼ of the Niskin bottle is filled with 5% HCl. The bottle is rotated and shaken while closed to ensure the 5% HCl comes into contact with the entire surface area. Lastly, the bottle is rinsed with Milli-Q by filling ¼ of the bottle and shaking it. The Milli-Q rinse is repeated twice to remove the 5% HCl. Once clean, the bottle can be used or stored in a clean storage bin. The Niskin bottle was not cleaned between samples during deployment due to the short 1-day deployment.

8.2.2 DNA Extraction and Sequencing

The Qiagen DNeasy plant mini kit was used to extract DNA from all samples using a modified protocol based on Zorz *et al.* 2019 [50] with the following additional modifications: samples

were incubated at 52 °C for 1 hour and the same 50 µl of elution buffer from Qiagen (AE buffer) was used to elute the DNA twice to ensure maximum DNA concentrations were extracted. After extraction, 10 µl of DNA from each sample was sent for Illumina sequencing at the Integrated Microbiome Resource Lab (IMR) at Dalhousie University. DNA was sequenced for the V4-V5 region of the 16S ribosomal RNA gene according to IMR standard operating procedure using primers 515F = 5'-GTGYCAGCMGCCGCGGTAA-3' and 926R = 5'-CCGYCAATTYMTTTRAGTTT-3' [51], [52].

8.2.3 Bioinformatics

Sequences were processed according to the Microbiome Helper developed by IMR [53] using QIIME2 2019.7 [54]. Deblur (QIIME2 plugin version 2019.7) [55] was used to denoise sequences as well as identify and label individual amplicon sequence variants (ASVs) [56]. ASVs are clusters of highly related DNA sequences that are treated as a single homogeneous unit; each is assigned to a particular taxonomic group such as species, with multiple ASVs potentially mapping to the same group. After identification, ASVs were classified using the SILVA 132 database [57], [58] as well as the PhytoREF database [59] for further classification of chloroplast sequences. Two ASV tables were created from this data: one with the raw ASV counts, and a second where raw ASV counts were rarefied to 4000 so relative abundance could be compared between samples. Rarefaction is a normalization process through which samples of differing sizes are subsampled to a normalized threshold [60]. The rarefaction curve for this deployment is illustrated in Figure 8.2. All plots were made using RStudio [61] using the following packages: UpSetR [62], Phyloseq [63], ggplot2 [64], and ggpmisc [65].

8.2.4 Results

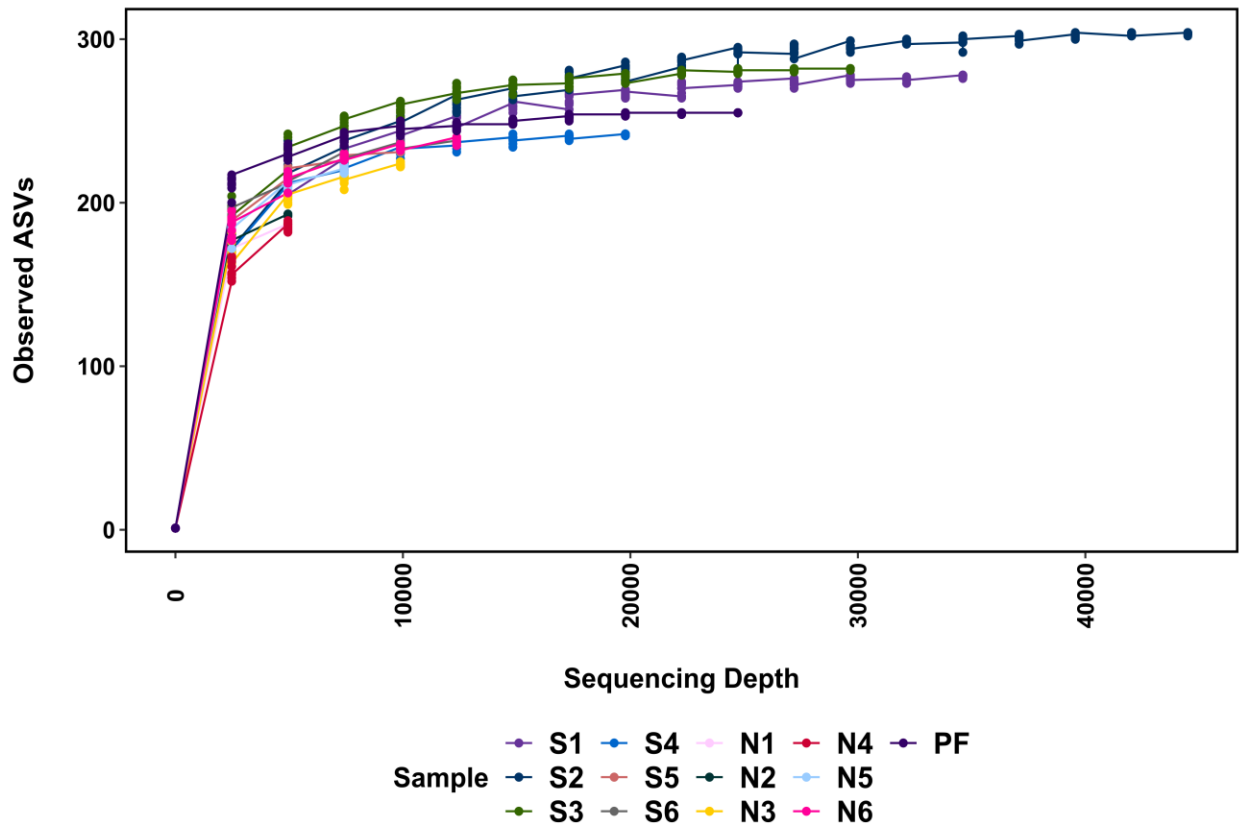


Figure 8.2: Rarefaction curves for all samples. S1 to S6 are the samples acquired from the eDNA sampler, while N1-N6 are the samples acquired from the Niskin bottle captures. PF is the 35 micron pre-filter on the eDNA sampler. Reprint from [43].

8.2.5.1 DNA Extraction and Sequencing

In total, 6 stations were sampled in the first field deployment of the eDNA sampler; the coordinates and the time at which samples were taken can be found in Table 8.1. The map of stations sampled is shown in Figure 8.3. At 2 out of the 6 stations, S2 and S6, the pre-set target volume was not reached. This was due to the transmembrane pressure reaching the threshold, with enough material accumulated to block the filter membrane, therefore the time threshold of staying on the station was met before the volume threshold. The remaining stations, S1, S3, S4, and S5 had 100% of the sample captured, as shown in Table 8.2. Table 8.2 outlines various

metrics regarding the extracted DNA and raw sequencing data for each transect sample and the pre-filter. Although eluted DNA concentrations were lower in samples collected using the sampler, when considering the difference in volume filtered, the original source DNA concentration (i.e. marine water) is comparable between the Niskin and sampler, but not identical as DNA extractions are not 100% efficient. As well, the pre-filter had a lower eluted DNA concentration and nearly 0 ng/mL in the original sample.

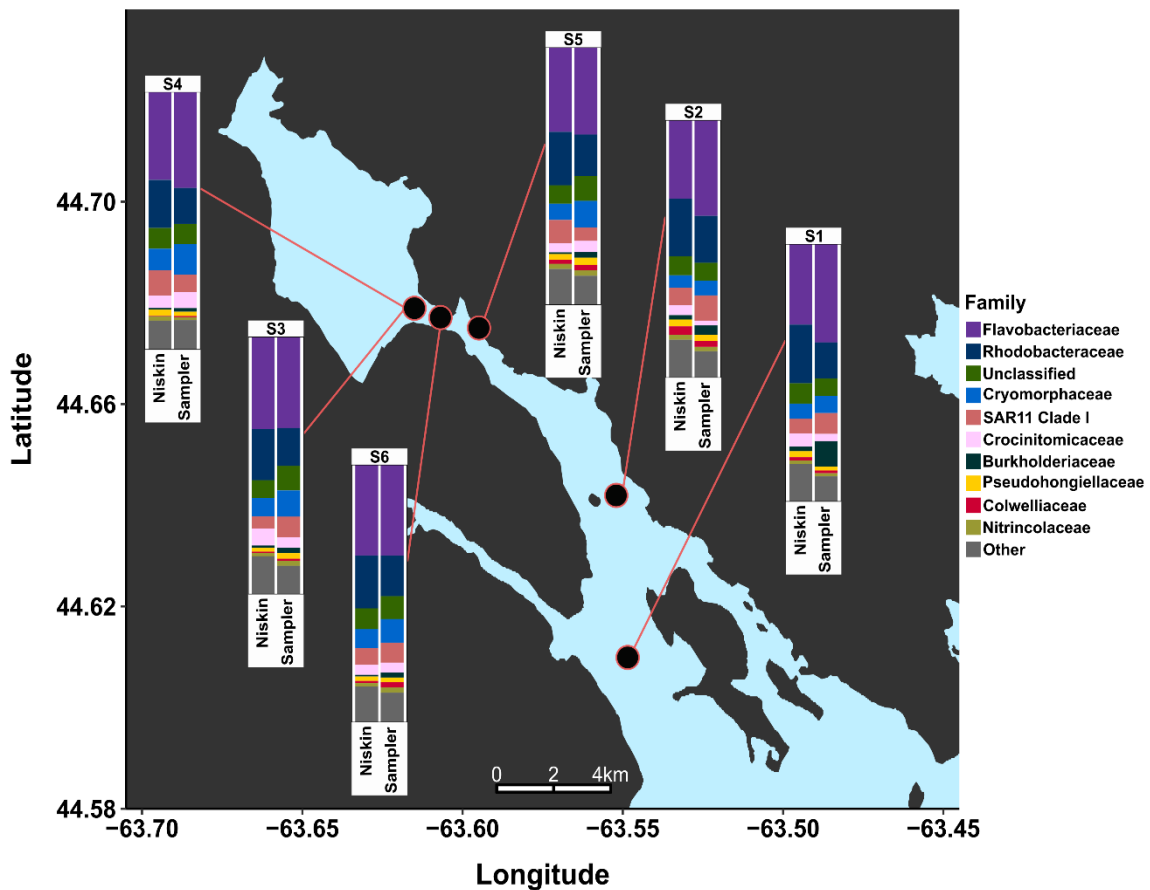


Figure 8.3: Map of Halifax Harbour sampling locations. Stations are numbered in sequential order with S1 being first and S6 last. Samples at S3 and S4 were taken at the same location approximately 2 hours apart. Stacked bar plots highlight the top 10 relatively abundant bacterial taxonomic families at each sampling station for all samples. All ASVs not within the top 10 families are represented as "Other". Reprint from [43].

Table 8.1: Coordinates and time sampled for each of the 6 stations where a successful deployment occurred. S3 and S4 represent samples taken at the same location at different times. Reprint from [43].

Station	Coordinates	Time Sampled
S1	44.36947 N, 63.32909 W	10:15
S2	44.640941 N, 63.552115 W	11:15
S3	44.680485 N, 63.622483 W	12:45
S4	44.680485 N, 63.622483 W	14:40
S5	44.674603 N, 63.595273 W	15:15
S6	44.670648 N, 63.592853 W	16:02

Table 8.2: DNA metrics of eDNA sampler and Niskin samples at each station (S1-S6) and the pre-filter (PF). DNA in the original sample was back calculated from the concentration of eluted DNA using the elution volume (50 μ L for all samples). The 260/280 ratio is presented as an indicator of purity. While 260/280 ratio values are expected to be 1.8 for DNA and 2.0 for RNA, the actual ratio is a factor of the nucleic acid composition as well as the pH of the solution [66]. Reprint from [43].

Station	Method	Sample Volume (mL)	Eluted DNA (ng/ μ L)	DNA in Sample (ng/mL)	260/280 Ratio	Number of Raw Reads	Number of ASVs
S1	Sampler	125	8.3	3.3	2.23	37081	278
	Niskin	760	97.3	6.4	1.91	5511	187
S2	Sampler	111	4.9	2.2	2.05	46863	304
	Niskin	740	57.8	3.9	1.9	5404	193
S3	Sampler	125	10.6	4.2	2.15	30270	282
	Niskin	770	93.8	6.1	1.86	11839	225
S4	Sampler	125	16.4	6.6	2.05	20218	242
	Niskin	660	55.1	4.2	1.89	6901	191
S5	Sampler	125	4.7	1.9	2.27	10675	233
	Niskin	880	35.5	2.0	1.92	8972	223
S6	Sampler	114	9.4	4.1	2.15	12667	238
	Niskin	1140	68.5	3.0	1.92	14000	240
PF	Sampler	875	3.1	0.2	2.48	25100	255

8.2.5.2 Community Composition

Figure 8.3 shows the 10 families with the highest relative abundance at each station for both collection methods, also shown side by side in Figure 8.4. The two collection methods returned the same top families in near-identical relative abundance, demonstrating that the sampler was able to capture the same community composition of common microbes as the Niskin. All of the 10 most-abundant families were found in all 12 samples, with Rhodobacteraceae having the greatest difference in relative abundance between Niskin and sampler at 5 out of 6 stations (9% in S1, 5% in S3-S6) and Flavobacteraceae having the greatest difference in S2 (6%). The difference between all other taxa at each station was less than 5% with the exception of Burkholderiaceae. The family Burkholderiaceae showed high variance at site S1 (sampler: 10%, Niskin: 2%) and to a lesser extent S2 (sampler: 4%, Niskin: 2%). This was due to a particular ASV classified as *Ralstonia picketti*, which was found in all of the sampler samples, but none of the Niskin samples. Though it is not shown, analysis of the phytoplankton community showed a strong bloom of Thalassiosirales which presented as a single ASV dominating both sample types (Niskin and sampler) at all stations, ranging from 30% of all chloroplast reads in S4 Niskin to 60% in S3 Niskin. No evidence of Thalassiosirales was found in the pre-filter sample.

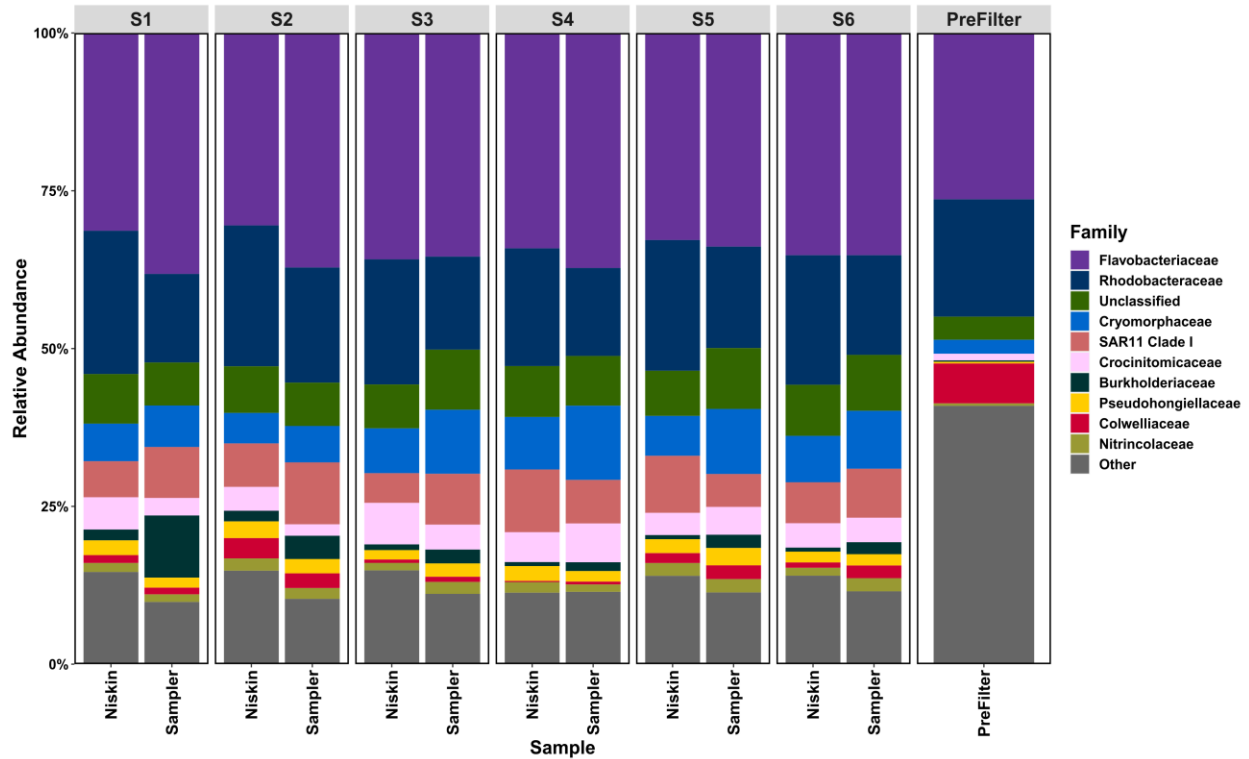


Figure 8.4: Stacked bar plot highlighting the top 10 relatively abundant bacterial taxonomic families at each sampling station for all samples as well as the pre-filter. ASVs were rarefied to 4000 to obtain relative abundance and all ASVs not within the top 10 families are represented as "Other". Reprint from [43].

The Niskin and eDNA sampler results were also quantitatively similar at the level of individual ASVs. Figure 8.5 shows the correlation between sampler ASVs and Niskin ASVs (both bacterial and phytoplankton) at each site. R^2 values ranged from 0.71 to 0.93, with later stations having higher R^2 values than stations S1 and S2. The *Ralstonia picketti* ASV mentioned previously is highlighted in red, and has higher counts in S1 and S2 (7.5% and 2% of total counts respectively), with lower abundance in stations S3-S6 ($\leq 1\%$ of total counts).

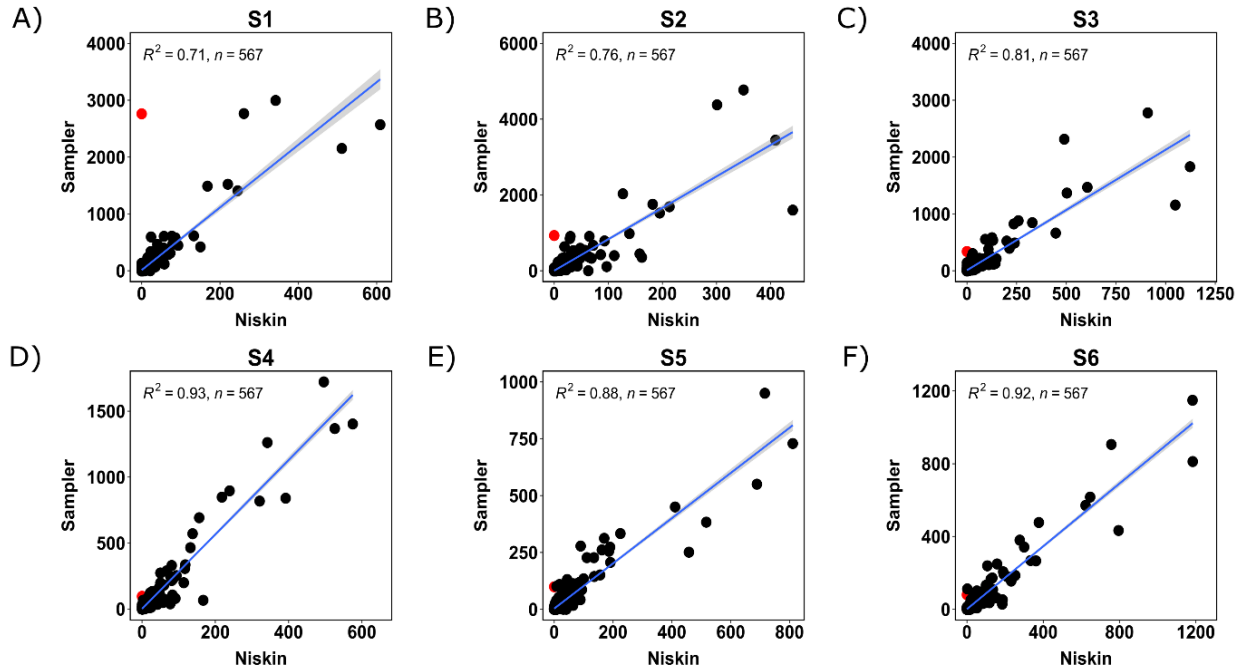


Figure 8.5: Scatterplots showing raw counts of all ASVs in samples from each collection method plotted against each other. The single red point indicates the raw counts of *Ralstonia picketti*, a potential contaminant found only in the sampler. The contaminant decreases with more utilization of the sampler, from S1 to S6, indicating that new samplers must be thoroughly cleaned after assembly to remove contaminants. Reprint from [43].

Lastly, we examined the patterns of presence and absence of each ASV across the 13 sampler, Niskin, and pre-filter samples. The most common presence/absence pattern included 190 ASVs that were found only in the pre-filter sample (Figure 8.6); however, these account for less than 10% (20,936 of 235,501 sequences collected from all samples). By contrast, only 65 ASVs were found in the pre-filter and at least one other sample. A total of 124 ASVs were found in all twelve Bedford Basin sample sites, 24 of which were also recovered from the pre-filter. Of these, the 100 ASVs recovered only from Bedford Basin sites accounted for 171,345 sequences (72.8%) while the 24 ASVs recovered from all samples accounted for 23,341 sequences (10.0% of all recovered sequences). No other presence / absence pattern was exhibited by more than seven ASVs, and the majority of patterns were observed once or twice in the pool of ASVs. These results further demonstrate the homogeneity of the samples across stations and the

consistency between the sampler and Niskin datasets. A total of 4308 sequences were assigned to the probable contaminant *Ralstonia pickettii* across all eDNA sampler samples; these decreased in count from 4308 in sample S1 to 80 in the final sample S6.

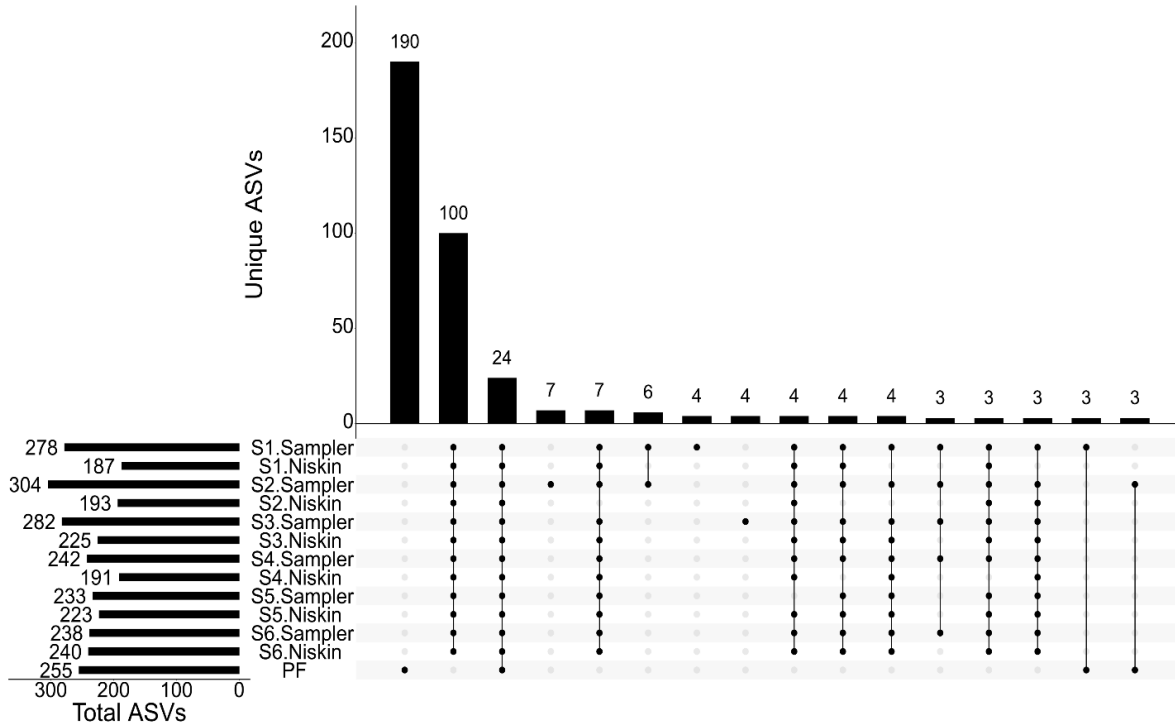


Figure 8.6: Upset plot of ASVs in each sample as well as the pre-filter (PF). Each column shows the count of ASVs with the occurrence pattern indicated by the black dots with the associated samples. The total number of ASVs associated with each sample is shown on the left. Sets of samples with 3 or more associated ASVs are shown here, with sample combinations returning ASVs occurring only once or twice not shown. Reprint from [43].

8.2.5 Discussion

The results presented in this chapter detail the successful testing and deployment of a novel eDNA sampler. When compared to the concurrent 7 Niskin bottle samples, the sampler captured a near-identical community for both bacteria and phytoplankton at all stations. This is despite differences in the protocol such as volume filtered and temporal resolution, aligning with prior studies, which have shown similar results [67], [68]. A recent study performed using the 3G ESP

also demonstrated that results were equivalent between autonomous and manual sampling [69]. Interestingly, sample volumes in the ESP study were reversed where the autonomous sampler filtered a higher volume (1 L), and the manual sampling filtered a lower volume (36 mL-100 mL) [69]. Our protocol generated comparable results with a lower autonomous sampler volume, which allows sampling time to be kept to a minimum.

Another difference between the sampler and Niskin methods is the 35 μm pre-filter fitted on the inlet of the sampler due to particle limitations on the pump and valves. However, results here show that the pre-filter did not affect results as the sampler still picked up the community in the water column. Keeping the pre-filter is advantageous because it allows the sampler to remain at a small, portable size, allowing for easier field deployment, particularly on small vessels with little deck space. The pre-filter also did not affect results through clogging, due to the cleaning protocol and pre-sample flushes which include a backflush through the inlet, thereby pushing material off the pre-filter.

The one noticeable discrepancy between samples was that an ASV classified as *Ralstonia picketti* was found in all sampler results but none of the Niskin results. This bacterium is commonly found in the environment and is capable of growing on plastics [70], meaning it was likely a form of contamination in the sampler from previous testing. Despite the prevalence of this bacteria, the raw counts and relative abundance decreased rapidly in subsequent sampling, indicating the cleaning protocol was clearing the bacterium out of the lines with each sample. Therefore, with optimization, the cleaning protocol can prevent contamination in the future.

The cleaning protocol can be optimized using different chemicals, increased concentration of chemical, flow rate optimization, and longer exposure time. Additionally, the use of different wetted materials can be explored so to minimize the risk of adhesion and growth of unwanted organisms such as *Ralstonia picketti* within the eDNA sampler. For biofouling on the outside of the instrument, copper material could be added.

In conclusion, these results demonstrate the successful testing and deployment of a novel, autonomous eDNA sampler capable of both cleaning and preservation, and includes a field-swappable cartridge. These aspects are beneficial for research and monitoring, particularly in remote locations and over extended periods of time in areas such as Marine Protected Areas (MPAs). Future studies of the system will include cleaning optimization as well as fluorometer integration and collaborative testing of the system in multiple deployment scenarios. Overall, this eDNA sampler will expand the use of eDNA in monitoring programs, making it more accessible and convenient than traditional sampling methods.

Chapter 9 Conclusion and Future Work

9.1 Thesis Conclusion

This thesis describes developing and testing a novel eDNA sampler starting from the ground up. Chapter 3 described the fluidic architecture of the eDNA sampler and the components required to operate the system fluidically. Chapter 4 describes the design of the eDNA samplers PCB, which is the core electrical component in the eDNA sampler. Chapter 5 described the software architecture that enabled the eDNA sampler to run in real time and perform sample capture. Chapter 6 described the unit tests to validate the eDNA sampler's software and fluidic design. Chapter 7 described the benchtop testing performed with the eDNA sampler to assess its ability to collect biological samples capable of being successfully sequenced. Finally, chapter 8 concludes the work done in this thesis by using turning the benchtop eDNA sampler into a submersible unit, then testing that submersible unit in the Halifax Harbour during a transect by comparing it to the gold standard of Niskin bottle samples. The submersible eDNA sampler produced results comparable to the Niskin bottle approach. The submersible eDNA sampler is at a Technology Readiness Level (TRL) 7 [71]. The prototype is at an operation level and demonstrated in the marine environment. However, to attain TRL 8 and 9 multiple month studies must be completed in a variety of conditions (temperature, pressure, turbidity). These have been planned for 2023/2024 and will be the focus of subsequent publications.

9.2 Suggested Future Work

The design of a submersible eDNA sampler was a success. Nevertheless, several approaches can be taken to improve the design of the eDNA sampler. These approaches include pairing the

eDNA sampler with a fluorometer, optimizing the sampling protocol used on the eDNA sampler and improving the power consumption on the eDNA sampler. The eDNA sampler has a limited amount of filters to use per deployment. As such, pairing a fluorometer would allow for triggering based on fluorometer readings above a threshold. This triggering type would increase the likelihood of capturing algae blooms and detecting the species causing them.

Optimizing the sampling protocol would allow the eDNA sampler to reduce cross-contamination and possibly reduce chemical usage so that the cost per deployment of the system is lessened. Finally, reducing the power consumption of the eDNA sampler during idle would allow for more extended system deployment times. I anticipate that the work done in this thesis will promote further improvements to the designed eDNA sampler and promote the use of this eDNA sampler in further studies.

eDNA analysis is being widely adopted globally in nearly every sector that is involved with biological/ecological systems. This adaption includes conservation efforts, fisheries, environmental engineering and public health [72]. With this adoption, eDNA has provided a non-invasive, time and cost-efficient method of monitoring the effects of offshore wind farms on the surrounding environment [73], surveying locations for endangered/declining population/invasive aquatic species [15], [17] and monitoring the biodiversity in MPAs [36], to state a few use cases. The novel eDNA sampler in this thesis is highly applicable to these global sectors.

References

- [1] J. C. Y. Ng and J. M. Y. Chiu, "Changes in biofilm bacterial communities in response to combined effects of hypoxia, ocean acidification and nutrients from aquaculture activity in Three Fathoms Cove," *Mar Pollut Bull*, vol. 156, p. 111256, Jul. 2020, doi: 10.1016/j.marpolbul.2020.111256.
- [2] E. Rastelli *et al.*, "A high biodiversity mitigates the impact of ocean acidification on hard-bottom ecosystems," *Sci Rep*, vol. 10, no. 1, p. 2948, Dec. 2020, doi: 10.1038/s41598-020-59886-4.
- [3] J. Rensel and J. N. C. Whyte, "Finfish mariculture and harmful algal blooms," in *Manual on harmful marine microalgae*, UNESCO, 2003, pp. 693–722.
- [4] D. M. Anderson, P. Hoagland, Y. Kaoru, and A. W. White, "Estimated Annual Economic Impacts from Harmful Algal Blooms (HABs) in the United States," Woods Hole Oceanog.Inst., Sep. 2000. Accessed: Sep. 08, 2022. [Online]. Available: <https://apps.dtic.mil/sti/citations/ADA386861>
- [5] "COP15 ends with landmark biodiversity agreement," *UNEP*, Dec. 20, 2022. <http://www.unep.org/news-and-stories/story/cop15-ends-landmark-biodiversity-agreement> (accessed Mar. 29, 2023).
- [6] K. D. Goodwin *et al.*, "DNA Sequencing as a Tool to Monitor Marine Ecological Status," *Front Mar Sci*, vol. 4, 2017, doi: 10.3389/fmars.2017.00107.
- [7] K. M. Ruppert, R. J. Kline, and M. S. Rahman, "Past, present, and future perspectives of environmental DNA (eDNA) metabarcoding: A systematic review in methods, monitoring, and applications of global eDNA," *Glob. Ecol. Conserv.*, vol. 17, p. e00547, Jan. 2019, doi: 10.1016/j.gecco.2019.e00547.
- [8] R. Hinlo, D. Gleeson, M. Lintermans, and E. Furlan, "Methods to maximise recovery of environmental DNA from water samples," *PLOS ONE*, vol. 12, no. 6, p. e0179251, Jun. 2017, doi: 10.1371/journal.pone.0179251.
- [9] M. Bentzon-Tilia, E. C. Sonnenschein, and L. Gram, "Monitoring and managing microbes in aquaculture – Towards a sustainable industry," *Microb Biotechnol*, vol. 9, no. 5, pp. 576–584, 2016, doi: 10.1111/1751-7915.12392.
- [10] T. Cordier, A. Lanzén, L. Apothéloz-Perret-Gentil, T. Stoeck, and J. Pawlowski, "Embracing Environmental Genomics and Machine Learning for Routine Biomonitoring," *Trends Microbiol*, vol. 27, no. 5, pp. 387–397, May 2019, doi: 10.1016/j.tim.2018.10.012.

- [11] C. Moncada, C. Hassenrück, A. Gärdes, and C. Conaco, "Microbial community composition of sediments influenced by intensive mariculture activity," *FEMS Microbiol Ecol*, vol. 95, no. 2, Feb. 2019, doi: 10.1093/femsec/fiz006.
- [12] M. Y. Stoeckle, J. Adolf, Z. Charlop-Powers, K. J. Dunton, G. Hinks, and S. M. VanMorter, "Trawl and eDNA assessment of marine fish diversity, seasonality, and relative abundance in coastal New Jersey, USA," *ICES J. Mar. Sci.*, vol. 78, no. 1, pp. 293–304, Feb. 2021, doi: 10.1093/icesjms/fsaa225.
- [13] S. E. Alter, C. D. King, E. Chou, S. C. Chin, M. Rekdahl, and H. C. Rosenbaum, "Using Environmental DNA to Detect Whales and Dolphins in the New York Bight," *Front. Conserv. Sci.*, vol. 3, p. 820377, Feb. 2022, doi: 10.3389/fcosc.2022.820377.
- [14] S. Huang, K. Yoshitake, S. Watabe, and S. Asakawa, "Environmental DNA study on aquatic ecosystem monitoring and management: Recent advances and prospects," *J. Environ. Manage.*, vol. 323, p. 116310, 2022, doi: <https://doi.org/10.1016/j.jenvman.2022.116310>.
- [15] A. C. Thomas, J. Howard, P. L. Nguyen, T. A. Seimon, and C. S. Goldberg, "eDNA Sampler: A fully integrated environmental DNA sampling system," *Methods Ecol. Evol.*, vol. 9, no. 6, pp. 1379–1385, 2018, doi: <https://doi.org/10.1111/2041-210X.12994>.
- [16] "EDNA SAMPLER BACKPACK COMBO," *Smith-Root, Inc.* <https://store.smith-root.com/products/edna-sampler-backpack-lith-combo> (accessed Mar. 05, 2023).
- [17] K. L. Pope, C. S. Goldberg, N. L. Nelson, A. K. Cummings, T. Seaborn, and J. Piovita-Scott, "Designing environmental DNA surveys in complex aquatic systems: Backpack sampling for rare amphibians in Sierra Nevada meadows," *Aquat. Conserv. Mar. Freshw. Ecosyst.*, vol. 30, no. 10, pp. 1975–1987, 2020, doi: 10.1002/aqc.3444.
- [18] K. P. Nolan *et al.*, "Detection of brook trout in spatiotemporally separate locations using validated eDNA technology," *J. Environ. Stud. Sci.*, vol. 13, no. 1, pp. 66–82, Mar. 2023, doi: 10.1007/s13412-022-00800-x.
- [19] *CLAM Application Sheet*. Aqualytical. [Online]. Available: <https://aqualytical.com/wp-content/uploads/2018/02/Application-Sheet-1.pdf>
- [20] A. L. Coes, N. V. Paretti, W. T. Foreman, J. L. Iverson, and D. A. Alvarez, "Sampling trace organic compounds in water: A comparison of a continuous active sampler to continuous passive and discrete sampling methods," *Sci. Total Environ.*, vol. 473–474, pp. 731–741, Mar. 2014, doi: 10.1016/j.scitotenv.2013.12.082.
- [21] *CLAM Product sheet*. Aqualytical. [Online]. Available: https://aqualytical.com/documents/Technical-Info-Library/Posters/CLAM-Poster_Product-Description.pdf

- [22] N. Formel, I. C. Enochs, C. Sinigalliano, S. R. Anderson, and L. R. Thompson, "Subsurface automated samplers for eDNA (SASe) for biological monitoring and research," *HardwareX*, vol. 10, p. e00239, 2021, doi: <https://doi.org/10.1016/j.ohx.2021.e00239>.
- [23] *PPS Datasheet*. McLane. [Online]. Available: <https://mclanelabs.com/wp-content/uploads/2022/03/McLane-PPS-Datasheet.pdf>
- [24] D. J. McGillicuddy *et al.*, "A red tide of *Alexandrium fundyense* in the Gulf of Maine," *Deep Sea Res. Part II Top. Stud. Oceanogr.*, vol. 103, pp. 174–184, May 2014, doi: 10.1016/j.dsr2.2013.05.011.
- [25] L. A. Winslow *et al.*, "Autonomous Year-Round Sampling and Sensing to Explore the Physical and Biological Habitability of Permanently Ice-Covered Antarctic Lakes," *Mar Technol Soc J*, vol. 48, no. 5, pp. 8–17, Sep. 2014, doi: 10.4031/MTSJ.48.5.6.
- [26] A. C. Trembanis, C. Cary, V. Schmidt, D. Clarke, T. Crees, and E. Jackson, "Modular autonomous biosampler (MAB) - A prototype system for distinct biological size-class sampling and preservation," in *2012 Oceans*, Hampton Roads, VA: IEEE, Oct. 2012, pp. 1–6. doi: 10.1109/OCEANS.2012.6405110.
- [27] K. M. Yamahara *et al.*, "In situ Autonomous Acquisition and Preservation of Marine Environmental DNA Using an Autonomous Underwater Vehicle," *Front. Mar. Sci.*, vol. 6, p. 373, Jul. 2019, doi: 10.3389/fmars.2019.00373.
- [28] H. Ribeiro *et al.*, "Development of an autonomous biosampler to capture in situ aquatic microbiomes," *PLOS ONE*, vol. 14, no. 5, p. e0216882, May 2019, doi: 10.1371/journal.pone.0216882.
- [29] B. Nguyen, K. Pechetratanapanit, C. Udell, C. Walter, J. S. Selker, and T. Levi, "PolyWAG (Water Acquired Genomics) System: A Field Programmable and Customizable Auto-sampler for eDNA," vol. 2019, pp. H53S-2076, Dec. 2019.
- [30] K. Roy *et al.*, "Updates on PolyWAG: Autonomous filtered water sampling for eDNA," presented at the Fall Meeting 2022, AGU, Dec. 2022. Accessed: Mar. 20, 2023. [Online]. Available: <https://agu.confex.com/agu/fm22/meetingapp.cgi/Paper/1096147>
- [31] N. Wandhekar *et al.*, "PolyWAG (Water aquired Genomics) Opensource 24-filter eDNA Water Sampler - Robotic DNA Collection with High Performance Sample Isolation and Preservation," presented at the AGU Fall Meeting 2021, AGU, Dec. 2021. Accessed: Mar. 24, 2023. [Online]. Available: <https://agu.confex.com/agu/fm21/meetingapp.cgi/Paper/943361>
- [32] A. F. Govindarajan *et al.*, "Improved biodiversity detection using a large-volume environmental DNA sampler with in situ filtration and implications for marine eDNA sampling strategies," *Deep Sea Res Part Ocean. Res Pap*, vol. 189, p. 103871, 2022, doi: <https://doi.org/10.1016/j.dsr.2022.103871>.

- [33] M. Schaeper, R. Bahlo, and R. Jaskulke, "Monitoring System with Event Controlled Sampling Operated by a MSP430 Microcontroller," *IFAC Proc. Vol.*, vol. 41, no. 1, pp. 103–106, 2008, doi: 10.3182/20080408-3-IE-4914.00019.
- [34] D. M. Pargett, J. M. Birch, C. M. Preston, J. P. Ryan, Y. Zhang, and C. A. Scholin, "Development of a mobile ecogenomic sensor," in *OCEANS 2015 - MTS/IEEE Washington*, Oct. 2015, pp. 1–6. doi: 10.23919/OCEANS.2015.7404361.
- [35] B. Nguyen, K. Pechetratanapanit, C. Udell, C. Walter, J. S. Selker, and T. Levi, "PolyWAG (Water Acquired Genomics) System: A Field Programmable and Customizable Auto-sampler for eDNA," *ESSOAr*, p. 1, 2020, doi: 10.1002/essoar.10501740.1.
- [36] N. K. Truelove *et al.*, "Expanding the temporal and spatial scales of environmental DNA research with autonomous sampling," *Environ. DNA*, vol. 4, no. 4, pp. 972–984, 2022, doi: 10.1002/edn3.299.
- [37] A. Kirtane, J. D. Atkinson, and L. Sassoubre, "Design and Validation of Passive Environmental DNA Samplers Using Granular Activated Carbon and Montmorillonite Clay," *Environ. Sci. Technol.*, vol. 54, no. 19, pp. 11961–11970, Oct. 2020, doi: 10.1021/acs.est.0c01863.
- [38] B. J. Sansom and L. M. Sassoubre, "Environmental DNA (eDNA) Shedding and Decay Rates to Model Freshwater Mussel eDNA Transport in a River," *Environ. Sci. Technol.*, vol. 51, no. 24, pp. 14244–14253, Dec. 2017, doi: 10.1021/acs.est.7b05199.
- [39] C. P. S. Kruse, P. Basu, D. R. Luesse, and S. E. Wyatt, "Transcriptome and proteome responses in RNA later preserved tissue of *Arabidopsis thaliana*," *PLoS ONE*, vol. 12, no. 4, p. e0175943, Apr. 2017, doi: 10.1371/journal.pone.0175943.
- [40] *Electro-Fluidic Systems Handbook*. Lee Company Limited. [Online]. Available: <https://www.theleeco.com/uploads/2021/04/EFS-9th-Edition-Oct-2019.pdf>
- [41] "PDS-85-2018-08-LFNSeries2-wayMicroInertSolenoidValve.pdf." Accessed: Jan. 30, 2023. [Online]. Available: <https://www.theleeco.com/uploads/2021/11/PDS-85-2018-08-LFNSeries2-wayMicroInertSolenoidValve.pdf>
- [42] A. D. Beaton *et al.*, "Lab-on-Chip for In Situ Analysis of Nutrients in the Deep Sea," *ACS Sens.*, vol. 7, no. 1, pp. 89–98, Jan. 2022, doi: 10.1021/acssensors.1c01685.
- [43] A. Hendricks *et al.*, "Compact and automated eDNA sampler for in situ monitoring of marine environments," *Sci. Rep.*, vol. 13, no. 1, Art. no. 1, Mar. 2023, doi: 10.1038/s41598-023-32310-3.
- [44] *STM32F411xC STM32F411xE Datasheet*. STMicroelectronics. Accessed: Mar. 12, 2023. [Online]. Available: <https://www.st.com/resource/en/datasheet/stm32f411ce.pdf>

- [45] DRV8834 Dual-Bridge Stepper or DC Motor Driver Datasheet. Texas Instruments, 2015. [Online]. Available: <https://www.ti.com/lit/ds/symlink/drv8834.pdf>
- [46] NEMA 17 Stepper Motor Datasheet. PCBLinear. [Online]. Available: <https://pages.pbcllinear.com/rs/909-BFY-775/images/Data-Sheet-Stepper-Motor-Support.pdf>
- [47] "E5 Optical Kit Encoder," *US Digital*. <https://www.usdigital.com/products/encoders/incremental/kit/e5/> (accessed Mar. 13, 2023).
- [48] A. Hendricks *et al.*, "A Miniaturized and Automated eDNA Sampler: Application to a Marine Environment," in *OCEANS 2022, Hampton Roads, 2022*, pp. 1–10. doi: 10.1109/OCEANS47191.2022.9977218.
- [49] E. A. Luy, S. C. Morgan, J. J. Creelman, B. J. Murphy, and V. J. Sieben, "Inlaid microfluidic optics: absorbance cells in clear devices applied to nitrite and phosphate detection," *J. Micromechanics Microengineering*, vol. 30, no. 9, p. 095001, Jun. 2020, doi: 10.1088/1361-6439/ab9202.
- [50] J. Zorz *et al.*, "Drivers of Regional Bacterial Community Structure and Diversity in the Northwest Atlantic Ocean," *Front. Microbiol.*, vol. 10, 2019, doi: 10.3389/fmicb.2019.00281.
- [51] A. E. Parada, D. M. Needham, and J. A. Fuhrman, "Every base matters: assessing small subunit rRNA primers for marine microbiomes with mock communities, time series and global field samples," *Env. Microbiol*, vol. 18, no. 5, pp. 1403–1414, 2016, doi: 10.1111/1462-2920.13023.
- [52] W. Walters *et al.*, "Improved Bacterial 16S rRNA Gene (V4 and V4-5) and Fungal Internal Transcribed Spacer Marker Gene Primers for Microbial Community Surveys," *mSystems*, vol. 1, no. 1, pp. e00009-15, Dec. 2015, doi: 10.1128/mSystems.00009-15.
- [53] A. M. Comeau, G. M. Douglas, and M. G. I. Langille, "Microbiome Helper: a Custom and Streamlined Workflow for Microbiome Research," *mSystems*, vol. 2, no. 1, pp. e00127-16, Jan. 2017, doi: 10.1128/mSystems.00127-16.
- [54] E. Bolyen *et al.*, "Reproducible, interactive, scalable and extensible microbiome data science using QIIME 2," *Nat Biotechnol*, vol. 37, no. 8, pp. 852–857, Aug. 2019, doi: 10.1038/s41587-019-0209-9.
- [55] A. Amir *et al.*, "Deblur Rapidly Resolves Single-Nucleotide Community Sequence Patterns," *mSystems*, vol. 2, no. 2, pp. e00191-16, Mar. 2017, doi: 10.1128/mSystems.00191-16.
- [56] B. J. Callahan, P. J. McMurdie, and S. P. Holmes, "Exact sequence variants should replace operational taxonomic units in marker-gene data analysis," *ISME J.*, vol. 11, no. 12, pp. 2639–2643, Dec. 2017, doi: 10.1038/ismej.2017.119.

- [57] C. Quast *et al.*, “The SILVA ribosomal RNA gene database project: improved data processing and web-based tools,” *Nucleic Acids Res*, vol. 41, no. D1, pp. D590–D596, Jan. 2013, doi: 10.1093/nar/gks1219.
- [58] P. Yilmaz *et al.*, “The SILVA and ‘All-species Living Tree Project (LTP)’ taxonomic frameworks,” *Nucleic Acids Res*, vol. 42, no. D1, pp. D643–D648, Jan. 2014, doi: 10.1093/nar/gkt1209.
- [59] J. Decelle *et al.*, “PhytoREF: a reference database of the plastidial 16S rRNA gene of photosynthetic eukaryotes with curated taxonomy,” *Mol Ecol Resour*, vol. 15, no. 6, pp. 1435–1445, Nov. 2015, doi: 10.1111/1755-0998.12401.
- [60] E. S. Cameron, P. J. Schmidt, B. J.-M. Tremblay, M. B. Emelko, and K. M. Müller, “To rarefy or not to rarefy: Enhancing microbial community analysis through next-generation sequencing,” *bioRxiv*, 2020, doi: 10.1101/2020.09.09.290049.
- [61] R Core Team, *R: A Language and Environment for Statistical Computing*. Vienna, Austria: R Foundation for Statistical Computing, 2022. [Online]. Available: <https://www.R-project.org/>
- [62] N. Gehlenborg, *UpSetR: A More Scalable Alternative to Venn and Euler Diagrams for Visualizing Intersecting Sets*. 2019. [Online]. Available: <https://CRAN.R-project.org/package=UpSetR>
- [63] P. J. McMurdie and S. Holmes, “phyloseq: An R package for reproducible interactive analysis and graphics of microbiome census data,” *PLoS ONE*, vol. 8, no. 4, p. e61217, 2013.
- [64] H. Wickham, *ggplot2: Elegant Graphics for Data Analysis*. Springer-Verlag New York, 2016. [Online]. Available: <https://ggplot2.tidyverse.org>
- [65] P. J. Aphalo, *ggpmisc: Miscellaneous Extensions to “ggplot2.”* 2022. [Online]. Available: <https://CRAN.R-project.org/package=ggpmisc>
- [66] Thermo Fisher Scientific, “260/280 and 260/230 Ratios,” Thermo Fisher Scientific, Wilmington, Delaware USA, T024-Technical Bulletin, Mar. 2009. [Online]. Available: https://dna.uga.edu/wp-content/uploads/sites/51/2019/02/Note-on-the-260_280-and-260_230-Ratios.pdf
- [67] A. R. Bramucci *et al.*, “Microvolume DNA extraction methods for microscale amplicon and metagenomic studies,” *ISME COMMUN*, vol. 1, no. 1, p. 79, Dec. 2021, doi: 10.1038/s43705-021-00079-z.
- [68] R. S. Cornman, J. E. McKenna, J. Fike, S. J. Oyler-McCance, and R. Johnson, “An experimental comparison of composite and grab sampling of stream water for metagenetic analysis of environmental DNA,” *PeerJ*, vol. 6, p. e5871, Dec. 2018, doi: 10.7717/peerj.5871.

- [69] P. A. Den Uyl *et al.*, “Lake Erie field trials to advance autonomous monitoring of cyanobacterial harmful algal blooms,” *Front Mar Sci*, vol. 9, p. 1021952, Oct. 2022, doi: 10.3389/fmars.2022.1021952.
- [70] M. p. Ryan, J. t. Pembroke, and C. c. Adley, “*Ralstonia pickettii* in environmental biotechnology: potential and applications,” *J Appl Microbiol*, vol. 103, no. 4, pp. 754–764, 2007, doi: 10.1111/j.1365-2672.2007.03361.x.
- [71] I. Government of Canada, “Technology readiness levels,” Jan. 23, 2018. <https://ised-isde.canada.ca/site/innovation-canada/en/technology-readiness-levels> (accessed Apr. 27, 2023).
- [72] L. E. Ogden, “The Emergence of eDNA: An interdisciplinary tool helps monitor biodiversity and health.,” *BioScience*, vol. 72, no. 1, pp. 5–12, Jan. 2022, doi: 10.1093/biosci/biab120.
- [73] M. Clavey, “Innovative fish eDNA project launched at offshore wind farm,” *NatureMetrics*, Mar. 10, 2022. <https://www.naturemetrics.co.uk/2022/03/10/innovative-fish-edna-project-launched-at-offshore-wind-farm/> (accessed Mar. 30, 2023).